

READING ROOM

OF-WTWI-1985-9

STRATIGRAPHY OF BEDDED HALITE IN THE PERMIAN SAN ANDRES FORMATION, UNITS 4 AND 5, PALO DURO BASIN, TEXAS

by

S. D. Hovorka
B. A. Luneau
S. Thomas

CAUTION

This report describes research carried out by staff members of the Bureau of Economic Geology that addresses the feasibility of the Palo Duro Basin for isolation of high-level nuclear wastes. The report describes the progress and current status of research and tentative conclusions reached. Interpretations and conclusions are based on available data and state-of-the-art concepts, and hence, may be modified by more information and further application of the involved sciences.

Prepared for the
U. S. Department of Energy
Office of Nuclear Waste Isolation
under contract no. DE-AC97-83WM46651

Bureau of Economic Geology
W. L. Fisher, Director
The University of Texas at Austin
University Station, P. O. Box X
Austin, Texas 78713

1985

RECEIVED
Reading Room/Data Center

APR 04 1985

BUREAU OF ECONOMIC GEOLOGY
UNIV. OF TEXAS AT AUSTIN

DRAFT

TABLE OF CONTENTS

Abstract

Introduction

Part I: Textural Study of Bedded Halite

Methods of preparation of detailed logs

Depth

Lithology

Sedimentary Structures

Halite Types

Interbeds and Description of interbeds

Zones

Description of San Andres Unit 4 and 5 Halite

Sedimentary Structures in Bedded Halite

Textural Classification of Halite

Chevron Halite Rock

Color-Banded/Vertically Oriented Halite Rock

Chaotic Mudstone-halite Rock

Equant Muddy Halite Rock

Equant Anhydritic Halite Rock

Displacive Halite

Cavity-Filling Halite Cement

Fibrous, Fracture-Filling Halite Cement

Halite As a Diagenetic Replacement of Other Minerals

Interbeds Within Halite

Mudstone Interbeds

Composition of Terrigenous Clastic Mudstone

Sedimentary Structures in Terrigenous Clastic Mudstone

Dark, Anhydritic Mudstone Insoluble Residue

Composition and Fabric of Anhydrite Interbeds

Part II: Stratigraphic Cross Sections

Correlation of Zones of Clean, Anhydrite, and Muddy Halite within San Andres Unit 4

Correlation Within San Andres Unit 5

Discussion

Depositional Environment of Halite

Depositional Environment of Mudstone Interbeds

Distribution of Mudstone Interbeds

Summary of San Andres Depositional Environments

Conclusions

DRAFT

ABSTRACT

Seven cored wells through the bedded halite of the San Andres Formation have allowed an unusual, detailed analysis of the fabrics in halite. A descriptive classification system identified eight textural types of halite. These are: chevron halite rock, color-banded/vertically oriented halite rock, chaotic mudstone-halite rock, equant muddy halite rock, equant anhydritic halite rock, displacive halite in other sediments, cavity-filling halite cement, and fibrous fracture-filling halite cement. Genetic interpretation of the depositional environment in which halite textures formed resulted from analysis of the relationships between textures and comparison to ancient, modern, and experimental halite analogs. Chevron and color-banded/vertically oriented halite are recognized as textures formed subaqueously as halite precipitated on the floor of brine pools. Chaotic mudstone-halite rock, equant muddy halite rock, equant anhydritic halite rock are recognized as diagenetic alteration products formed by karstification and diagenetic recrystallization occurring at least partly in the subaerial environment. Displacive halite in other sediments, cavity-filling halite cement, and fibrous fracture-filling halite cement are products of precipitation of halite within the sediment during early diagenesis.

Very detailed logging of the halite fabrics and anhydrite and mudstone interbeds and partings in the seven cored wells allowed correlation on a meter scale between cores. A basinwide pattern of alternation between zones of anhydritic halite with preserved brine pool fabrics and zones of halite with mudstone interbeds and altered textures was identified. These alternating zones can be traced as much as 100 km between the wells, providing evidence that the entire study area was one broad low relief evaporite shelf. Net mud maps of the muddy intervals suggest that the geometry of mudstone beds might be broad, poorly-defined lobes. Isopachs of the anhydrite interbeds show variation in the facies pattern in each genetic cycle. Some anhydrite beds thicken toward southern Swisher County, while others are thickest to the west, in Deaf Smith County.

This report describes research carried out by staff members of the Bureau of Economic Geology that addresses the feasibility of the Palo Duro Basin for isolation of high-level nuclear wastes. The report describes the progress and current status of research and tentative conclusions reached. Interpretations and conclusions are based on available data and state-of-the-art concepts, and hence, may be modified by more information and further application of the involved sciences.

CAUTION

DRAFT

INTRODUCTION

The investigation of the Permian bedded halite of the Palo Duro Basin, as a potential site for a nuclear waste repository, has provided a need and a unique opportunity to study the stratigraphy and depositional environment of a thick and extensive evaporite section containing bedded halite. Reconnaissance studies comparing bedded halite units in the basin (Presley, 1979a, 1979b) have been followed by a coring and research program focusing on the potential repository horizon, the halite of informally named units 4 and 5 of the San Andres Formation.

The character of the San Andres Formation and its lateral and vertical relationships with other units in the Palo Duro Basin (fig. 1) have been reviewed by Presley (1981b, 1981c) and Budnik and Smith (1982). Regional studies utilizing geophysical logs have permitted recognition of five cyclic sequences in the lower San Andres (Presley, 1979a) and an interpretation of the general regressive nature of Permian evaporite sequences in the Palo Duro Basin (fig. 2).

Construction of detailed regional cross sections using geophysical logs and acquisition and examination of nine cores through most of the San Andres Formation have permitted development of a detailed model for the San Andres cyclic evaporites (fig. 3) (Hovorka, 1982, Fracasso and Hovorka, 1984). The textures observed in these cyclic sequences reflect rapid transgression followed by increasing salinity of a shallow marine-marginal water body due to decreasing communication with the normal marine environment. The initial sediment of each cycle is a thin, dark, anhydritic mudstone, derived at least in part from the dissolution of the underlying halite during transgression. The sediments deposited during the phase of increasing salinity are: skeletal limestone, dolomite, anhydrite which has replaced laminated gypsum, and bedded halite. Many cycles are not complete. The cycle may be initiated by hypersaline water, resulting in a thin or nonexistent carbonate. The cycle may be interrupted by a new transgression before halite saturation was reached, resulting in the absence of halite. The halite part of the cycle may be removed during the following transgression, resulting in concentration of the insoluble components from the halite as a residue. Numerous thin complete and incomplete cycles can be recognized throughout the Palo Duro Basin through all but the upper 60 m of the San Andres Formation. The basal insoluble residue-mudstone units

DRAFT

and carbonate units of thin San Andres cycles can be correlated using geophysical logs over an area in excess of 26,000 km² (Fracasso and Hovorka, 1984).

The significance of this regional geometry is that the depositional environment in which San Andres evaporites formed was an uninterrupted, broad, shallow shelf. Textural evidence from petrographic studies indicates that most of the evaporites were deposited in shallow, subaqueous environments. Evidence that the San Andres limestone, laminated anhydrite, much of the dolomite, and nodular anhydrite were deposited in subaqueous environments is discussed elsewhere (Fracasso and Hovorka, 1984).

The extent to which the San Andres halite was formed in a similar, uninterrupted shallow water body will be investigated here. Recent models of halite-precipitating environments are in supratidal environments (Shearman, 1970; Gavish, 1980; Weiler and others, 1974; Handford, 1982). In the most extensive modern evaporite flats, the Ranns of Kutch of the eastern coast of India, deposition takes place in subbasins with physically or geochemically different sediment accumulation histories (Glennie and Evans, 1976). Handford and Bassett (1982) constructed a generalized model for the Palo Duro Permian, contrasting an isolated, small salt pan facies as part of the "mud-rich sabkha system" with an extensive, subaqueous halite-precipitating environment as part of the "mud-poor sabkha system." The San Andres Formation, based on its relatively low clastic content, would probably fall in the extensive salt-precipitating environment of the mud-poor model. Bein and Land (1982), considering mostly geochemical data, constructed an alternate model where the lower San Andres units 2, 3, and 4 were deposited subaqueously in a large shelf basin or lagoon, while in the upper San Andres and unit 5, both the carbonate and halite parts of the cycle were deposited in smaller, separated water bodies.

Handford (1981) studied bromide content of halite, a trace constituent which is useful for interpreting the composition of the brine from which the halite formed, and found no apparent trend in the San Andres unit 4 halite. Ruppel and Ramondetta (1982) mapped the salt quality (mudstone content) of the San Andres units 4 and 5 based on gamma-ray log response. The trends shown on the salt quality maps are spotty and difficult to interpret. The irregularity of

DRAFT

the pattern might be interpreted to suggest that subbasins existed during deposition of units 4 and 5 halite. The implication of such a model is that the character of the halite might vary greatly from area to area, so that information gathered about the stratigraphy, geochemistry, or other properties of halite at one location might not be applicable to another locale.

The present study was undertaken after recognition that zones of clean or anhydritic halite and zones of abundant mudstone interbeds appeared to be correlatable between cores based on reconnaissance lithologic logging. The areal extent over which these zones can be traced without change in character indicating facies change, provides information about the continuity or isolation of the halite-precipitating environments. Improved understanding of the halite-precipitating environments allows better prediction of areal variation in the character of the halite. This information, combined with the detailed logs produced during this study, should be useful information for repository siting.

PART I: TEXTURAL STUDY OF BEDDED HALITE

Methods of Preparation of Detailed Logs

The present study utilized information and techniques developed during examination of 5,000 meters of core from seven wells drilled through Permian halite and associated strata in the Palo Duro Basin by the U.S. Department of Energy. Generalized logs of these cores have been published (Handford, 1980; McGowen, 1981; Ruppel and Hovorka, 1983a, 1983b; Hovorka and others, in prep. a, b, c.) For this study, the San Andres units 4 and 5 halite intervals were relogged at an expanded scale to permit recording detailed information (Plates 1-14). Consistency was emphasized so that comparison of subtle features between logs could be made with confidence. The three authors prepared detailed lithologic logs during an eight-month period and the senior author proofed all logs against the core. An additional check on the accuracy of the data was comparison of these detailed logs to less detailed draft logs prepared by ONWI (1983) and the reexamination of those intervals in which discrepancies were identified.

The locations of the cored wells are shown in figure 4, and the stratigraphic position of the logged unit 4 and 5 intervals in the cored part of the San Andres Formation is shown in figure 5. In the detailed logs, unit 4 and unit 5 are contiguous along match lines at the top of unit 4 and base of unit 5. Each log shows eight columns of data. From left to right, these are: depth, lithology, structures, halite type, interbeds, description of interbeds, comments, and zone number (key, fig. 6). The methods used in acquiring and recording the data in each column are discussed below.

Depth

The depth shown on detailed logs (Plates 1-14) in feet below kelly bushing corresponds to the depths painted on the core according to BEG Specific Work Instruction WSCL 001, Revision 02. Core depths typically vary from geophysical log depths for a corresponding bed by a few feet, with an apparent maximum variance of five feet, due to cumulation of measurement errors.

Greatest uncertainty as to accurate depth occurs in intervals of poor recovery or core loss, where uncertainty as to the exact interval in which the loss occurred is arbitrarily dealt with by recording loss at the top of the core run involved. Also shown in the depth column are intervals where logging is less precise, because the core was unavailable at the time of logging, and older records were used. Intervals labeled "PC" refer to determination of the percent lithology shown in the second column by point counting.

Lithology

Visual estimates of mineralogic composition of Plates 1-14 for each foot of core examined were recorded in the lithology column; the key to the symbols used is shown in figure 6. The scale is arithmetic, showing volume percent, and totaling 100 percent. The constituents identified are: terrigenous clastic sand, terrigenous clastic silt, terrigenous clastic mud, terrigenous clastic clay, calcite, dolomite, anhydrite, halite, and possible trace amounts of polyhalite. Reconnaissance petrographic studies (Hovorka and others, 1982; Hovorka, 1983) and X-ray diffraction, whole rock geochemistry, and grain-size analysis studies confirm that these are the dominant components and that visual determination of mineralogy is accurate within the limits discussed below.

Sandstone and siltstone are rare in San Andres units 4 and 5, but are readily identified by comparison in the binocular microscope with a set of standards. The standards are typical clastics from cores of Permian Palo Duro sediments in which grain size has been determined petrographically and by grain-size analysis. The sandstone/siltstone boundary is transitional, and visual estimates may err in the proportion of each size shown. Sandstone and siltstone compositions throughout the Permian including the San Andres Formation are arkose, subarkose, lithic arkose, and arkosic litharenite (Hovorka and others, 1982; Kolker and others, in prep.)

Mudstone is a mixture of clay-size and silt-size material. Accurate determination of the percentages of these components is not possible during logging, because of the fine grain size. The discrimination of siltstone (less than 33 percent clay-size materials) and claystone (less than 33 percent silt-size material) is somewhat arbitrary, based on crude tests such as gritting

mud between teeth (test for silt size) and slow drying and "clayey" smell (test for the presence of clay). Discrimination between mudstone, claystone, and siltstone is very difficult without laboratory analysis when they are admixed with carbonate or anhydrite, as they are at the base of cycles in unit 5.

San Andres carbonates are readily identified by distinctive appearance. The percentage of calcite is determined by etching the slabbed core with dilute hydrochloric acid. Identification of other materials such as siliciclastic silt within dolomite or dolomitic limestone is difficult prior to laboratory analysis, as is identification of dolomite as a minor constituent in terrigenous clastics and halite.

Anhydrite is identified because of its distinctive appearance. Minor amounts of anhydrite in halite are visible because they are left in relief on the etched surfaces of the core. Minor amounts of anhydrite as cement or nodules in terrigenous clastics are identifiable because of the increased hardness to scratch test and lighter color of such intervals.

Halite is identified by taste and because it is etched on outside and slabbed surfaces of the core. Minor amounts of halite as cement or diagenetic replacement of other lithologies are deeply etched in many samples. Apparent pores require careful examination and most are found to have contained halite which was dissolved during coring or slabbing procedures.

Possible polyhalite ($MgCaSO_4 \times H_2O$) has been indicated in thin zones in several cores because of the distinctive orange or pink color of the sulfates in these zones. Microprobe analysis (Long-Cheng Liang, personal communication, 1983) has confirmed the presence of polyhalite at one location (2,325.7 feet, San Andres unit 5, #1 G. Friemel core) where it was petrographically identified by Larry M. Fukui of Bendix Field Engineering (written communication, 1-27-1983). Additional possible examples of polyhalite have been submitted for laboratory analysis. Other petrographically identifiable components within the halite, such as diagenetic limpid dolomite, celestite, dark pigment (organic material), hematite, and other diagenetic opaque minerals are present only in trace quantities and are not commonly identifiable on slabbed core.

Accuracy of the percentage estimates for each lithology was checked at frequent intervals by point counting. This technique uses 100 dots marked in a grid on a sheet of plastic, 1 foot by 10 centimeters, which covers the slabbed surface of the core. This technique is preferred to thin section point counting because the fabric of the halite is typically strongly inhomogeneous, both laterally and vertically, so that a thin section does not include a large enough area to be representative of the interval. Insoluble residues, thin sections, and geochemical analysis are being prepared to improve the accuracy of the percent lithology column.

Sedimentary Structures

All of the core not allocated to engineering tests requiring whole core has been slabbed. This has greatly improved recognition and understanding of fabrics in all lithologies. Techniques used to recognize subtle fabrics in halite are cleaning and lightly etching the core in water, examining it wet, which allows better resolution of features within and between the crystals, then examining the etched surface after it has dried, which emphasizes insoluble components and the size and shape of the halite crystals. Halite crystal boundaries are visible when the core is held oblique to room light so that the light reflects off the crystals showing the differences in their orientation.

Structures shown on the logs may be slightly enlarged and generalized because of scale considerations. Structures shown to the right of the column are features such as the nature of the contact between two lithologies, fractures, and structures within thin beds which would have been obscured if plotted with the other structures. Symbols for sedimentary structures are shown in the key (fig. 6).

Halite Types

The salt classification used here is described elsewhere in this paper. The classification was developed to quickly describe the common fabrics recognized in Palo Duro halite and categorize halite crystal size, crystal shape, amount, composition, distribution of impurities, and other aspects of fabric.

Interbeds and Description of Interbeds

The composition, location, thickness, and character of bedding for interbeds of other lithologies in halite are highlighted in this column. Terrigenous clastic beds, dominantly mudstone, are shown with a solid line; anhydrite is shown as a patterned line. The continuity of a bed through the 10 cm diameter of the core is shown graphically. The sawtooth pattern in the upper, lower, or both surfaces of beds indicates the irregularity of the bedding surfaces. The interbed lithology and estimated average thickness in millimeters are shown in the description column. Also shown in the description column are any generalizations required because of the scale. In locations where many interbeds were present per foot, only two or three are shown with symbols, and the number of interbeds each symbol represents is shown in the description. Comparison of correlated intervals of adjacent cores indicates that little significant information is lost by this generalization. Individual partings within one-foot intervals could not be correlated over the distances between the cored wells used in this study even when looking at actual cores so all features could be considered. The locations of all interbeds of any thickness are shown graphically. Those for which no thickness is recorded are partings averaging less than 1 mm thick.

A limit to the accuracy of these logs in locating interbeds is inherent in the use of a 10-cm-diameter core. Inhomogeneities, such as karst pits and small-scale collapse features, truncate areally extensive interbeds and partings so that they are no longer represented in the core. Alternatively, mudstone and anhydrite accumulations on pit floors and along small-scale fault planes which are not equivalent to regionally persistent beds may not be distinguishable in core from regional beds. An attempt was made, however, to recognize such features in the core. Accumulations of impurities which were interpreted as pit fills or localized along faults, are shown in the structures column. Discontinuous accumulations of impurities of more uncertain origin are shown in the interbed column as discontinuous features with irregular bedding surfaces. Many of these discontinuous, irregular beds may actually also be local pit fills. Zones of abundant mudstone impurities with no defined bedding are shown with a stippled

pattern. These intervals correspond to the chaotic mudstone-halite salt type, described later in detail.

Many interbeds are mixtures of mudstone and halite, mudstone and anhydrite, or anhydrite and halite, as noted in the description column. A pragmatic approach is used in defining interbeds. Beds composed of irregularly spaced and interconnected partings or beds with many halite masses within them and irregular bedding surfaces may, therefore, have an average composition of greater than 50 percent halite. Discrimination between anhydritic mudstone and muddy anhydrite is difficult in core and, therefore, somewhat arbitrary.

Zones

The numbers in the rightmost column identify zones which have been interpreted as correlative and correspond to the numbered zones on Plates 15 and 16. These zones are not intended as formal stratigraphic units, but as work units for convenience of comparison of approximately equivalent zones in different wells. The numbered zones are based on sequences of beds which can be recognized in most of the seven cores used in this study. The upper and lower boundaries of the zones are somewhat arbitrarily placed at the uppermost or lowermost mudstone bed of a sequence, which may or may not have been correlated with the uppermost or lowermost mudstone bed in the equivalent sequence in the adjacent core. This procedure is justified because, although the sequence is correlated with confidence, correlations on a less than one-foot scale cannot be made with certainty over the distances between cores. In some cases, the boundaries between zones are drawn along lithofacies boundaries. In cases where lithofacies boundaries are unclear or complex, boundaries are drawn along correlation lines, and several lithofacies are combined together in one zone with the uniting characteristic of complexity.

Description of San Andres Units 4 and 5 Halite

The study interval contains the section from the base of the halite of San Andres unit 4 to the uppermost interval of halite in unit 5 (fig. 5). The carbonate/anhydrite interval of unit 4 is omitted from this study. Carbonate and anhydrite rocks of unit 5, however, are part of thin

cyclic sequences, each of which locally culminates in halite. The omission or separation of the unit 5 carbonate/anhydrite from the halite rocks would, therefore, be arbitrary and unnecessarily confuse the sections. Fabrics in carbonate/anhydrite sequences in San Andres unit 5 are further discussed by Fracasso and Hovorka (1984).

The halite sections of both unit 4 and unit 5 are composed of halite, mudstone, anhydrite, and minor constituents best identified in thin section or by geochemical analysis. Halite rock (greater than 50 percent halite) is by definition the dominant component in halite intervals. Impurities occur both as minor components disseminated through halite rock and as concentrations in interbeds. For example, in the San Andres unit 4 halite in the J. Friemel core, 70 discrete mudstone beds were identified on the detailed log. The average mudstone bed thickness is 3.5 cm, and the maximum mudstone bed thickness is 47 cm. The estimated average composition of these mudstone beds is 70 percent mudstone. The 165-foot thick unit 4 halite interval averages about 7 percent mudstone (calculated from the detailed log, Plate 2), so discrete mudstone beds contain about half the mudstone in the interval. The rest of the mudstone is disseminated in halite rock. Most of it is concentrated in the 17 percent of the interval logged as mudstone/halite rock (salt type D), which averages 10 to 15 percent mudstone in irregular masses in halite. A minor amount of the mudstone is disseminated through relatively clean halite, which contains an average of 1 to 2 percent mudstone in isolated masses. Anhydrite makes up 6 percent of the unit 4 halite interval in the J. Friemel core. Ninety-five anhydrite beds were identified. Most are partings of unmeasurable thickness. Anhydrite is abundant along halite grain boundaries and as irregular masses in halite. Halite makes up 87 percent of the unit 4 interval in the J. Friemel core and exhibits a variety of primary and diagenetic fabrics. Similar compilations of compositions drawn from the detailed logs are shown in Table 1.

Sedimentary Structures in Bedded Halite

Special conditions are required for the study of textures in halite rock. Halite has both a high solubility in water, creating a potential for reactivity during diagenesis, and low strength,

causing it to flow in many geologic settings. These processes cause destruction of initial fabrics, so that study of primary fabrics is not possible in many salt deposits. Additionally, study is limited because halite does not crop out in most climates. Coring techniques using saturated brines are required for good recovery of halite. Conditions for textural study are near optimum in the Palo Duro cores. A wide variety of well-preserved primary fabrics are present. Abundant examples of the relationships between primary and altered fabrics permit interpretation of diagenetic processes. The technique of slabbing and light etching in water was especially useful for textural studies allowing identification of features not visible on the outside of the cores. The availability of seven cores through the San Andres Formation allows examination of spatial relationships. Halite core from other Permian halite units in the Palo Duro Basin provided important contrasts with the textures observed in the San Andres Formation.

Textural studies of halite have been published by Dellwig (1955) of the Silurian Salina salt of Michigan, Wardlaw and Schwerdtner (1966) of Devonian salt in Saskatchewan, Arthurton (1973) of Triassic halite in Cheshire, England, Lowenstein (1982) of the Permian Salado Formation of the Delaware Basin, New Mexico, and Holdoway (1978) of Permian salt in the Nippewalla Group of Kansas. Gornitz and Schreiber (1981) present a graphic summary of the varieties of fabrics described in these studies.

Figure 7 illustrates the suite of fabrics identified in San Andres halite and comparable fabrics from the literature. These fabrics are vertically-oriented bottom-nucleated crystals, cumulates of detrital or suspended crystals, equant mosaic fabric, growth zones defined by fluid inclusions (chevron structures), color bands due to variations in the amount and type of included material, partings and interbeds of argillaceous materials or anhydrite, truncation surfaces, small-scale karst pipes and pits, recrystallized, altered, and diagenetic fabrics.

Bottom-nucleated crystals form as a crust on the floor of the brine pool. They are nucleated on detrital halite grains; as they enlarge, competition for space on the crowded floor of the brine pool favors those with the fast growing cube corners and edges directed upward (Arthurton, 1973; Wardlaw and Schwerdtner, 1966). The resulting fabric, in which the favorably

oriented crystals have grown upward until truncated by a changing condition, appears in slab as a mosaic of similarly-oriented vertically elongated halite crystals (figs. 8 and 9). This fabric is very common in San Andrés units 4 and 5.

Halite in modern environments is commonly observed crystallizing at the air-water interface (Arthurton, 1973). Minute crystals are held in suspension by surface tension and commonly coalesce to form rafts, which eventually founder and form cumulates on the bottom. Weiler and others (1974) have identified detrital forms of halite accumulating in brine pans, including rippled, soft halite mud, and halite ooids. The "mud" is composed of 0.2 mm cube-shaped crystals, and the ooids resemble carbonate ooids except that they have a smaller diameter. Relict detrital grains of halite or foundered rafts are sparse in Palo Duro halite although they are an important halite fabric in modern and experimental environments (Arthurton, 1973). One explanation for the paucity of such fabrics in Palo Duro examples is the coarse average crystal size in Palo Duro halite. Apparently, the diagenetic conditions during and after cementation of any unconsolidated halite deposits consistently favored larger crystal sizes and most original accumulations of fine grains have been recrystallized and are no longer recognizable. Fine halite crystals of probable cumulate origin are preserved in a matrix of anhydrite (figs. 10 and 11).

Equant mosaic fabrics are common in Palo Duro halite rocks (fig. 12). These fabrics have not been identified in Recent environments. A possible origin of equant mosaic fabrics is recrystallization of any other fabric to the most stable crystal shape, similar to the growth of neomorphic spar in carbonates (Bathurst, 1975). Alternatively, halite could have accumulated with an equant fabric, perhaps by slow, noncompetitive growth of crystals on a brine pool floor.

Fluid inclusion concentrations along relict growth faces in halite known as "chevrons" and "coronets" are abundant in San Andres halite rocks and are very similar to those described in the literature (figs. 13 and 14) (Arthurton, 1973; Wardlaw and Schwerdtner, 1966; Holdoway, 1978; Shearman, 1970). The growth bands in chevrons show that the halite crystals were oriented with the cube corners upward, while in coronets the cube faces are upward. Chevron and coronets indicate crystals were bottom nucleated.

Roedder (1982) has examined chevron fluid inclusions from the San Andres Formation of the #1 Rex White core. He interpreted the regular banding as due to diurnal variation in the saturation of the precipitating water. This model requires precipitation of halite in extremely shallow water only a few feet deep, so that the brines supersaturated at the surface could reach the brine pool floor without homogenizing.

Color banding due to variations in the amount and composition of impurities is common in San Andres halite. The commonest type of banding is dark gray to black bands of halite alternating with clear or white bands (fig. 15), although red-brown color bands alternating with clear bands are also found. Bands are typically 1 to 10 cm thick and occur repetitively, but with irregular spacing. Petrographic and geochemical studies of the pigmenting agents in these bands have not been completed, but preliminary results identify disseminated anhydrite, mudstone, and organic material in dark bands. Total organic carbon in similar-appearing lower Clear Fork salt was measured by Handford (1980) as 0.8 weight percent. Light bands are clear or colored white by anhydrite or fluid inclusions. Fluid inclusions in color banded halite do not typically show well-formed zonation. Color bands may be associated with anhydrite partings and truncation surfaces or occur in uninterrupted halite.

The sedimentary structures and character of mudstone and anhydrite interbeds and partings will be discussed in detail later in this report. Regularly spaced interbeds are lacking throughout the halite of the San Andres Formation. This is an important distinction between it and the regularly banded "jahresringe" halite rocks such as those of the Silurian of the Michigan Basin (Dellwig, 1955), Devonian of Saskatchewan (Wardlaw and Schwerdtner, 1966), and some Zechstein salt beds (Reading, 1978, p. 200), and "varved" salt of the Permian Castile Formation of the Delaware Basin, New Mexico (Dean and Anderson, 1982). Relationships between and variability of types of San Andres interbeds are complex and appear random. Detailed correlations discussed below, however, show that groups of mudstone or anhydrite interbeds can be traced long distances across the basin.

A well-displayed suite of features which crosscut the fabrics described above can be seen in San Andres cores. On the smallest scale, corrosion surfaces cut across vertical crystals or

chevron structures (fig. 16). Most commonly, the corrosion surfaces are highlighted by an anhydrite parting or a thin interbed. Small-scale truncation relationships can rarely be identified beneath mudstone beds because the adjacent halite is typically recrystallized. Small pits and other irregularities on the truncation surface can be identified where preservation of primary textures is good enough to define them. Palo Duro corrosion surfaces are similar to those examined by Shearman (1970) in Salina Ometepec, Baja California, Mexico. In Salina Ometepec, dissolution of previously deposited halite along its upper surfaces, truncating vertical crystals, and along grain boundaries, forming small pits, occurs when salinity is lowered by input of new low salinity brine. The initial precipitate of the new brine is a thin layer of gypsum after which halite precipitation resumes. The origin of the Palo Duro truncation surfaces is believed to be similar. The source of lower salinity water could either be input of less highly evaporated marine-derived brine across the shelf or freshening by input of meteoric waters by rain or intermittent flood event. Fisher and Hovorka (1984) attribute the moderate bromide/chloride ratio of chevron salt to a process of precipitation alternating with input of lower salinity marine-derived (?) brine.

Dramatic, larger-scale crosscutting features are identified as karst pits and pipes. Pipes (B. C. Schreiber, oral communication, 1983) is the term applied to narrow vertical flaws in the bedded halite fabric (fig. 17 and 18). Widths are typically 1 to 3 cm. Lengths are difficult to determine in core, but may be a few centimeters up to an observed maximum of two meters. Pipes are generally tubes of relatively equant diameter, but features with a planar geometry extending the 10 cm width of the core have been identified. The pipes have a strong vertical orientation, but deviate enough to enter and leave the plane of the slabbed core face. The pipes can be differentiated from the host halite because of the slightly coarser crystal size of the halite within them and the absence of primary fabrics. In most examples, it is difficult to draw a sharp division between pipe fill and host halite.

Some pipes are partly or completely filled with mudstone (fig. 19). In other examples, anhydrite partings can be observed as broken and discontinuous fragments sagging into the pipe. Pipes containing nonhalite materials which collapsed into them must have been open void space

at some time; the coarse halite in them therefore was precipitated as void-filling cement. However, recrystallization of halite along the pipe walls clearly played a role in causing the fabric discontinuity at the pipe, as evidenced by the difficulty in identifying the edge of primary halite. Some pipes may have only been fractures along which fabrics were diagenetically altered.

In contrast to pipes, pits are wide features which clearly were once open void space although halite cement now fills all pores (fig. 20). Pits range from 3 cm to greater than the 10 cm core width in width, and may be a few centimeters to 2 m deep. Pit floors are marked by an accumulation of anhydrite and/or mudstone, which is typically similar in composition to the insoluble components in the host halite. Most pits are filled with coarse halite cement, but mudstone pit fills are not uncommon. The host halite was recrystallized for a few millimeters or a few centimeters adjacent to the pit. Beds of insoluble material project as ledges a few centimeters out from the pit wall host halite. The geometry of pits is difficult to determine because of their size relative to the size of core available, but they appear, like pipes, to have a general vertical orientation and an equant cross section, complicated by the presence of anastomosing vertical passages and widening into horizontal rooms. Some pits are bottle-shaped with a narrow top, widening toward the floor. In complexly shaped pits, insoluble residue materials drape all horizontal surfaces (fig. 21). Rotated blocks of bedded halite collapsed into pits attest to the presence of interconnected open spaces analogous to karst in carbonates. Intervals of core with well-defined parallel bedding and banding and normal brine pool textures rotated 5 to 30 degrees extending for up to one meter vertically (fig. 22) suggest the presence of some fairly large-scale collapse pits although the pit which caused the collapse cannot be identified in core. The dipping beds are overlain by normal horizontally bedded halite. In some examples there is a suggestion of angular truncation of the dipping beds by the overlying horizontal beds, indicating that collapse occurred in the depositional environment.

The origin of pits and pipes in San Andres halite is interpreted as due to karstic solution of cemented halite rock. The pipes and pits crosscut the brine pool fabrics and, therefore, are presumed to have formed in response to a change in environment. This change in environment

is interpreted as a change from subaqueous halite-precipitating conditions to subaerial(?) halite-dissolving conditions. Karst pits in halite have been noted, but not described, by Weiler and others (1974) in supratidal zones of halite-cemented halite ooids on the shores of the Dead Sea, Israel, and by Hunt and others (1966, p. 62, 64) in halite pans in Death Valley. Features similar to the pits in the San Andres can be seen in the Permian Salado Formation. Maps of drift walls of the WIPP mine, east of Carlsbad, New Mexico (D'Appolonia Consulting Engineers Inc., 1983) show abundant anomalies, commonly 1 to 2 feet wide (maximum 11 feet) and 1 to 2 feet deep (maximum, same pit, more than 6 feet deep). These features are recognized where they cut through the partings and bands within the halite. The change from primary fabrics to coarser equant fabrics is not identifiable on drift walls, partially because of the rough mine wall exposure. However, in test core samples from the WIPP site, the senior author identified features on a 10 centimeter scale which truncate primary textures by coarse cavity filling halite, very similar to the pits observed in the Palo Duro San Andres. D'Appolonia researchers (verbal communication, 1983) believe that many of the anomalous features in the WIPP site are channel-form, although no lateral mapping of them has been undertaken. In potash mines in the Devonian Prairie evaporites of Saskatchewan, Baar (1974) has mapped in larger-scale anomalous features, interpreted by him to be due to dissolution of salts at exposed surfaces by isolated rainstorms, when the dissolving waters scoured channels and then evaporated or seeped into central sinks. Some channels have a clay residue derived from dissolved salts and are filled with salt. Salt-filled fractures are identified parallel to the channels. Channels are as much as 1,000 feet long, and 10 to 20 feet wide. Smaller-scale features were not described.

There are several problems with the interpretation that San Andres pits have a karst origin. No traces other than the pits and pipes themselves remain of any vertical fractures controlling the movement of fluids, but presumably some such control existed during the stage of dissolution. Vertical fractures of poorly understood but possible early origin are common in mudstone beds and carbonate units associated with the halite section, and lend support to the theory that now-healed vertical fractures may initially have formed in the halite. Salt polygons with cracks defining their edges are common in modern environments (Handford, 1982; Hunt and

others, 1966). An additional difficulty in the karstic solution model for the origin of pits is the apparent depth of several meters to which dissolution occurred. Development of several meters of hydrologic head to circulate the dissolving fluids is difficult to envision on the extremely low relief surface on which San Andres evaporites were deposited (Fracasso and Hovorka, 1984). However, the same problem pertains to the examples in the Salado Formation at the WIPP mine and the Saskatchewan potash mines. Little is known about the hydrology of such extensive evaporite flats; therefore, models made at this time are purely speculative.

Abundant recrystallized, altered and diagenetic fabrics can be identified in the Palo Duro evaporites. All halite rocks show some alteration, evident in the rather coarse average grain size, loss of chevron fabrics along grain boundaries (fig. 23), ubiquitous occurrence of diagenetic blades of anhydrite along grain boundaries and within grains (fig. 24), and the common presence of diagenetic multifaceted dolomite crystals along grain boundaries (fig. 25). Naimen and others (1983) have examined diagenetic dolomite in detail. Many examples of halite rock show relict primary fabric which has been largely destroyed by alteration processes such as pit and pipe formation, dissolution and recrystallization, grain enlargement or grain boundary migration. Halite rock which lacks identifiable primary textures, may represent alteration events of which no traces remain.

Suites of the textural features discussed here occur repetitively throughout the section. The following classification recognizes common associations and permits identification of common textures, so that stratigraphic and other patterns which may correlate to halite rock textures can be recognized.

Textural Classification of Halite

A classification of halite based on crystal size, crystal shape, amount and composition of impurities, distribution of fluid inclusions, and characteristic sedimentary structures has been developed during examination of Palo Duro cores. The eight classes of fabrics range from those originating as primary brine-pool precipitates to those formed during diagenesis.

CAUTION
This report describes research carried out by staff members of the Bureau of Economic Geology that addresses the feasibility of the Palo Duro Basin for isolation of high-level nuclear wastes. The report describes the progress and current status of research and tentative conclusions reached. Interpretations and conclusions are based on available data and state-of-the-art concepts, and hence, may be modified by more information and further application of the involved sciences.

DRAFT

Most of the halite core examined has been from the San Andres Formation; however, examination of other formations in the Palo Duro Basin which contain halite indicates that this classification will be useful for all halite in the Palo Duro Basin. No attempt to expand this classification to include fabrics from halite rocks in other basins has been made, although interpretations based on other basins and modern halite-precipitating environments have been utilized to select important fabrics.

The fabrics used to classify halite and the resulting eight classes are shown in Table 3. Each halite type is identified by a letter symbol, used for measured sections and geochemical data, and a type name. Typical crystal size, shape, composition and location of impurities, and fluid inclusion distribution are given for each type. The associated halite types, a summary of identifying characteristics, and a sketch of typical fabric are shown. The first five classes (chevron halite rock, color-banded/vertically-oriented halite rock, chaotic mudstone-halite rock, equant muddy halite rock, and equant anhydritic halite rock) are fabrics arranged, left to right, from those showing the most primary fabrics to those showing the most altered fabrics. The remaining four classes of halite (displacive halite, cavity-filling halite cement, fibrous fracture-filling halite cement and replacive halite) are fabrics produced by halite introduced into sediments during diagenesis.

Chevron Halite Rock

Chevron halite rock is characterized by abundant, minute (less than 50 micron) fluid inclusions (fig. 26). Variation in the density and size of the inclusions defines relict growth faces of crystals (chevron structures), showing that the crystals grew upward as a crust on the brine-pool floor. Most crystals are elongated in a vertical direction as a result of competition for space (fig. 27). The zonation of fluid inclusions shows that most crystals grew with cube corners oriented upward. Crystals range from 5 mm tall to 5 cm tall, averaging about 2 cm tall, and have a height/width ratio of 3:2 to 4:1. Some chevron halite crystals appear to be oriented obliquely to bedding, perhaps occurring as rosettes, rather than isolated crystals (fig. 28).

Most beds of chevron halite are transected by equant halite containing a few large fluid inclusions. The equant halite is interpreted as halite cement filling karst pits and pipes (fig. 15 and 17). In some intervals of chevron halite, pits are partly filled with red mudstone.

Many, but not all, intervals of chevron halite are bedded. Corrosion surfaces which truncate chevron crystals are marked by anhydrite laminae (fig. 16). Anhydrite laminae may be horizontal or gently irregular, conforming to the shape of the truncation surface. Anhydrite occurs within and between crystals as well as in partings, and is the most common impurity in chevron halite, typically making up 1 to 5 percent of the rock. In combination with the abundant fluid inclusions, anhydrite imparts a conspicuous white color to the rock. Chevron halite lacking bedding is characterized by variable crystal size, including some unusually large crystals.

The preservation of the primary fluid inclusions is evidence that this halite has not been extensively recrystallized. Recrystallization would have caused expulsion, agglomeration, or other disruptions in the fluid inclusion distribution. The chevron zonation typically is truncated toward the edges of crystals, suggesting that some recrystallization has occurred (fig. 14, 23 and 27). This recrystallization at crystal edges may have been brought about by the same early diagenetic fluids which precipitated the anhydrite and dolomite observed along grain boundaries.

Color-Banded/Vertically-Oriented Halite Rock

Halite rock which displays the primary brine pool fabrics of vertically elongated crystals and/or bedding defined by variation in halite color but lacks the abundant well-zoned fluid inclusions typical of chevron halite is categorized as color-banded/vertically-oriented halite rock. Vertically-elongated halite grains, like those found in chevron halite, are 0.5 to 5 cm tall, average 2 cm tall, and have length/width ratios of 3:2 to 4:1. Finer halite grains are typically present in anhydritic zones. The shape of the crystals is visible on the slabbed surface of core when it has been lightly etched in water. Some crystals are rimmed with anhydrite blades which apparently replaced halite along grain boundaries during diagenesis. The anhydrite remains in relief when the halite is etched, defining grain boundaries (fig. 9). In vertically-

oriented crystals lacking anhydrite along grain boundaries, halite grain shapes can be seen by the glint of light reflected from the etched surface after it has been wiped dry. Many, but not all, halite rocks with vertically-oriented crystals exhibit bedding, expressed either as anhydrite partings formed along dissolution surfaces or as minor variations in the amount and composition of impurities included within the salt. Impurities cause the color of the halite to vary from white or clear to black or red brown and include anhydrite, mudstone, and organic material. Some intervals of halite rock with well-defined color banding have equant rather than vertically-oriented crystals. These are included in this category as part of a continuum of fabrics from vertically-oriented crystals in halite rock which lacks defined bedding to well-bedded halite rock with equant crystals.

Color-banded/vertically-oriented halite characteristically is a darker color than chevron halite, even though it may contain no higher percentage of impurities than chevron halite. There appears to be a correlation between the presence of minor amounts of clay and/or organic material and the sparse occurrence of abundant minute fluid inclusions which define the growth bands in chevron halite. It is not yet known to what extent this is due to a different depositional environment or to diagenetic destruction of fluid inclusions.

Color-banded/vertically-oriented halite, like chevron halite, commonly contains abundant vertical pits and pipes. In samples with very abundant pits and pipes, much of the primary fabric is lost, and the halite rocks are classified as chaotic mudstone-halite, or equant muddy or anhydritic halite.

Chaotic Mudstone-Halite Rock

Halite with masses of mudstone between and within halite crystals (typically 10 to 25 percent of the rock volume is mudstone) and an absence of definable bedding is classified as chaotic mudstone-halite (fig. 29). Halite crystals are coarse (0.3 to 3 cm in diameter), equant, and may express cube faces (fig. 30) or anhedral, complex corroded-appearing faces against mudstone masses (figs. 29 and 31). The mudstone masses most commonly contain anhydrite as stringers and compressed nodules which highlight the disrupted, compressed, stretched, or intraclastic fabrics characteristic of the mudstone (fig. 32). The composition of the mudstone

in chaotic mudstone-halite is petrographically indistinguishable from mudstone present in discrete beds (discussed below) and the clay minerals within halite are under study. Some of the equant halite crystals in some examples of chaotic mudstone halite have a red-brown color similar to the color of the fibrous halite which fills vertical fractures in other lithologies, but the origin and significance of the pigment has not yet been investigated.

Although chaotic mudstone-halite fabric is a common fabric in halite intervals which contain abundant mudstone, its origin is somewhat difficult to interpret because of the characteristic absence of interpretable sedimentary structures within it. Smith (1971) identified three possible origins for clastic-salt mixtures in Permian evaporites of Yorkshire, England: (1) primary precipitation of halite from a halite-saturated water body, which was then mixed with clastics during recrystallization; (2) simultaneous precipitation of halite and deposition of clastics, which were then redistributed during diagenesis; and (3) secondary formation of halite within sediment during early diagenesis or following burial. Based on the absence of sedimentary structures, Smith interpreted the Yorkshire halite-clastic mixture as forming by the third possible origin in a vadose zone in subaerially-exposed sediment. Brine was introduced by flooding from above, capillary recharge from below, or lateral recharge in response to salinity gradients. Smith suggested the term "haloturbation" for the resulting disruption of fabric. Holdoway (1978) identified chaotic mudstone-halite as the dominant texture in halite of the Permian Nippewalla Group in western Kansas. She interpreted some of those mudstone-halite mixtures in which some bedding in the enclosing mudstone is preserved and halite has euhedral shapes as forming by displacive growth of halite in soft, silty mud. Mixtures with a higher ratio of halite to mudstone exhibit a chaotic mottled texture, which she interpreted as "haloturbation" by repeated solution and precipitation of halite. Handford and Bassett (1982) interpreted the textural similarity between the Palo Duro mudstone-halite and sediments observed by Handford (1982) in Bristol Dry Lake, California, as indicating a possible similar origin, that is, displacive growth of halite crystals in brine-soaked mudstone sediment with a possible overprint of dissolution and reprecipitation. Gornitz and Schreiber (1981) describe isolated displacive skeletal halite crystals in Recent carbonate mudstones in the Dead

Sea, formed either by downward diffusion of brines under submerged conditions, or by upward diffusion of connate brines under present subaerial conditions. Mudstone in mudstone-halite-polyhalite mixtures in the Salado Formation was interpreted by Adams (1969, p. 96) as airborne dust contributed into the evaporite-precipitating environment, because of its intimate association with polyhalite deposits indicating advanced evaporation of brine.

In our studies, examples of mudstone-halite mixtures formed by a variety of methods have been identified. Most of the chaotic mudstone-halite rock abundant in the San Andres Formation appears to have a common origin as Smith's (1971) first option: primary halite altered and mixed with mudstone by diagenetic processes. However, within mudstone beds (distinguished from mudstone-halite rock because they are greater than 50 percent mudstone), clear examples of displacive growth of halite and haloturbation due to alternation of displacive growth of halite and dissolution of halite, (Smith's third option) were recognized. These features will be discussed below in the section on interbeds. Possible examples of Smith's second option—precipitation of halite simultaneously with accumulation of clastic sediment—are not well understood. Intervals of evenly distributed mudstone and finely crystalline halite (fig. 33) which lack any of the features described below for typical chaotic mudstone halite and may initially have been deposited as mixtures. The best examples of this homogeneous rather than chaotic texture are in the Artesia Group and study of them has not been undertaken. Some chaotic mudstone-halite mixtures may be due to diagenetic alteration of depositionally mixed sediments such as the intervals of finely interbedded mudstone and halite found in parts of the San Andres units 4 and 5. Typical examples of San Andres mudstone-halite are 10 to 25 percent mudstone, and, therefore, have a halite-supported fabric with isolated masses of mudstone within and between halite crystals. The high ratio of halite to mudstone, the presence of relict remnants of bedding and other brine pool halite fabrics, and examples of halite with textures intermediate between bedded brine pool halite and chaotic-mudstone halite suggest that much of the San Andres chaotic mudstone-halite rock was originally bedded halite sediment.

Relict bedding in San Andres chaotic mudstone-halite rock is defined by discontinuous zones of anhydrite in halite (fig. 34). The anhydrite is concentrated along grain boundaries or relict grain boundaries of what were originally small (0.5 cm tall), vertically-oriented crystals. Anhydrite may also occur along one or more horizontal partings truncating crystals. Other primary fabrics such as chevrons or zones of vertically-oriented crystals typically cannot be identified. Many of the vertical crystals outlined by anhydrite have been recrystallized to coarser poikilotopic crystals. The anhydrite appears altered and was possibly partially mobilized. The anhydritic beds are discontinuous through the diameter of the core, truncated against mudstone masses or vertical masses of cleaner halite; however, the continuation of similar anhydritic fabric in a horizontal direction is definite enough in some examples to lend credibility to other less defined examples of similar texture. In a few examples of chaotic mudstone halite rock, relict chevrons, or relict color banding are preserved in a few locations. Examples of isolated, frequently somewhat dish-shaped, horizontal but not laterally traceable mudstone and anhydrite beds are abundant in some beds of chaotic mudstone-halite rock (fig. 35). These accumulations are interpreted as the insoluble residue formed on the floors of karst pits. The original host halite has now recrystallized and is indistinguishable from the pit-filling halite. Vertically elongated mudstone masses are also interpreted as former pits which were filled with mudstone.

Examples of halite intermediate between bedded brine-pool halite and chaotic mudstone/halite are abundant and provide additional support for the interpreted genetic relationship between the two halite types. Figure 36 illustrates an example of color-banded/vertically-oriented halite rock, which is truncated by a mass of chaotic mudstone halite rock. The mudstone/halite appears to be filling a wide vertically-oriented pit in the color-banded halite. The genetic sequence interpreted for this example is (1) dissolution of a pit in the banded host halite, (2) precipitation of less than one centimeter of clear halite cement rimming the pit, (3) accumulation of mudstone in the pit, probably accompanied by additional dissolution of halite, disrupting any fabric present in the mudstone, and (4) displacive growth of

poorly-formed skeletal halite crystals within the mudstone, further disrupting its texture. Recrystallization of the host halite during pit formation did not occur in the example shown in figure 36, but is present in many other examples. If in either diagenetic process, pit formation or recrystallization had been more prolonged or intense and had altered fabric any further, the primary halite fabric would have been destroyed and the sample would have become chaotic mudstone halite rock.

In some chaotic mudstone-halite, partial dissolution of halite crystals along grain boundaries and halite-mudstone contacts accompanying recrystallization may have removed halite and aided in disruption of such fabric. Partial dissolution of halite would increase the ratio of mudstone to halite. The corroded appearance of mudstone halite contacts and disrupted, collapsed, and soft sediment microfaulted textures in mudstone beds and masses affirm the importance of halite dissolution (figs. 29 and 31). However, euhedral and skeletal halite-mudstone boundaries and textures in mudstone masses which appear compressed indicate that displacive growth of halite is an important process (figs. 30 and 32). The highly disrupted fabric characteristic of most chaotic mudstone-halite suggests that an alternation of both dissolution and displacive growth processes during diagenesis, as was described above for the well-preserved sample shown in figure 36, may be common.

Equant Muddy Halite Rock

Equant, muddy, halite rock is a catchall class for halite with no identifiable primary fabric and no evidence of the kind of intense alteration which has affected chaotic mudstone-halite rock. Halite crystals are equant, with average to coarse crystal size (1 to 5 cm). A minor amount (1 to 10 percent) of mudstone is present, but it is not concentrated in pits or in beds (fig. 37). In many examples, anhydrite is present in indeterminate amounts. Samples of halite which contain enough mudstone to pigment the halite red-brown or dark gray are included in this class. The origin of this equant fabric in halite is not clear, but probably all intervals identified as equant muddy halite rock do not have the same origin.

Equant fabrics can form as a result of recrystallization of halite with primary fabrics. Examples exhibiting vertical and horizontal gradation from color-banded/vertically-oriented halite to equant halite which recrystallized under the influence of waters penetrating along grain boundaries or along now-obsolete fractures provide evidence of this process. Clay or gypsum co-deposited with halite may have released enough water during diagenesis to recrystallize halite. Alternatively, equant fabrics may be primary, not recrystallized. Equant halite crystals and absence of recognizable bedding surfaces is common in chevron halite. Equant crystals are also found in many examples of color-banded halite. If the particular conditions which created the chevron zones or the dark bands were absent, primary brine pool origin of chevron and color-banded halite could not be recognized. Equant halite is found within well-defined beds in Permian salt of the Paradox Basin, Utah (R. J. Hite, verbal communication, 1983). San Andres equant halite fabrics formed in primary precipitates cannot be petrographically discriminated from fabrics formed by diagenetic recrystallization.

Equant Anhydritic Halite Rock

Equant anhydritic halite rock is similar to equant, muddy halite in its absence of identifiable fabric but lacking mudstone other than trace amounts (fig. 38). Like equant muddy halite rock, the extent to which textures are recrystallized or primary cannot be determined in most examples by methods used in this study. Lateral and vertical gradation of chevron halite rock into equant anhydritic rock is commonly observed. Increased intensity or duration of the diagenetic processes can alter chevron halite to equant recrystallized halite. In equant anhydritic halite formed by recrystallization of chevron halite relict primary fabrics, such as corroded remnants of chevron texture in a few grains, concentrations of insoluble components marking former pit floors and discontinuous anhydrite partings defining bedding are identifiable.

Most of the thin intervals of halite with a pink or orange color have equant anhydritic halite fabric. A recrystallization origin, due perhaps to the diagenetic fluids responsible for the pink or orange color (polyhalitization/iron oxide staining), is tentatively proposed for these samples. Most possible polyhalitic rocks have some relict primary fabrics such as sulfate

partings or sulfate outlining relict vertical crystals, but lack chevron fabric or color banding. Petrographic and geochemical studies of these samples are underway to resolve questions about mineralogy and diagenetic alterations.

Examples of equant anhydritic halite of apparently primary origin are also abundant. Most chevron halite has zones of equant, clear crystals above anhydrite partings and below the chevrons (fig. 39). These clear zones may have been slightly altered during diagenetic release of the waters of hydration from the probable original gypsum in the parting as it dehydrated to anhydrite. However, the stratiform character of the clear zones suggests that the origin of the texture is a stage of precipitation of clear equant halite before precipitation of halite with chevron fabric. This indicates that, if the right conditions exist, primary equant halite can be precipitated in ordinary San Andres environments. Crusts of subhedral to euhedral halite crystals have been observed forming in the bottom of the restricted estuary, Bocana de Virrila, Peru (Brantley and others, 1984).

Displacive Halite

Displacive halite, in contrast to the halite rock types discussed previously, is a minor element in other lithologies such as mudstone and siltstone interbeds within halite rock. Displacive halite also occurs in anhydrite beds within, beneath, or overlying halite rocks, and in a few locations is found within carbonate rocks close to halite. Displacive halite forms cubes (fig. 40), slightly skeletal crystals (hopper crystals) (fig. 41), and extremely skeletal crystals (fig. 42). Displacive halite is similar in morphology and occurrence to displacive skeletal crystals described by Gornitz and Schreiber (1981), but lacks the very fine skeletal fabrics described by Southgate (1982), probably because of the coarser grain size of the host mudstone in the San Andres. Matrix mudstone is typically too highly disrupted to reveal the displacive character of the halite (fig. 41). In well-bedded examples, deformation of adjacent beds due to displacive growth of the halite crystal can be identified. There is a tendency for the halite crystals to be nucleated in the more clay-rich laminae of the sediment (fig. 42). This is not expulsion of clay during growth of the halite crystal as postulated by Holdaway (1978), but

halite nucleation apparently controlled by preexisting variation in grain size of the host sediment.

Halite Cavity-Filling Cement

Halite cavity-filling cement is most abundant in karst pits. In these locations the crystals can be extremely coarse, in many examples larger than the 10 cm core width (fig. 43). The presence of some pits is deduced from an interval of very coarse halite. The halite cavity-filling cement is typically clear, impurity-free halite with large fluid inclusions. Impurities associated with the halite are the insoluble residue materials, anhydrite and mudstone, which fell into the pit as cement was precipitating and define the pit floor (figs. 20 and 21). In some cases, it is difficult to determine how much of coarsely crystalline halite was formed as cement and how much originated as finer halite which has been recrystallized, a problem analogous to discriminating between cement and neomorphic spar in carbonates.

Halite occurs as a pore-filling cement in all other lithologies. Halite-filled pores are abundant in clean sandstone and carbonate grainstones (fig. 44). The cement is poikilotopic with crystals up to 3 cm across. Halite cement in nonhalite rocks may have been deposited under very different conditions than halite cement in pits within halite rocks, because of the potential differences in timing of precipitation.

Fibrous Fracture-Filling Halite

Fibrous, fracture-filling halite is common throughout the halite section, especially in mudstone interbeds within halite rock (fig. 45). It also occurs within fractures in carbonate rocks and dark, anhydritic mudstone beds at the base of cycles. Halite-filled fractures have not been observed in anhydrite beds.

The fibrous, fracture-filling halite is very similar in appearance in all lithologies. It characteristically has a red to deep orange color. All fractures have a vertical orientation. Most fractures do not appear to widen upward toward paleosurfaces, indicating that they are formed in the subsurface. A few examples examined in thin section (fig. 46) are tentatively believed to have formed later than most diagenetic features, such as multifaceted dolomite and

anhydrite, but before precipitation of these phases ceased, constraining the timing of fibrous halite precipitation as the last early diagenetic process.

Halite As A Diagenetic Replacement of Other Minerals

Halite occurs commonly as a diagenetic replacement of other minerals in San Andres rocks. Halite pseudomorphs after gypsum crystals in anhydrite matrix are very common in San Andres anhydrite rocks (fig. 47). Preservation of fine anhydrite laminae within many of the pseudomorphs indicates that the replacement of gypsum by halite took place without formation of void space; therefore, the halite is a replacive, as distinguished from a cement, texture. No evidence of collapse or geopetal fabrics, which would indicate formation of void space prior to halite precipitation, have been found in anhydrite. The replacement of larger gypsum crystals by halite is identified as one of a series of early diagenetic events during deposition of the cyclic evaporite (Fracasso and Hovorka, 1984).

Halite-filled molds of ooids and skeletal grains are common in carbonates (fig. 44), but the extent to which this is halite cement precipitated in a mold formed by dissolution of aragonite or is replacement of aragonite without formation of a void has not been determined. Oomolds in which the cube corners of the halite filling are visible suggest that, at least minor replacement of carbonate by halite is possible, because the mold formed by dissolution of the ooid would have been round. No examples of preservation of fine structures within halite-filled ooids or skeletal grains have been identified to confirm that entire grains can be replaced.

Interbeds Within Halite

Accumulations of non-halite components within halite rock are identified as interbeds if they are interpreted, based on continuity through the slabbed core, to be areally extensive features representing episodes of accumulation of materials other than halite. An attempt has been made to discriminate between areally extensive interbeds and local features, such as mudstone fillings in pits and insoluble residues in pit floors. For this study, interbeds of any thickness were identified, including partings less than one millimeter thick.

Terrigenous clastic mudstone and anhydrite are the materials which make up most interbeds. A few siltstone and claystone interbeds have been identified. Mixtures of materials, such as anhydrite nodules and displacive halite crystals in mudstone, mudstone disseminated in anhydrite, or composite mudstone-anhydrite beds with a layer of one material on top of the other are common.

Mudstone Interbeds

Composition of Terrigenous Clastic Mudstone.--The mudrock classification of Folk (1974, p. 30) is used in discriminating between siltstone, mudstone, and claystone. Siltstone has greater than 67 percent silt-size grains, claystone has greater than 67 percent clay-size grains, and mudstone is composed of the subequal amounts of silt and clay-size material. A few grain size analyses of samples from a variety of Permian sediments suggest that many of the rocks visually identified as mudstone are silt rich and may actually be muddy siltstones (Seay Nance, verbal communication, 1984). Three grain-size analyses of San Andres mudstones (Table 4) showed a range from 73 to 57 percent silt. Petrography of thin sections of halite rocks and interbeds in halite rock through the San Andres interval in three wells (DOE-Gruy Federal No. 1 Grabbe, Stone and Webster No. 1 Mansfield, and DOE-Gruy Federal No. 1 Rex White, Appendix 1) indicates that the mixture of silt and clay-size material is present in almost all mudstone beds.

The grain-size distribution of siliciclastic sediments in the San Andres appears to be similar to other Palo Duro Permian sediments (Kolker and others, in prep) in that the most abundant grains are coarse silt size. Fine and very fine sand is present in the thick clastic intervals, but coarser sand grains are sparse. Clay-size material and the finer silt sizes are rare in comparison to the large amount of coarse silt. A mechanism of eolian transport is suggested to explain the unusual coarse silt-rich grain-size distribution. Kukul and Saadallah (1973) documented a similar high silt (4 to 6 phi) grain size in a variety of depositional environments in the Persian Gulf, and traced its origin to the silt-rich dust storms which transport an estimated 2 centimeters per year of sediment into the area. Regional facies relationships and

sedimentary evidence is presented by Kolker and others (in prep.) that clastic environments marginal to many of the Palo Duro evaporite environments have a dominant eolian influence. An eolian contribution might therefore be expected in clastics interfingering with evaporites.

Petrographic examination of typical examples of mudstone show that the silt fraction is dominantly angular quartz grains with approximately 10 percent orthoclase feldspar (fig. 48). A few percent opaque grains, petrographically identified as "ilmenite/magnesite, limonite, hematite and leucoxine" and trace amounts of muscovite, chlorite, and biotite are present in the silt fraction. Microprobe analysis of the silt-size fraction of one sample confirms this mineralogy (Seay Nance, verbal communication, 1984). Kolker and others (in prep.) studied sandstones and clean siltstones through the entire Permian evaporite section and documented a quartz-rich lithic arkose composition. The average quartz:feldspar:rock fragment ratio for 33 samples is 72:19:9. The compositional variations through the evaporite section are minor, indicating stability of clastic source areas. It is predicted that additional study will show similar compositional homogeneity of the silt-size material in the mudstone. The clay fraction is composed of fine, felted to optically aligned clay with low to moderate birefringence and, typically, a deep-red stain. The clay mineralogy of the evaporite section has been studied by Bassett and Palmer (1981). Clay minerals identified in thirteen samples in mudstone beds within the San Andres Formation include chlorite-smectite mixed layer clays, corrensite (swelling chlorite), vermiculate-chlorite mixed layer clays, and chlorite. Illite is present in all samples. The same clay assemblage that is found in clastic beds occurs in mudstone impurities in halite rock (S. Fisher, verbal communication). The clay assemblage is interpreted as representing diagenetic alteration of detrital clays in high-Mg evaporite brines.

Most of the Permian clastics have red brown colors (10R4/6, 10R5/4). In thin section, the red color appears as a stain, presumably iron oxides, associated with clays. In clean sandstone and siltstone, the pigment occurs in thin clay coats (cutans) on siliciclastic grains. Interbeds and mudstone masses within salt generally have darker grayish red colors (10R4/2) than thicker mudstone intervals, perhaps indicating slightly more reducing conditions.

Mudstone and siltstone with gray, green, or black colors are abundant within the salt section as beds and mottles with red sediments. Areas with the more reduced colors appear in thin section to be identical to the adjacent red sediments, except for the absence of stain in the clays. Reduced colors are probably due to slightly less oxidized diagenetic microenvironments. Pyrite or organic material are rare as pigmenting agents in San Andres clastic-halite sequences, although they are common within carbonate-anhydrite intervals. Pyrite is common in black anhydritic mudstones residues between the halite at the top of one cycle and the carbonate or anhydrite at the base of the next cycle. The pyrite is presumed to have formed in response to diagenetic conditions established during deposition of the overlying carbonate or anhydrite. The total organic carbon of two samples of one dark mudstone bed at the base of San Andres unit 4 in the DOE-Gruy Federal No. 1 Rex White core was 0.10 and 0.16 percent (S. Dutton, 1980; unpublished report from GeoStrat).

Sedimentary Structures in Terrigenous Clastic Mudstones.---Mudstones in the San Andres Formation typically have a highly disrupted fabric. Out of the approximately 100 discrete mudstone beds or partings within the San Andres unit 4 halite, each of the seven cores examined, 3 to 13 beds have well preserved sedimentary structures, and a similar number have disrupted fabric in which remnant bedding is preserved. The remainder are homogenized or are composed of unsorted, unoriented intraclasts with poorly defined shapes (fig. 41). This fabric is described as disturbed intraclastic fabric. The most abundant preserved structures are small-scale (1 to 5 mm) ripple cross-laminae in siltstone or muddy siltstones alternating with thin mudstone or claystone drapes (figs. 49 and 50). Some of the thicker, siltier clastic beds, notably the "pi" marker bed in the upper San Andres, contain abundant microscour features, up to 1 cm deep and a few centimeters across, and associated size-sorted and imbricated granule to coarse sand-size claystone rip-up clasts. In most mudstone interbeds, the grain size contrast between the rippled material and the drape material is small enough so that rippleforms are poorly defined, but scours appear to be minor or lacking. Parallel stratification is fairly common in mudstone and muddy siltstone, but the fabric is not well-defined enough to determine whether

this is real parallel lamination due to vertical accretion or translent strata formed by ripple migration. Graded bedding has not yet been identified in core or thin section. In the San Andres Formation, mudstone interbeds in halite with preserved fabric tend to be part of a sequence of thin clastic beds with preserved fabric, interbedded with thin beds of halite also with preserved fabric (fig. 51). The tops of some thick mudstone beds are ripple laminated above the lower disrupted part (fig. 52). In many beds, zones of disrupted intraclastic fabric alternate with well-preserved structures.

The origin of the disrupted fabric is not obvious in most samples. Disrupted fabrics in San Andres mudstones might be attributed to burrowing or to intraclastic fabrics interpreted as rip-up conglomerate. Evidence collected in this study suggests that the origin of most, if not all, of the disrupted intraclastic fabric in San Andres mudstones is due to displacive growth of halite and/or collapse after dissolution of halite, a process known as haloturbation. Although modern halite-saturated environments can contain abundant organisms such as brine shrimp, no evidence of such organisms, such as fecal pellets or well-preserved burrows have been found in Palo Duro halite rocks or in interbeds within them. It seems unlikely that burrows would only occur in the most highly disturbed strata, and never in isolated occurrences where the diagnostic burrow fabrics could be clearly recognized. A rip-up clast origin is also rejected for most San Andres mudstone beds with disrupted fabrics, because they lack the diagnostic features of rip-up clasts. The poorly defined intraclasts exhibit no trace of sorting by clast size and have no horizontal or imbricated preferred orientation. The clasts are most commonly the clean silt fraction in a more clay-rich mudstone matrix. In normal rip-up clasts, the clasts are claystone or mudstone, because of the greater cohesiveness of unlithified clayey sediments. Small size-sorted clay rip-up clasts are recognized in a few intervals as discussed above.

Evidence for the origin of San Andres (disturbed) intraclastic fabrics by haloturbation is:

- (1) the adjacent facies relationships between disturbed intraclastic fabric and bedded halite and
 - (2) the presence of partially disrupted fabric in which a sequence of events can be reconstructed.
- The more elastic-rich formations in the section show large-scale facies sequences in progress and current status of research and tentative conclusions reached. Interpretations and conclusions are based on available data and state-of-the-art concepts, and hence, may be modified by more information and further application of the involved sciences.

This report describes research carried out by staff members of the Bureau of Economic Geology that addresses the feasibility of the Palo Duro Basin for isolation of high-level nuclear wastes. The report describes the progress and current status of research and tentative conclusions reached. Interpretations and conclusions are based on available data and state-of-the-art concepts, and hence, may be modified by more information and further application of the involved sciences.

DRAFT

which stratified or massive clastics vertically grade into disturbed intraclastic fabrics, then to disturbed intraclastic fabrics containing preserved halite crystals, and finally to chaotic mudstone-halite or bedded halite rock. This sequence is interpreted as reflecting increasing duration of halite precipitating conditions in an environment alternating between clastic sedimentation and halite precipitation. Halite did not precipitate in the sedimentary environment of the bedded clastics. Displacive halite crystals were precipitated during intermittent flooding of the disturbed intraclastic sediment by brine, but were dissolved during long intervening terrestrial intervals. In environments more frequently flooded by brine the chances of halite preservation within the sediment are high. Clastic sediments with displacive halite are found adjacent in the facies tract to bedded or chaotic mudstone-halite deposited where halite precipitating conditions are frequent compared to clastic input.

A similar facies relationship can be seen on a smaller scale within the San Andres where individual mudstone beds with preserved lamination generally contain few displacive halite crystals and occur in association with halite with preserved primary fabric. Preservation of sedimentary structures in both mudstone and halite indicate that the processes of displacive growth and/or collapse and dissolution of halite, which cause the process of haloturbation, had been relatively inactive in these beds (fig. 51). In comparison, intervals of mudstone with homogenized or disturbed-intraclastic texture interpreted as due to haloturbation commonly contain displacive halite crystals and are associated with chaotic mudstone-halite fabric formed as discussed previously by haloturbation processes.

Textural evidence that haloturbation is an important process in forming disrupted-intraclastic fabrics is shown in figures 52 and 53. Growth of halite crystals occurring displacively within sediments deforms initially well-stratified sediments. Small halite crystals crusting the sediment surface were dissolved during or after the deposition of the overlying sediment, leaving silt-filled molds and collapsed fabrics. More complex fabrics result from displacive growth of halite followed by dissolution. Crystals with cube faces expressed equally on all sides or which deform original stratification are accepted as evidence of displacive

growth. Casts of cubic crystals, collapse fabrics, and corroded halite masses in mudstone are interpreted as evidence of dissolution of halite. Most mudstone-interbed environments appear to have favored alternation between halite precipitation and halite dissolution, forming intensely disrupted fabrics.

Mudstone beds exhibit a variety of relationships with adjacent halite. Completely horizontal, nonpenetrative contacts between mudstone beds and host halite are rare. Typically the contact is slightly irregular and the halite and mudstone are mixed. The mixture may result from (1) deposition of mudstone over an irregular halite surface, (2) corrosion of halite during or after mudstone deposition caused mudstone to collapse into pits in the halite (figs. 36 and 48), or (3) displacive growth of halite in the mudstone (fig. 54). In most examples, the initial mud/halite relationships have been obscured by haloturbation processes. Upper surfaces of mudstone beds are also irregular in many examples. The origin of the irregular upper contacts is unclear. Displacive growth of halite within the mudstone bed before, during, or after resumption of halite precipitation of the overlying bed is one explanation.

Most mudstone beds in the San Andres Formation have been fractured and the fractures filled with fibrous red halite. Fractures have been observed in similar occurrences through the entire Permian salt section, from Clear Fork to Salado-Tansill. Fractures occur in mudstone and carbonates, but truncate against or are invisibly healed in halite and anhydrite. The fractures have a strong vertical orientation, although they may deviate in response to lithologic inhomogeneities in the host material. They may be up to several meters long and greater than the 10 cm core diameter in width. Fractures intersect at high angles, indicating that they may form polygons in plan view. The fractures do not otherwise have the same morphology as surficial desiccation cracks. They do not widen upward toward a paleosurface, but appear to pinch out to unfractured host material with equal frequency upward and downward. An additional argument against a surficial mudcrack origin is that no similar appearing features filled with any material other than halite have been seen. If these fractures were surficial features in mudstone host, some fractures should have been filled with carbonate or siliciclastic

mud sediments during flooding of the desiccated surface. The halite fillings suggest that the fractures formed in the subsurface environment where the fractures were sealed against input of detrital sediments.

The halite in the fractures is composed of fibers several millimeters in cross sectional diameter. Fibers are perpendicular to the fracture walls and may be elongated enough to extend from wall to wall of the host fracture. The distinctive red-orange color appears, in a few thin sections, to be due to red stain at the edges of the fibers. Zonation parallel to the vein walls defined by variation in the red color and the fibrous character of the vein fills suggests that the opening of the fracture may have coincided with the precipitation of the halite.

The relationships between the halite-filled fractures and other evaporites is obscure. In many examples, a fracture in a mudstone bed appears to have fractured an anhydrite nodule within the mudstone, but, where the nodule was broken, the fracture has been healed by anhydrite rather than halite (fig. 55). Where halite-filled fractures in mudstone beds truncate against the overlying and underlying halite, relationships are unclear. There is no evidence that the fracture either extended into the halite, or that there has been shear between the mudstone and halite beds to take up the differential deformation. In many cases, red fibrous halite in fractures appears to terminate into displacive, red or clear, slightly skeletal halite crystals in mudstone.

Evidence of the timing of formation of these fractures is inconclusive. The fracture walls are characteristically not perfectly parallel, indicating the sediment, once fractured, was able to deform plastically as the fracture opened but the fractures have not been deformed by compaction. The halite in some fractures contains diagenetic replacive anhydrite and multifaceted dolomite similar to that which occurs in most other halite. These diagenetic minerals are typically small, and sparse or absent, however, as if the fracture filling halite formed during and not before completion of the phases of diagenesis during which these minerals precipitated. However, if the fibrous halite-filled fractures in the carbonates have a common origin with the similar appearing fractures in the mudstone interbeds in halite, the

fracturing must have occurred after the carbonate was removed from its depositional environment. Halite could have been supplied from brine pools some tens of meters or more above the fracture. Alternatively, halite could have been supplied at any time by brines squeezed from adjacent sediments. A study of the orientation of these fractures based on Fracture Identification Logs indicates that they have the same preferred orientation as fractures of other kinds (E. Collins, verbal communication). The timing of formation of halite veins has been further discussed by Luneau (in prep.).

Dark Anhydritic Mudstone Insoluble Residue.---Mudstone beds occur at the contacts between halite at the top of one cycle and the carbonate or anhydrite at the base of the next. Although in reconnaissance studies the mudstone at the base of cycles appears to be compositionally similar to other mudstone beds in halite, it differs in that it is colored gray or black and contains more anhydrite in nodules, beds, or wisps than most mudstone beds. The fabric is strongly disturbed, although horizontal bedding defined by compositional variations is present. Disruption, in most cases, is extensive enough that little fabric can be identified. Structures such as disrupted ripple laminae, soft sediment microfaults, folds, and apparent load casts can be seen (fig. 56 and 57). The upper part of some base of cycle black mudstone beds is ripple laminated. Migration of ripples deposited distinctive 1- to 3-mm thick lenses of silt in a dark mudstone matrix (fig. 58). No scour is apparent at the base of ripples. Similar structures characteristically occur also in overlying carbonate mudstones indicating continuity of depositional processes. The upper part of the mudstone at the base of unit 4 is fissile and appears to have a high organic content. Textural characteristics and facies relationships suggest that a significant part of the mudstone accumulated as a residue left as halite dissolved in the near normal salinity waters introduced during transgressions during initiating the overlying cycle. The mudstone and anhydrite, deposited as interbeds or as disseminated masses, within the halite was concentrated when the host halite dissolved. Soft sediment deformation, which took place as the residue draped over the irregularities on the surface of the underlying corroded halite, is diagnostic of this method of accumulation. Bedding in the residue is defined by variations in

sediment composition formed due to original variation in the proportion of impurities in the source bedded salt. Anhydrite, in most examples, appears to have been partly mobilized during diagenesis and forms beds of small nodules, a fabric not present in the preserved halite (fig. 59). Discrete, coherent mudstone and anhydrite originally present as interbeds within the halite were included in the residue following dissolution. If such interbeds were thick, they may be the dominant component in the residue, which then appears to be red clastic beds or anhydrite beds deposited in the base of the next cycle. The only feature which allows identification of these former interbeds is the overlying residue from the beds of halite rock initially deposited in the top of the interbed but this residue may be thin or difficult to identify.

The distribution of dark anhydritic mudstone beds is the second factor in identifying them as insoluble residues. These beds have some strong compositional similarities to the red or gray mudstone beds within the halite because they are derived from such beds; however, the occurrence of dark color, bedding defined by compositional variation, and higher than average anhydrite content corresponds, in almost all cases, to beds beneath dolomite or thick anhydrite beds at the base of cycles. The thickest residue beds in the San Andres occur beneath the San Andres unit 4 carbonate, which is thick and contains evidence of deposition under normal marine conditions, such as diverse fauna, abundant burrows, brachiopod shells with intact spines, and early generations of carbonate cement (Hovorka, 1983; Fracasso and Hovorka, 1984). Residues beneath sparsely burrowed, rippled dolostone deposited in more hypersaline waters are thinner, characteristically a few tens of centimeters. Comparative residues beneath thick anhydrite beds deposited in moderately saline brines are typically 10 cm or less in thickness, and residues may be nonexistent beneath thin halitic anhydrite beds deposited by brines which were close to halite saturation. This relationship between the thickness of the dark anhydritic mudstone and the lithology at the base of the overlying cycle is additional evidence that the mudstone accumulated as a residue after dissolution of halite. More normal marine carbonate producing waters apparently dissolved more halite than more hypersaline anhydrite precipitating waters and, therefore, thicker residues accumulated beneath them.

Another factor contributing to the amount of residue accumulated is the amount of impurities within the salt. An example of a residue which is thick because the halite which dissolved to form it contained a high percent of insoluble material occurs at the base of the third cycle within San Andres unit 5. Several discrete anhydrite beds make up over half the thickness of this residue. The dissolved halite contained a high insoluble content in the form of anhydrite beds. Discrete mudstone beds which originated as interbeds in halite can be identified in some residues. Distinguishing between the residues formed by dissolution of thin sequences of halite with a high percentage of impurities from residues formed by dissolution of thicker sequences of purer halite is difficult.

A third factor which may contribute to the formation of the dark mudstone at the base of cycles is the addition of new clastic material to form the rippled or fissile tops of many dark mudstone beds. Hite (1968) has interpreted black shale in the cyclic evaporitic Hermosa Formation in the Paradox Basin of Utah and southwestern Colorado to have formed because of increased transportation of clastics during maximum transgression. Because Paradox cycles include both a transgressive and a regressive phase, the black shale was deposited on top of the carbonate of the transgressive phase, so dissolution of halite is not a contributing factor in this situation. Hite (1966) described anhydritic insoluble residues formed by the initiation of the transgression that ended halite deposition and initiated anhydrite deposition. In the Palo Duro San Andres, however, transgressive deposits did not accumulate to separate dark mudstones from insoluble residues. The anhydritic black mudstones may be partly equivalent to the Paradox model, with the lower part of the mudstone formed as an insoluble residue during initiation of transgression, and the upper part formed by transportation of clastics into the basin during maximum transgression. Alternatively, the rippled tops of the San Andres dark anhydritic mudstone beds could have been formed by reworking of insoluble residue mudstone within the basin. Adams (1969, p. 102) has discussed a similar residue/transported origin for thin magnesite-terrigenous clastic beds beneath thick anhydrite beds in the Salado Formation of the Delaware Basin.

Composition and Fabric of Anhydrite Interbeds

Anhydrite beds are typically mixed with trace or minor amounts of dolomite and/or mudstone; some beds are anhydrite/halite mixtures. The fabric of anhydrite interbeds has been mostly destroyed by diagenetic alteration. Beds thicker than about 30 cm typically have fabrics resembling the anhydrite part of the San Andres evaporite cycle, most typically laminae and halite pseudomorphs after large vertically oriented gypsum crystals (fig. 58). Very thick anhydrite beds in San Andres unit 5 contain the moderate salinity facies represented by dolomite and nodular mosaic anhydrite. These units are best thought of as the lower part of well-developed cycles rather than interbeds within halite, and are discussed in more detail by Fracasso and Hovorka (1984). The upper approximately 30 cm of anhydrite beds beneath halite typically have a strongly altered, variable fabric. Coarse blades of anhydrite floating in halite matrix, weakly defined contorted bedding, large masses or eyes of halite between contorted beds, and small halite pseudomorphs after gypsum in halite matrix, defined only by thin rims of anhydrite which outline the pseudomorphs are typical fabrics in these anhydrite-halite transition intervals (figs. 60 and 61). In thin anhydrite beds, these anhydrite-halite transition fabrics may make up the entire bed. These fabrics appear to be due to extensive replacement of sulfates by halite. A model is proposed for the origin of such replacements, based on the consistent occurrence of these fabrics at the halite-anhydrite transition, where early reaction between sulfate sediments and halite saturated brines in the overlying brine pool occurred. The initial sediment was gypsum sand or mud, similar to that which commonly served as matrix to large bottom-nucleated gypsum crystals. Rationale for interpreting the origin of sulfates as gypsum rather than anhydrite is the presence of recognizable pseudomorphs after twinned gypsum crystals in many intervals, and the prevalence of gypsum as the precipitated phase in analogous subaqueous environments (Schreiber, 1978). The gypsum sediment began to dehydrate to anhydrite in the shallow burial environment in response to increasing salinity which favors anhydrite over gypsum (Bock, 1961; Herrmann and others, 1973). When the salinities of the overlying water body increased to halite saturation, the interstitial waters depleted in CaSO_4

became capable of dissolving any remaining gypsum in the sediment and precipitating halite. The details of the mechanism by which this replacement occurs have not been determined. The sulfate which had already dehydrated to anhydrite was stable enough to be preserved because of its slightly lower solubility compared to gypsum in halite-saturated solutions. Therefore, the uppermost gypsum sediments, which had little time under burial conditions to dehydrate before halite precipitation began, have been extensively replaced by halite. In comparison, in sediments a few decimeters below the top of the anhydrite, only the large gypsum crystals, mostly the bottom-nucleated, twinned crystals remained to be replaced by halite. In bedded or nodular anhydrite a few meters from the top of the anhydrite bed, little or no gypsum remained at the time halite precipitation began in the overlying brine pool and, therefore, these sediments contain little halite. Preservation of fine textures within many pseudomorphs is the evidence that the gypsum-to-halite transformation occurred as a replacement process rather than by a dissolution-cementation process involving development of a void space by dissolution of gypsum and subsequent fill by halite cement.

Mixtures of siliciclastics with anhydrite are common. Thin mudstone beds, interpreted as insoluble residues, occur at the base of many anhydrite beds. These are reduced to gray colors beneath most thick anhydrite beds, but may have preserved red colors beneath thin anhydrite beds. Mudstone beds at the top of anhydrite beds are also common. Mudstone beds in this position exhibit complex fabrics. Anhydrite may be mixed with mudstone as nodules, as laths of anhydrite in mudstone, or as poikilotopic mosaic cement. Mudstone typically occurs as masses in anhydrite. Mudstone fills cavities which resembled small karst cavities and collapsed halite pseudomorphs after gypsum. Halite in skeletal displacive crystals further disturbs the fabric in many of these beds.

Strongly irregular bedding surfaces have been observed in some fairly thin (one meter thick) anhydrite beds within halite. Core with nearly vertical division into two lithologies has been found. Anhydrite with halite matrix makes up one side of the core; halite with discontinuous anhydrite or mudstone partings or masses occur in the other (fig. 62). These

features are interpreted as pits or enlarged fractures in the anhydrite host filled with halite. Bedded halite overlies these features. Several anhydrite beds with irregular bedding surfaces due to collapse into pits in the underlying halite were cored (fig. 63). The pits in the halite are filled with mudstone insoluble residue and collapsed blocks of anhydrite; the remaining voids are filled with halite cement. Structures in the example shown indicate that the formation of the pit in the halite was going on contemporaneously with deposition of anhydrite. The bedding surfaces in the anhydrite, covered with small pseudomorphs after bottom-nucleated gypsum are tilted from their initial horizontal orientation to near 45 degrees at the base of the bed. The dip of the bedding decreases upward until the uppermost bed is nearly horizontal.

A third type of irregularity in anhydrite beds appears to be a growth fabric, where beds of gypsum with bottom-nucleated gypsum crystals produced mounds as sediment accumulated. The gypsum crystals in these beds have a radial orientation perpendicular to the deformed bedding. There is no evidence that any type of soft sediment deformation produced these mounds, and no evidence of a contribution by algal activity. Preservation of primary fabric within the mounds is good. The mounds appear to be a growth form of laminated gypsum host with bottom-nucleated blades of gypsum.

PART II: STRATIGRAPHIC CROSS SECTIONS

Correlation of Zones of Clean, Anhydritic, and Muddy Halite

Within San Andres Unit 4

Stratification of San Andres halite is defined by conspicuous zones of abundant mudstone interbeds and chaotic mudstone-halite alternating with zones of dark- or light-colored halite lacking mudstone interbeds. Detailed logging allows description of these zones.

Zones with abundant mudstone interbeds and chaotic mudstone-halite are 30 cm to 3 m thick, averaging 1.3 meters. A few mudstone beds occur isolated within clean halite, but commonly, mudstone beds are concentrated in some intervals and absent from others. Most

beds of chaotic mudstone-halite also occur below or within zones of abundant mudstone beds. The most common halite fabric between mudstone beds is dark halite with vertically oriented crystals. Equant muddy halite and equant anhydritic halite occur less commonly in the muddy zones. The average composition of these zones is estimated as 5 to 15 percent mud, 0 to 5 percent anhydrite, and 80 to 95 percent halite. Most of the mudstone is in interbeds and as masses in chaotic mudstone halite; some is present in pit floor residues, pit fills, and disseminated mudstone in cleaner halite. Anhydrite interbeds are present in some zones; in other zones anhydrite is present along halite crystal boundaries or as nodules in mudstone beds and masses.

Zones lacking mudstone interbeds are 60 cm to 4.3-m thick, averaging 2.2-m thick. Halite brine pool fabrics, including chevron halite and color banded-vertically oriented halite, are the most common fabrics in these zones. Abundant pipes and pits result in intervals in which brine pool fabrics grade laterally into recrystallized equant halite textures. Horizontal beds of halite with equant anhydrite and equant muddy halite fabrics may be depositional textures or the result of recrystallization. Mudstone masses are abundant as pit fills in some intervals in which the texture is described as chevron halite altering to chaotic mudstone-halite or color banded-vertically oriented halite altering to chaotic mudstone-halite. Anhydrite partings are abundant in many zones, but mudstone beds are sparse. Anhydrite is also present along grain boundaries. The estimated average composition of these zones lacking mudstone interbeds is 1 to 10 percent anhydrite, 0 to 5 percent mudstone, 90 to 99 percent halite.

Two assumptions were made during the initial phases of constructing the correlations between wells and are stated here to assure reproducibility of results: (1) Anhydrite interbeds a few centimeters to a few meters thick present in each of the halite intervals logged are probably correlatable; (2) Sequences of muddy and anhydritic halite undergo only conservative changes in thickness and lithology from well to well. These assumptions are defended using the evolving San Andres depositional model. Anhydrite interbeds are interpreted as the sediments accumulated following input of lower salinity water. The lower salinity is probably related to a

slight deepening of water allowing better circulation. During the deep phases of the brine pool, minor topographic irregularities might be drowned, and the anhydrite deposited over broad areas. Anhydrite interbeds might provide a basis of correlation between cores. The positive philosophy adopted toward correlation of zones of muddy halite and anhydritic halite between cores is justified because good correlations with very little change of lithology, fabric, and thickness are possible in the carbonate and anhydrite parts of the section (Fracasso and Hovorka, 1984). Validation of these assumptions used in constructing correlations is based on the extent to which the results of the correlations conform to normal stratigraphic relationships and produce a plausible depositional model.

Initial correlations were made between the thicker anhydrite beds. In San Andres unit 4 in the Swisher County cores, a sequence of three anhydrite beds (zones 14, 16, and 26, Plate 15) provided a strong basis for correlation. A single thin anhydrite bed (zone 14) provided a probable point of correlation of the Deaf Smith cores, but the relationship of this bed with the three anhydrite beds of Swisher County was not apparent. Correlation was continued upward and downward from the anhydrite beds; zones containing abundant mudstone beds were correlated with other zones of mudstone beds. Zones of many anhydrite partings and clean halite were also correlated. Most of these correlations were made with ease.

Comparison of the clean and muddy halite zones between anhydrite beds in detail confirms that these techniques define meaningful units. Strong textural similarities within some zones indicate that the conditions within the brine pool were similar throughout the area studied. Zone 23, for example, is dominantly chevron halite with abundant anhydrite interbeds (fig. 64). There is some variation in the amount of equant halite admixed with the chevron halite and in the distribution of anhydrite partings. The No. 1 Harman core is almost all chevron halite with dark color bands and anhydrite partings at the top and bottom. Bedding in the middle of the intervals is weakly defined by discontinuous anhydrite partings. A mudstone parting is present at the top zone 23, the distribution of halite textures is similar in the No. 1 Zeek core, except that the upper and lower intervals with dark color bands and abundant

anhydrite partings are thicker and the poorly bedded chevron halite correspondingly thinner. The mudstone parting at the top of the interval in the Zeeck core does not appear to be in exactly the same stratigraphic position as any of the mudstone partings in the Harman core and might be a residue on the floor of a pit which cuts out any correlative mudstone partings. The No. 1 Grabbe core differs from the other two in that the upper part of the interval is equant muddy halite. Discontinuous anhydrite partings and patches of relict vertical crystals through the interval suggest that it may originally have had a bedded texture like this interval in the other two cores, but have lost primary fabric during diagenetic alteration.

The correlation of many zones of muddy, anhydritic and clean halite follows easily after defining and aligning a few marker beds. Correlation of individual beds within the zones is difficult or impossible, because there is enough lateral variability so that the number, thickness, and character of the beds is different in each core. For example, zone 24, San Andres unit 4 halite, between the No. 1 Zeeck and No. 1 Grabbe wells is clearly defined (fig. 64). The thick mudstone bed has similar thickness and bedding character in both areas, but the number and spacing of the thin mudstone beds, mudstone partings, and anhydrite partings varies. Two interpretations of correlations of anhydrite partings are shown in figure 65. Correlation A of figure 65 shows an interpretation where the rate of sediment accumulation is the same in both cores, with the difference in the thickness of the section due to dissolution of halite during deposition of the mudstone bed. Correlation B of figure 65 shows an interpretation where the sedimentation rate was faster in the Zeeck core than the Harman core during deposition of the upper part of the salt. Both interpretations are reasonable and no evidence to suggest one is more likely than the other has been identified. Most correlations on a scale finer than the meter thick zones have this degree of uncertainty.

Other zones show greater textural variability, but are still identifiable both on the percent composition log and the sedimentary structures log as zones of relatively clean halite between muddy zones. Zone 21 in San Andres unit 4 is an example of a somewhat variable, but still traceable zone (fig. 66). In the No. 1 Harman core, zone 21 is composed of chevron halite

with anhydrite partings and interbeds, extensively replaced by chaotic mudstone halite in a pit filling and coarsely crystalline anhydritic halite in a bed or pit fill. In the No. 1 Zeeck core, the equivalent stratigraphic interval is well bedded chevron halite and equant anhydritic halite with abundant anhydrite partings. In the No. 1 Grabbe core, the equivalent interval is muddy and anhydritic equant halite with small areas of preserved primary fabric. A more muddy zone in the middle of the interval is chaotic mudstone-halite.

Some of the reasons for lateral variability in halite can be interpreted from the relationships shown in figure 67. The thinning in zone 25-24 of San Andres unit 4 halite in the Zeeck core is interpreted as being due to dissolution of the upper part of the halite during the minor transgression which produced the overlying anhydrite bed. Evidence that dissolution is the process most likely responsible for thinning is the presence of a mudstone residue at the base of the anhydrite while the thicker halite sections lack mudstone at the base of the anhydrite. Occurrence of the thin halite and residue corresponds to a thick overlying anhydrite bed, suggesting that more dissolution may have occurred in response to a phase of sulfate precipitation which was either more prolonged or had a higher rate of sedimentation. The exact amount of salt dissolved cannot be calculated because of the gradational contact of the fairly clean halite of zone 25 with the underlying sequence containing mudstone beds.

Another style of lateral variability is demonstrated in zone 19 of the San Andres unit 4 halite (fig. 68). In the Harman and Grabbe cores the interval is dominantly muddy and anhydritic equant halite with scattered evidence of brine pool deposition capped by a 30-cm thick mudstone bed with a disrupted fabric and abundant anhydrite nodules. The equivalent interval in the Zeeck core is chaotic mudstone-halite in the upper half and vertically oriented color banded halite in the lower half. The mudstone bed at the top of the interval is three times as thick as the equivalent mudstone in adjacent cores and is interpreted as being genetically related to the presence of chaotic mudstone halite. More mudstone may have been contributed to the area around the Zeeck core during deposition of both the halite and the mudstone bed. The geometry of this area of increased percent mud might reflect the mud

distribution pattern, but percent mud or net mud maps have not been attempted on this fine a scale. Alternatively, the accumulation of the thick mudstone may have been accompanied by intense pit formation and diagenetic alteration of the underlying halite to form chaotic mudstone-halite might be local features intersected by the well, perhaps as small as a few tens of centimeters in diameter.

The relationships between regionally extensive beds in zone 14 and zone 16 and the intervening halite bed, zone 15, summarize some of the facies variations in anhydrite beds (fig. 69). Lateral equivalence of anhydrite and halite can be seen in the zone 16 anhydrite. Gypsum appears to have been deposited continuously in the No. 1 Zeeck area, while halite deposition interrupted gypsum deposition in the areas of the No. 1 Harman core. Textural evidence suggests that no major breaks in sedimentation or removal of large volumes of sediment occurred in either location and the intervals are the same thickness in both cores. If these statements are true, then halite was being precipitated in the Harman area while gypsum was being precipitated contemporaneously 10 miles to the southeast at the Zeeck area. The same interval of the No. 1 Grabbe core, 10 miles east of the Harman well is a thin, single anhydrite bed. This may be due to deposition of zone 17 halite as a facies equivalent to the middle and upper parts of the Zeeck zone 16 anhydrite and to the halite and upper anhydrite of the Harman zone 16. If correlations are drawn as in figure 69, the mudstone beds near the base of zone 17 in the Grabbe core are correlative with mudstone beds in zone 16 in the Harman core, but no equivalent mudstone was identified in the Zeeck core. These zone 16 and 17 mudstones appear, therefore, to be confined to the halite facies.

The zone 14 anhydrite also is thick in the Zeeck core and thinner in the more northern cores. Several feet of distinctive ripple laminated siltstone interbedded with anhydrite with pseudomorphs after bottom-nucleated gypsum indicates that the lower part of the Zeeck, zone 14 anhydrite is correlated to the entire zone 14 anhydrite in the Harman core, as shown in figure 69. The ripple laminated siltstone is not typically a part of the facies sequence, but represents a time of influx of clastic sediments into the area, and, therefore, should be

considered as more of a time stratigraphic unit than the halite and sulfate, which are deposited as facies equivalents. The anhydrite lithofacies correlations are drawn with a base representing a rapid transgression. If the subsidence rate and corresponding rate of sediment accumulation was similar in all the cores, the upper part of the zone 14 anhydrite in the Zeeck core is the probable time equivalent of the halite with abundant anhydrite partings in zone 15 of the more northern cores. This is additional evidence for the model that anhydrite partings represent influx of marine derived brines which are undersaturated with respect to halite into the halite precipitating brine pool. The fabrics of the upper part of the Zeeck zone 14 and zone 16 anhydrite has the complex fabrics of the halite-anhydrite transition, which may indicate episodic increases to halite saturation during sulfate deposition.

The relationships between zone 16 and the underlying halite appear to be due to dissolution of the underlying halite and accumulation of an insoluble residue by the same processes discussed for the zone 26 anhydrite. Stratigraphic control at the zone 16-zone 15 contact is good enough to calculate the possible amounts of halite dissolved (fig. 70). The correlation shows 6 feet of halite dissolved. The estimated composition in volume percent averages 9 percent mudstone and 3 percent anhydrite. If the halite were all dissolved from this interval, it would leave a residue 0.7 ft thick, 75 percent mudstone, and 25 percent anhydrite. The actual residue is one foot thick, 65 percent mudstone, 15 percent anhydrite, and 20 percent halite. If this is recalculated to remove halite, the residue would be 0.8 ft thick, 80 percent mudstone, and 20 percent anhydrite. This is very good agreement given the accuracy of the percent estimates and confirms the model for the origin of insoluble residues. Not all residues are this similar in composition or thickness to the halite rock from which they are derived, due to facies changes in the halite or addition or removal of residue materials by sediment transportation or diagenetic processes.

Careful examination of the relationships within the interval in the Swisher County cores with three anhydrite marker beds for good control shows that correlation of zones of mudstone beds and intervening clean or anhydritic halite conforms to normal stratigraphic principles and

with interpretations of depositional environments based on textural evidence. These zones are, therefore, traced out of the areas of anhydrite marker beds allowing the Deaf Smith County cores to be correlated with each other (Plates 15, 16). Correlation over the 31 mile distance between #1 G. Friemel core and the #1 Harman core proved possible throughout the San Andres unit 4 halite although more facies changes occurred over this distance than in the shorter distances. Zones 23 and 14 and the contact of the halite with the unit 4 anhydrite were used as initial correlations, and corresponding muddy zones matched between them (Plate 16). The 30-mile correlation between the No. 1 Grabbe log and the No. 1 Rex White log was the most difficult, and was accomplished by recognizing thin equivalents of the zone 26, 16, and 14 anhydrite beds and zone 23 halite. The correlation of muddy zones was made from No. 1 Rex White, both to the No. 1 G. Friemel log to the west and the No. 1 Grabbe log to the south. Greatest uncertainty of correlations is in the lower part of the No. 1 Rex White core, because the interval from the base of the halite to the zone 14 anhydrite is approximately 20 feet thicker in the No. 1 Grabbe core. The underlying San Andres unit 4 carbonate section is correspondingly thin (fig. 71). The relationship is, therefore, drawn with probable time transgressive lithofacies boundaries, indicating that salinities in the north reached halite saturation and precipitated halite while carbonate rocks were still accumulating 30 miles to the south and west. An alternative model approximates time equivalence of initiation of halite deposition but faster rates of halite accumulation in the No. 1 Rex White area. Detailed correlation within the unit 4 carbonate may clarify the relationships.

The overall pattern within unit 4 halite is one of lateral continuity with minor facies variation overprinted. Only a few areas of apparently more rapid local subsidence and correspondingly faster halite accumulation were identified (fig. 72). Greatest thickness of anhydrite beds is recognized in the Zeeck core and adjacent Swisher County cores, with marked thinning or absences toward the north or west. The thin anhydrite of zone 14 can be traced throughout the entire study area, an area at least 95 km east-west and 75 km north-south (fig. 73a). These units are below the resolution of geophysical logs, so the isopachs cannot be

extended beyond, or data points added between, areas where information can be obtained from cores.

The San Andres unit 4 halite in the area of core control accumulated under conditions where halite deposition was interrupted only briefly by marine transgressions contributing calcium-sulfate-precipitating brines. In unit 4 the anhydrite beds thicken toward Swisher County and pinch out toward the north and west (figs. 73a, b, c). Continued thickening of anhydrite toward the south can be recognized on regional cross sections based on geophysical logs where several anhydrite beds thick enough to be recognized on geophysical logs are identified in the next available log 14 miles south of the No. 1 Zeeck well (Fracasso and Hovorka, 1984). Examination of the anhydrite beds of San Andres unit 4, zones 14, 16, and 26 contributes to understanding of the geometry of the updip pinch-out of anhydrite beds (fig. 74). This illustration reflects facies changes in an area of extremely low depositional slope and, therefore, may not be applicable in more structurally complex areas if syndepositional deformation created steeper or complex depositional topography.

Insoluble residues are found in the downdip areas of anhydrite deposition, indicating that relatively low salinity water extensively corroded underlying halite. Residues occur in areas where bedding in the underlying halite is interpreted as having low-angle truncation relationships with the overlying insoluble residue (fig. 69). Insoluble residues are absent updip, indicating that transgressing waters were more saline, reflecting either increased salinity halite dissolved as they moved over downdip halite beds or increased salinity due to evaporation.

The top of the anhydrite beds interfinger with halite as restriction of circulation by shallowing of the brine pool by sediment accumulation increased salinity to halite saturation. Detailed correlations document halite with abundant anhydrite partings equivalent to anhydrite 10 miles downdip (figs. 69 and 74) which is interpreted as a lateral facies change. The fabric of the anhydrite deposited as a lateral equivalent of halite has the distinctive disrupted fabric with coarse anhydrite blades in halite cement discussed earlier as characteristic of the anhydrite-halite contact and interpreted as representing conditions where gypsum was immersed in halite-

saturated brine, soon after or during gypsum deposition. The lateral facies sequence in anhydrite matches the vertical sequence with the thin, farthest updip beds of anhydrite composed entirely of anhydrite-halite mixture with a disrupted fabric, while those downdip have anhydrite-halite mixture with disrupted fabric overlying bedded anhydrite with halite pseudomorphs after gypsum. The updip equivalent of the thin anhydrite beds, seen by tracing zones 14, 16, and 26 northwest into Deaf Smith County, is bedded halite with abundant anhydrite partings.

If the textural sequence, correlations of the top of the anhydrite bed, and insoluble residue mudstones are understood correctly, the base of the anhydrite bed represents rapid transgression and can be interpreted as an approximately synchronous event throughout its extent. Transgression slow enough to be represented by sediment accumulation should be recognizable by interfingering relationships between anhydrite and halite, and by superposition of normal bedded anhydrite with halite pseudomorphs after gypsum on the anhydrite-halite mixture with disrupted fabric. These relationships have not been observed, although, if they were very thin, they might have been destroyed by dissolution of halite and diagenetic overprint of the disturbed fabric anhydrite-halite mixtures by development of nodules. The interpretation that transgressions were rapid, and, therefore, a significant amount of sediment did not accumulate during transgression based on small-scale relationships observed in San Andres unit 4 anhydrite beds agrees with interpretations based on complete cycles throughout the San Andres (Fracasso and Hovorka, 1984).

The same theme of lateral continuity of lithology overprinted by local variations can be identified in the mudstone units. Some intervals of abundant mudstone beds such as San Andres unit 4, zone 6 extend over the entire study area with only minor variations in thickness and sequence. The mudstone beds in these zones have a sheetlike geometry in the study area.

CAUTION

Other intervals of mudstone such as zones have significant variations in thickness and sequence

(fig. 75 and 76). This report describes research carried out by staff members of the Bureau of Economic Geology that addresses the feasibility of the Palo Duro Basin for isolation of high-level nuclear wastes. The report describes the progress and current status of research and tentative conclusions reached. Interpretations and conclusions are based on available data and state-of-the-art concepts, and hence, may be modified by more information and further application of the involved sciences.

DRAFT

McGookey and Goldstein (1982) have presented a model for distribution of mudstone in the San Andres unit 4 halite based on gamma-ray log response in the Potter and Oldham County areas, north of the area of core control. They recognize low mudstone content in areas of more rapid subsidence, corresponding to structural lows and sediment thicks. Their model suggests that clastics might be spread fairly evenly over the area, possibly by eolian processes. The variation in the percent mudstone in the halite would then be primarily a function of how much halite was deposited to dilute the mudstone.

In the area of core control, the lateral continuity and even thickness of most correlatable zones suggest that variations in the subsidence/sediment accumulation rate in this area were minor. No relationships between high mudstone concentration and thinning of the zone have been identified. The lateral variation, instead, shows that zones defined by regionally extensive mudstone beds in some areas contain more numerous and thicker mudstone beds, resulting in areas of increased percent mudstone. This implies that the mudstone is not distributed evenly throughout the area. However, almost all zones of mudstone beds can be recognized at least in two or three other cores, so the typical distribution pattern is fairly broad. Regional control based on geophysical logs is not sufficient in density or resolution to identify the geometry of the mudstone distribution pattern of individual zones, but a broad, lobate form (fig. 76) is plausible based on available data.

It is apparent on the maps shown in figure 76 that these lobes are not stacked and that mud depocenters shifted frequently. If percent mudstone is averaged throughout the entire interval, the interference due to overlap of these lobes might produce a spotty pattern in which no trends would be identified. The map of average mudstone in unit 4 based on gamma-ray logs exhibits such a spotty pattern in this area (Ruppel and Ramondetta, 1982).

Correlation Within San Andres Unit 5

The San Andres unit 5 logs were correlated using the same techniques as unit 4 (Plate 16). The anhydrite beds in zones 14, 17, and 19 were used as datums. Anhydrite beds were assumed

to be correlatable episodes of influx of lower salinity waters. Zones of clean and muddy halite could then be correlated between wells.

Unit 5 differs from unit 4 in that it is a composite of four to seven cycles. The lowest cycle is composed of an insoluble residue in the west (zone 1), overlain by areally extensive anhydrite (zone 2), and a small remnant of halite (zone 3) preserved only in the #1 Harman and #1 Grabbe cores. The second cycle is composed of the residue at the base (zone 4), carbonate and anhydrite (zone 5), and a remnant halite (zone 6), which was removed from the Deaf Smith County area. Zone 7 is the residue at the base of the third cycle in San Andres unit 5. The third cycle carbonate-anhydrite (zone 8) is overlain by a thick halite sequence (zones 8 through 22) with a complex stratigraphy. Correlations within this halite are complex, because it contains three anhydrite beds (zones 15, 17, 19) which locally would be interpreted as the bases of cycles where they are thick with mudstone residues at their bases, but are not areally extensive. The upper cycle of unit 5 is composed of 4 to 6 m of anhydrite with complex facies changes (zones 23, 24, and 25) overlain by 0.6 to 4.5 m of halite (zone 26).

The cycles of unit 5 offer interesting examples of the possible variations in salinity gradients and corresponding facies changes. In unit 4, the facies pattern both in the carbonate at the base of the cycle and in the anhydrite interbeds within the halite part of the cycle defined a subtle but definite pinch-out of carbonate and anhydrite into halite from south to north. The thickest and probably most prolonged accumulation of low salinity facies in the area of core control centered in Swisher County. The anhydrite beds within the unit 4 halite are thin and represent the most updip deposits of marine transgressions.

Unit 5 represents changed conditions in which deposition of thin dolomite beds and thick anhydrite beds accumulated alternately with halite. Transgressions interrupted halite deposition more frequently and for longer duration than in the unit 4 halite. In unit 5, the direction from which transgressing waters were supplied shifted from the southerly direction observed in unit 4. Each cycle in unit 5 exhibits a shift in apparent source of transgressive water, including due west, southwest, south, east or southeast, and complex combinations, as discussed below.

The cycle which initiated San Andres unit 5 is composed of residue (zone 1), anhydrite-carbonate (zone 2), and halite (zone 3). The lowest salinity deposits, dolomitic anhydrite, are centered in Deaf Smith County (fig. 77), representing a source of transgression from the west of the area of core control. The #1 G. Friemel core in Deaf Smith County contains carbonate rocks, and the adjacent #1 Detten and #1 J. Friemel cores contain thicker anhydrite than the corresponding interval in the eastern cores.

The area of the lowest salinity facies in Deaf Smith County corresponds to a thin halite sequence in the top of unit 4 above the anhydrite marker bed of zone 26 (fig. 78). This thinning in Deaf Smith County is attributed to truncation of initially continuous beds in Deaf Smith County, based on application of the methods of correlating clean and muddy zones in halite (fig. 79). However, because the clean and muddy zones are correlated based on a sequence of alternations and not on characteristics specific to each zone, alternative models not requiring dissolution are possible. The thinning of the halite could be due to migration of anhydrite and carbonate facies into the Deaf Smith County area, while halite precipitation continued to the east. This model is rejected, however, because it would require slow transgression allowing accumulation of sediment as low salinity facies migrated westward. The well-preserved sequence of lithologies and fabrics in the halite at the top of unit 4 and the carbonate and anhydrite in unit 5 records no evidence of transgressive deposits. The unit 4 halite shows no evidence of interfingering with anhydrite; it contains instead many mudstone beds and intervals of chaotic mudstone-halite. The unit 5, zone 2 anhydrite and carbonate records a generally regressive salinity-increasing sequence, marked by dolomitic anhydrite overlain by nodular anhydrite, in turn overlain by laminated anhydrite.

Another alternative model requiring no dissolution of halite from the top of unit 4 would involve recorrelation of the clean and muddy zones of the thick halite of the eastern cores to individual mudstone and halite beds in the western area of thin halite. In this interpretation, a slow sedimentation rate would be responsible for thinner halite in the west. This model is rejected because the overlying anhydrite is thick in the west, which would require an

unexplained and improbable reversal of controls on sedimentation rate from slow in the west during halite deposition to fast in the west during anhydrite deposition.

Recognition of the correlation between the areas of low salinity facies at the base of unit 5 and the thin halite at the top of unit 4 suggests that dissolution during the transgression initiating unit 5 was responsible for removal of some halite at the top of unit 4. Further evidence supporting a dissolution origin for the proposed unconformable relationship is between the top of unit 4 and the base of unit 5 is the presence of an anhydritic mudstone interpretation as an insoluble residue in the area of thin halite. The anhydritic mudstone is absent in areas of thick halite (figs. 78 and 79). Dissolution as a cause for unconformable relationships between anhydrite beds and underlying halite has been discussed above for San Andres unit 4, zones 15-16 and 25-26. While in all cases an element of uncertainty remains about the original thickness of the removed halite, the mechanism of dissolution during transgression seems to be valid. The proposed model for the relationship between units 4 and 5 is (1) deposition of a complete unit 4 section (zones 27 to 31) maintaining low-angle topography and (2) transgression from the west of near normal marine water, which in the west, where salinity was low, dissolved the upper halite of unit 4 and accumulated an insoluble residue. In the east, where waters were nearly saturated with halite dissolved from the west, anhydrite deposition on halite began with apparent conformable relationships. The thickness of the anhydrite and carbonate in the west may be partly a function of creation of a topographic depression by dissolution of halite, which then could accumulate a thick sequence of sediment. Probable pinch-out toward the top of the anhydrite bed by regressive facies migration replacing calcium sulfate precipitating environments with halite precipitating environments cannot be documented, because the halite at the top of this cycle is completely altered and almost completely dissolved by dissolution at the base of the next cycle.

The second cycle of unit 5 (zones 5 and 6, Plate 17) is fairly even thickness throughout the area of core control. A relationship is observed between the presence of carbonate at the base of this cycle and the complete removal of halite from zone 3 at the top of the underlying cycle

(fig. 80). The halite of the lower cycle was preserved in the two wells in which the second cycle contains only anhydrite (No. 1 Harman and No. 1 Zeeck). The geometry of the source and circulation pattern of the transgressing waters cannot be determined based on these few points, but may have a main western and a minor southern component. It is interesting that the furthest north core, No. 1 Rex White, has absent halite and basal carbonate rocks, while halite was preserved and carbonate absent in the cores 30 miles to the south, indicating the salinity gradient was not north-south as observed in unit 4.

The second and third San Andres unit 5 cycles (zones 6, 7, and 8) exhibits complications and contradictions from the model demonstrated so far. The halite at the top of the second cycle (zone 6) is thick in Swisher County, thins to the north, and is entirely absent in the west in Deaf Smith County (fig. 81). The diagenetic fabrics in anhydrite of the second cycle in the Deaf Smith County cores indicate that halite saturated brine was present within the sediment during early diagenesis and, therefore, the second cycle (zone 6) halite is probably absent because of dissolution from Deaf Smith County rather than nondeposition. The carbonate-anhydrite of the overlying third cycle (zone 8) has an even thickness over the area of core control, but contains thick carbonate rocks in Swisher County directly overlying preserved halite (fig. 81). Thinner carbonate sequences interfingering with anhydrite are present in Deaf Smith County, where halite has been completely dissolved from the second cycle, and in the #1 Rex White core where the halite is thin. The residue thicknesses in zone 7 are variable and do not appear to correspond to the amount of halite missing. Models to explain these relationships require too much speculation to be productively discussed based on available information.

The third unit 5 cycle (zones 7 through 14) is composed of a thick sequence of interfingering dolomite, anhydrite, and halite. Within zone 8 a thin dolomite overlying the residue at the base of the cycle throughout the area is overlain by a thick bed of nodular anhydrite, except in the No. 1 Zeeck and No. 1 Harman wells, where dolomite deposition continued without interruption. The top of zone 8 contains a thicker dolomite bed capped by nodular and bedded anhydrite. This sequence probably represents two regressive, cyclic pulses,

but no halite or residue after halite is present in cored wells. At the top of the third San Andres unit 5 cycle a regionally identifiable sequence composed of a thin halite bed (zone 9) overlain by a thin anhydrite bed (zone 10) confirms the correlation at the base of the halite sequence and establishes that environmental conditions are responding in the same way over the entire area. Alternation of anhydritic halite to muddy halite to anhydritic halite can be traced between core in zones 11 through 14.

Zone 15 is a 4-m-thick section of anhydritic, chevron halite (similar to zone 23 of the unit 4 halite) throughout most of the area but in the two easternmost cores (No. 1 Rex White and No. 1 Grabbe), appears to be correlative with a 4-m-thick anhydrite bed (fig. 82). This anhydrite has a distinctive, ripple-laminated siltstone and very-fine sandstone at its base. The clastics are interbedded with the overlying ripple-laminated anhydrite with abundant, tall, well-formed halite pseudomorphs after gypsum. The lateral facies change between halite and anhydrite occurs between the No. 1 Grabbe and the No. 1 Zeeck cores, a distance of 16 km, which is a relatively abrupt change. Note that the incomplete cycle of zone 15 shows that transgressing waters were lowest salinity in the east or southeast, a change in pattern from the previous cycles.

The pair of anhydrite beds in zones 17 and 19 show an almost inverse distribution pattern (figs. 83 and 84). These anhydrite beds can be traced between most of the cores, with the greatest thickness cored in the Zeeck well, but thin toward the east. Zones 17 and 19 anhydrite beds are thin in the No. 1 Grabbe core and absent in the No. 1 Rex White core. Good correlations are possible in the anhydritic and muddy halite above these anhydrite beds (zones 20 through 22).

The uppermost cycle of unit 5, anhydrite-carbonate-halite of zones 23, 24, and 25, and overlying halite (zone 26) exhibits a complex pattern of lateral facies variation (fig. 85). The relationship with the underlying halite is also complex, but the stratigraphy in this halite is not defined well enough to interpret relationships. Several carbonate beds are present in central Swisher County, however, the thickest anhydrite section in the No. 1 Rex White core contains

no dolomite. A thick anhydrite section is also present in the J. Friemel core, but is separated from the other thick anhydrite sections by the eastern Deaf Smith County cores, both of which contain a halite interval, separating two thin anhydrite beds. The geometry of the source and circulation pattern of the transgression cannot be defined based on these few points. The abrupt facies and thickness changes between fairly closely spaced wells are unusual and imply slightly higher depositional slopes than have been identified in other cycles.

DISCUSSION

Depositional Environment of Halite

Halite textures including structures and vertically-oriented crystals indicate, by analogy with modern and experimental halite ponds, that most or all the bedded San Andres halite accumulated subaqueously as crusts nucleated on a brine pool floor. Correlations based on detailed core logging indicate that zones of bedded halite can be traced over the entire area of core control, an area of 5,000 km². The zones of bedded halite are parallel to anhydrite beds, which are interpreted as representing an approximately synchronous episode of transgression. The zones of bedded halite, therefore, are also interpreted as approximately synchronous rather than time-transgressive deposits, indicating that the halite-precipitating water body was extensive and uninterrupted. Similar 1- to 20-foot-thick massive halite marker beds in the Salado Formation of the Delaware Basin have been traced over areas of 12,000 square miles (Adams, 1969).

The abundant corrosion surfaces marked by anhydrite partings within the bedded halite represent episodes of lowered salinity and addition of calcium sulfate-bearing brines. The calcium sulfate source is tentatively identified as marine, because abundant anhydrite partings appear to be equivalent to thicker anhydrite beds downdip. An updip meteoric/fluvial source for calcium sulfate is possible, but is considered less likely because anhydrite is typically present only in minor amounts (nodules making up less than one percent of the sediment) in

updip terrigenous clastic red beds. Evidence within the halite indicates that the halite environment was not completely isolated from the marine environment. The paucity of evaporite minerals deposited from brines evaporated beyond halite precipitation and the moderate bromide-chloride ratio in halite (Fisher and Hovorka, 1984) indicate that the halite-precipitating water body was not evaporated much beyond concentrations to initiate halite precipitation. Bittern and bromide-enriched brines efficiently refluxed and were removed from the system. The frequent input of undersaturated brines producing corrosion surfaces and anhydrite partings and the reflux or more highly evaporated brines are probably related and indicate that the halite-precipitating water body was connected to the marine environment. No system of topographic barriers separating evaporites in the Palo Duro Basin from potential southern and eastern marine sources has been identified, and any barriers present must have allowed circulation of water between or through them. The textural, geochemical, and stratigraphic evidence together indicate that halite deposition took place in an environment similar to the preceding carbonate and anhydrite environments, best described as a shallow, increasingly hypersaline shelf.

Textural evidence within the bedded halite indicates that the precipitating water body was at some times very shallow and that the halite was episodically dissolved and altered. Roedder (1982) argued that the regularly-banded chevron halite formed in water less than a few feet deep. Although no maximum water depth can be interpreted from halite, the generally shallow water character of the anhydrite and carbonate rocks deposited in each genetic cycle prior to halite deposition place a general constraint on the maximum water depth. The abundant pits and pipes within the halite are interpreted as karst developed in halite. No recent examples of such features have been described against which the San Andres features can be compared. The pits and pipes have a dominantly vertical geometry and are up to two meters deep, and commonly filled with mudstone or are truncated at the top by a mudstone bed. This contrasts with the small-scale pitting and anhydrite partings which are characteristic of horizontal corrosion surfaces in the halite. Pits and pipes are, therefore, attributed to a

different process than the apparently subaqueous dissolution which formed the corrosion surfaces. The accumulation on the pit floors of a layer of insoluble residue similar in composition to the insoluble components in the missing halite is evidence of the origin of the features by dissolution of halite rock. This process is envisioned as occurring under subaerial conditions, when the supply of halite-precipitating brine was shut off. The evidence for subaerial exposure is the association with mudstone beds, many of which form under subaerial conditions (discussed below) and the strongly vertical orientation of the pipes and pits, which implies existence of hydrologic head to draw the dissolving waters through the sediment. In limestone karst systems, which is the only available analog, vertical pit development is characteristic of the vadose zone. The mechanism for lowering the groundwater table to cause the apparent hydrologic head, however, is not understood, and, in the absence of other examples of karst from halite rock, doubt remains about the origin of pits.

Twenty to 50 percent of the San Andres unit 4 and unit 5 halite section is composed of halite lacking the textures diagnostic of subaqueous deposition. Criteria to distinguish which of these fabrics are primary and which are due to destruction of primary fabrics by diagenetic alteration have not yet been developed; however, many examples of halite with only relict primary fabric indicate that diagenetic alteration is an important process. Most, if not all, chaotic mudstone-halite rock in San Andres units 4 and 5 is interpreted as originating by intensive and repeated episodes of pit formation, accumulation of mudstone in pit fills and insoluble residue on pit floors and accompanying recrystallization of remaining host halite. This interpretation is based on the presence of relict fabrics indicating former bedded character in many examples of chaotic mudstone-halite. Some equant anhydritic or muddy halite with equant crystals also contains evidence of former better-bedded character including discontinuous anhydrite partings, remnants of chevron structure, and insoluble residue accumulations marking the location of former pit floors.

Correlations of detailed core logs show that the same patterns of association between halite types observed in vertical sequence are also lateral equivalents. Chevron halite is most

commonly associated with equant anhydritic halite, indicating either that equant anhydritic halite is a common diagenetic alteration product of chevron halite or that they are formed under similar conditions. Sequences of alternating equant anhydritic halite and chevron halite do not match the sequence of the same lithologies in adjacent cores. The alternation is, therefore, due to local rather than regional depositional or diagenetic conditions. Chaotic mudstone-halite is commonly laterally correlative to zones of bedded halite with mudstone interbeds. In some examples it occurs immediately beneath mudstone interbeds. These relationships agree with the interpretation that chaotic mudstone-halite originates due to alteration and karstification during the times of lengthy or repeated subareal exposure during which the mudstone beds were deposited.

Depositional Environment of Mudstone Interbeds

Mudstone beds within the halite of the San Andres units 4 and 5 exhibit strong similarities to each other. They have grain sizes in the silty end of the mudstone range and the dominant silt-size grains are quartz and potassium feldspars. Most mudstone beds have a fabric described as disturbed intraclastic, which is interpreted as a fabric produced by alternating displacive growth and dissolution of halite crystals within and beneath the sediment. Remnant fabrics in the intact clasts in the disturbed interbeds are similar to those in the less haloturbated interbeds and include small-scale ripple cross lamination, small-scale scours, granule-sized claystone rip-up clasts, thin mudstone or claystone drapes, and parallel stratification.

Individual mudstone interbeds in halite range from a few millimeters thick to a maximum of almost 1 meter. Individual beds are difficult to trace from core to core, but the zones in which numerous mudstone beds occur are readily traceable across the basin. Mudstone beds, even thin beds, can commonly be clumped into zones of abundant mudstone interbeds in halite 30 cm to 3 m thick, representing times when influx of mudstone was an important process. The mudstone distribution pattern appears to be broadly lobate, with thicker and more numerous mudstone beds defining the center of the lobe. In all areas, mudstone deposition alternates with

halite deposition, and the rate of sediment accumulation appears to be constant within the limitations of the correlations throughout the area of core control. In the area of core control, positions of greatest accumulation of mudstone shifted frequently, so the muddy lobes are not stacked. Mudstone deposition was episodic, with halite deposition resuming when mud was not accumulating.

Recent analogs for deposition of mudstone mixed with halite on an extensive shelf are not available. Three influences on sediment transport and deposition can be recognized within the interbeds in halite: (1) eolian, (2) subaqueous reworking, and (3) subaerial exposure.

The silt-rich grain size of the San Andres clastics is interpreted as evidence of eolian transport, based on the following arguments. The entire evaporite section is characterized by an abundance of very fine sand and coarse silt (Kolker and others in prep.) and is correspondingly impoverished in grains coarser than 0.25 mm average diameter and clay-sized materials. The silt-rich grain size distribution is unusual compared to other clastic sediments, in which sand-size and coarser grains are present as a result of mechanical weathering of source materials and clay-sized clay minerals which are present as products of chemical weathering (Pettijohn, 1976, chapter 3). The probable source areas for Palo Duro middle and upper Permian clastics are the generally granitic and metamorphic Ancestral Rockies (Kolker and others, in prep.) which should have contributed a wide range of grain sizes to alluvial fan deposits adjacent to these uplifts. The unusual grain size distribution in the Palo Duro Basin is, therefore, due to sorting by grain size during transport and not to the character of the source rocks.

Eolian transport is an effective mechanism in winnowing sediments by grain size. The silt-size fraction is the size transported by desert dust storms, which is the mechanism which produces silt-rich sediments to a variety of depositional environments in the Permian Gulf (Kukal and Saadallah, 1973). A similar desert dust storm origin for San Andres and other Palo Duro silty sediments is supported by the presence of extensive Permian red beds and eolian sandstones on the Colorado Plateau and the Dalhart Basin (Presley, 1981a) to serve as sources

for dust (Baars, 1962). The clastic units within the Palo Duro evaporite section also show evidence of eolian transport (Kolker and others, in prep.). Very good sorting, positively (fine)-skewed and bimodal grain size distributions, rounded, frosted sand grains, eolian (?) climbing ripple cross stratification, and a few high angle dune cross beds are interpreted as evidence supporting eolian influence. Eolian transport of sediments is a plausible mechanism in an area in which extreme aridity is evidenced by thick halite deposits. However, mudstone beds with evidence of deposition by eolian processes have not been identified. If dust settled out over a halite-precipitating water body, the water body was shallow or agitated enough to prevent development of graded bedding as the dust settled through the water body.

Thin, horizontal, ripple laminated mudstone beds which overlie thin beds of halite with well-preserved primary fabrics may have resulted from transport of mudstone as eolian dust or by halite-saturated water into a shallow halite-precipitating brine pool. The ripple laminated fabrics characterized by thin, silty laminae which pinch and swell within a darker, more clay-rich matrix or drape. The base of the siltstone laminae is sharp and exhibits little evidence of scour. The laminae are only a few millimeters thick, contain internal cross lamination and have a sharp or slightly gradational top. These beds resemble the ripple laminated mudstones in the Green River Formation interpreted as shallow lake margin deposits (Smoot, 1983), the flaser and lenticular bedding representing alternation of high current energy and waning current energy (Reineck and Singh, 1980), or the lenticularly laminated fine sand, silt, and clay of the mudflat environment of saline lakes (Hardie and others, 1978). The absence of corrosion of the underlying halite rules out deposition of these mudstone beds in dominantly subaerial environments. Even if the flood waters which transported the mudstone were saturated with halite before deposition took place, the subaerial environment would allow exposure of the halite to rain and dew, which should mobilize some halite and disrupt fabric, as is not seen in these beds. A subaqueous shallow shelf depositional environment is therefore postulated for these beds. Mudstone might be transported over broad areas as eolian dust which was reworked in shallow water by wave action. Alternatively, mud introduced by any process might be held in

suspension in shallow, wave-agitated, halite-saturated water, and transported to other areas. A mechanism of transportation of low salinity mud-laden water by density-stratified flow across halite-saturated brine, as was implied for San Andres mudstone beds by Bein and Land (1982) is unlikely because graded beds, which are characteristic of such deposition, have not been observed.

Most mudstone beds have disrupted fabrics interpreted as being due to haloturbation. Although the alternation between halite precipitating and halite dissolving interstitial waters within the mudstone could have been caused by changes in composition of an overlying standing water body, such changes in salinity are characteristic of intermittently flooded but dominantly subaerial settings, similar to mudflats surrounding saline lakes (Hardie and others, 1978). Episodic flooding of the flat by ephemeral streams results in dissolution of halite crusts and corrosion of halite within the sediment. Rain or dew on the flat may also contribute to mobilization of halite. Evaporation of water and dissolution of evaporites cooperated to increase the salinity of pore waters to halite saturation, allowing regrowth of halite within the sediment. Addition of halite to the sediment occurred when the mudstone beds were flooded by halite-saturated waters, producing abundant displacive crystals within the sediment, a fabric similar to saline mudflats rimming saline lakes (Smoot, 1983) or the continental playa sediments of Bristol Dry Lake (Handford, 1982). In Palo Duro evaporites, the facies position of the mudstone beds with displacive halite crystals and disrupted fabric between bedded halite and well-bedded terrestrial red beds indicates that the main source of the sodium chloride was from the adjacent marine-derived halite-precipitating water body. The bromide/chloride ratio of the displacive halite crystals and cements in mudstone interbeds in the San Andres is also moderate to high (R. S. Fisher, unpublished analysis) which is in agreement with a marine source of the depositing brines. Mudstone beds with haloturbated textures characteristically contain 1 to 10 volume percent displacive anhydrite nodules and trace amounts of aphanocrystalline dolomite. These minerals could have been derived from remobilized detrital anhydrite and dolomite deposited with the sediment, or could have been transported in solution by the same brines which precipitated the halite.

The common association of mudstone beds with corroded contacts with the underlying halite, mudstone beds which contribute mudstone fillings to karst pits in halite, or mudstone beds overlying chaotic mudstone-halite rock suggests a genetic relationship between mudstone beds and these features. However, not all of these subaerial features are restricted to occurrence beneath mudstone beds, indicating that either the features are related to a mudstone bed an unknown distance above them, or that not all episodes of exposure which produced these features are represented by a mudstone bed.

Distribution of Mudstone Beds

The mudstone beds are formed by increase of the ratio at the rate of accumulation of mud over the rate of accumulation of halite due to four interacting processes: (1) more efficient eolian transport, (2) cessation of halite precipitation, (3) halite dissolution, and (4) more efficient fluvial processes.

(1) Small amounts of fine-grained terrigenous clastics are present in most lithologies in the San Andres including carbonate, anhydrite, and bedded halite. These sparse but pervasive clastics are not confined or concentrated in a position in the facies tract and are generally silt-rich, suggesting that they may be reworked eolian dust deposited over a broad area. Dust transport into the halite-precipitating environment might be more frequent and more volumetrically important than in the anhydrite and carbonate rocks if the dust source area was nearby during halite deposition. The location of updip edge of the halite-precipitating water body where it interfingers with adjacent mudstone has not been defined for the San Andres. Modification of the section to the north and east, because of salt dissolution (Gustavson and others, 1980) has prevented definition of the depositional edge of halite, but the suggestion that clastic environments moved basinward some unknown amount during halite deposition is reasonable given the regressive nature of the San Andres cycles.

(2) The brine supply to the shallow extensive halite-precipitating shelf could be easily decreased or shut off by subtle changes in circulation due to changes in wind, topography, and

flooding events. This would cause the previously deposited halite to be subaerially exposed and halite precipitation to stop. A mudstone bed would then accumulate, because no halite precipitated to dilute the persistent eolian dust.

(3) Some mudstone may have been concentrated by dissolution of associated halite. This is interpreted as one important reason for formation of insoluble residue mudstones at the top of halite beneath the base of the next cycle. Partial dissolution of halite may also be a concentrating mechanism in some chaotic mudstone-halite rocks, producing collapsed fabrics in mudstone and corroded appearance in halite.

(4) When the supply of halite-precipitating brines diminished and the previously deposited halite was subaerially exposed, processes which transport mud may have operated more efficiently. Intermittent streams, in particular, could transport mudstone across the dry surface, but would deposit it near shore when the area was flooded. The drying of the flat would allow rapid progradation of subaerial mudflat environments across halite. The dominant sedimentary structures in both the mudflat environment of clastic units and the mudstone interbeds in halite is haloturbated, initially ripple laminated mudstone, supporting this interpretation.

Mudstone beds are concentrated in zones and the zones can be traced through the area of core control. Chaotic mudstone-halite also most commonly occurs in the zones of mudstone beds. The combination of processes responsible for deposition of mudstone beds was therefore cyclic and simultaneously affected broad areas. A similar cyclic alternation of mud-free halite grading up to muddy halite in the Salado Formation of the Delaware Basin, New Mexico is interpreted by Lowenstein as a shallowing upward sequence, representing progression from a perennial lagoon to a dry salt pan.

Summary of San Andres Depositional Environments

The environment in which the San Andres halite is deposited was a broad, low relief shelf. Circulation was restricted enough to cause brines to precipitate halite, but frequent, episodic

addition of marine water and reflux of more saline brines prevented deposition of potassium or other salts, and contributed anhydrite partings to the halite depositional environment. Bedded halite was deposited subaqueously, but facies relationships and textural features indicate that the water was shallow, from a few centimeters to perhaps a few meters deep. Terrigenous clastic mudstones of eolian origin were deposited either in subaqueous or subaerial environments. Transport of clastics under subaqueous conditions was either by turbulent suspension by wave action in shallow water or by eolian dust storms. Reworking of subaqueous sediment by waves produce lenticular and flaser bedding. These beds commonly are closely spaced, with bedded halite with preserved primary fabric between them, and represent episodes when clastic input into the environment was frequent.

Mudstone beds deposited or modified under conditions of subaerial exposure have haloturbated fabric, reflecting alternating precipitation and dissolution of halite. Relict ripple lamination within them represents episodes of flooding by shallow ponds or by rare sheetwash activities. Karst pits, corrosion of halite, and recrystallized chaotic fabrics result from dissolution of previously deposited bedded halite by fluvial and meteoric water. Displacive, euhedral halite crystals result from flooding of the dry mudflat by halite-saturated, mostly marine-derived water. Nodules of anhydrite were also precipitated. Dissolution alternating with precipitation occurred repeatedly in most beds, haloturbating initial fabric. Episodic return to halite-precipitating conditions caused mudstone beds to be interbedded with halite. Common halite fabrics were partially destroyed during the next exposure episode.

A precise model for the San Andres halite-precipitating environment is difficult to develop without a close modern analog. Most of the deposition of bedded halite occurred under shallow shelf conditions. However, significant amounts of time are represented by subaerially deposited and altered mudstone beds. The subaqueous-subaerial boundary of the facies tract

occurs, then, within the mud-rich zones of the halite part of the cycle, representing conditions of very shallow water on a low relief **CAUTION** shelf, where minor changes in circulation of brine cause large areas to alternate between wet and dry.

This report describes research carried out by staff members of the Bureau of Economic Geology which addresses the feasibility of the Palo Duro Basin for isolation of high-level nuclear wastes. The report describes the progress and current status of research and tentative conclusions reached. Interpretations and conclusions are based on available data and state-of-the-art concepts, and hence, may be modified by more information and further application of the involved sciences.

DRAFT

CONCLUSIONS

This study demonstrates that facies relationships and sedimentary textures and structures within bedded halite give information which can be used to interpret the depositional environment in which the sediment accumulated. Recent studies, for example Castens-Seidell (1984), Hardie and Eugster (1971), Schreiber and Kinsman (1975), Loucks and Longman (1982), Schreiber (1978), and Warren (1983), have demonstrated that facies study of calcium sulfate rocks can be productive. Halite, with well preserved sedimentary structures, however, is rare and integrated facies studies have hitherto not been undertaken.

The following facies have been identified within the halite of the San Andres Formation: (1) chevron halite with or without abundant anhydrite partings, (2) halite with color bands and/or vertically oriented crystals, (3) equant, structureless halite with minor amounts of mudstone or anhydrite as impurities, (4) chaotic mixtures of halite with mudstone, (5) paleo-karst features cutting across other fabrics, (6) mudstone interbeds with disturbed to intraclastic fabric or small scale ripple lamination, (7) anhydrite interbeds, and (8) dark mudstone beds with insoluble residue textures at the base of cycles. Petrographic study of features in core interpreted based on analogy with sparse examples from modern and other ancient halite environments was coupled with study of the regional distribution patterns of these facies shown on cross sections. A model for San Andres halite deposition emerged from this integration. Facies can be traced for long distances, in many intervals over the entire area where information from cores was available, indicating that the depositional environment was a broad and uninterrupted shelf. For example, San Andres unit 4, zone 23 is a 3 to 4 m thick sequence of dominantly chevron halite throughout the study area. The rapid vertical fluctuation between one facies and the next over broad areas provides evidence that each zone represents an approximately simultaneous event which affected a broad area, rather than a result of migration of narrow facies belts or tracts of facies mosaics. The widespread character of carbonate and anhydrite facies throughout the San Andres Formation is documented by Fracasso and Hovorka (1984).

Where lateral facies changes occur, they show interesting relationships which better define the depositional environments. Dolomite and anhydrite represent the most marine facies within the San Andrés. Episodes of deposition of these facies are interpreted as transgressions. A thinning of the halite and a less pronounced thickening of the dark mudstone insoluble residue at the base of the transgressive cycle can be identified beneath most of the dolomite and anhydrite beds, and is interpreted as a result of dissolution of the most halite in areas where the transgressing waters had the lowest salinity. The location of the lowest salinity transgressing waters shifts from cycle to cycle, occurring repetitively in unit 4 in southern Swisher County but varying in unit 5 between southern Swisher County and eastern Deaf Smith County.

Where anhydrite beds pinch out updip, they are laterally equivalent to mud-free anhydritic halite with textures including chevron halite, vertically oriented and color banded halite, abundant anhydrite partings and equant anhydritic and muddy halite. The laterally equivalent facies relationship between anhydrite and chevron halite with abundant anhydrite partings can be seen, for example, in Swisher County in San Andres unit 4, zone 15 and in San Andres unit 5, zone 15. The chevron halite is interpreted as the fabric most typical of brine pool deposition of halite. Crystals of halite nucleated on the bottom of the brine pool compete for space, producing vertically elongated crystals. Variations in the density of fluid inclusions trapped at the crystals growth faces reflect fluctuations, possibly diurnal, in the brine pool conditions. Similar vertically oriented and color banded halite is characterized by a generally darker color and lack of well defined fluid inclusion banding. Modern and experimental analogs for the dark, color banded type of halite have not been found. Color-banded/vertically oriented halite is speculatively interpreted to have formed in slightly deeper or more strongly density stratified water conditions where the fluctuations in water chemistry were buffered and dark colors better preserved by reducing conditions. Abundant anhydrite partings are interpreted, by analogy with modern environments, to represent episodes of flooding by marine derived waters which were initially saturated with gypsum but not halite. Dissolution of a minor amount of halite and precipitation of a thin layer of gypsum preceded evaporation to concentrations where

the precipitation of halite was renewed. This textural evidence of repeated interaction with marine waters complements geochemical and mineralogic evidence that the brine pool never became much more highly concentrated than required for halite precipitation.

The other suite of halite facies, including chaotic mudstone-halite mixtures, halite karst, and mudstone interbeds is interpreted as the result of intermittent drying of the halite flat. The main lines of evidence that these features represent at least intermittently dry conditions are (1) the need for hydrologic head to develop microkarst pipes and pits with a strong vertical orientation, (2) the haloturbated textures characteristic of the mudstone interbeds, which require alternate wetting with brine and drying and dissolution of halite, (3) the absence of graded bedding characteristic of density stratified subaqueous environments, and (4) the typical gradational character of the facies transition from bedded halite through haloturbated silty mudstone to eolian clastics, for example, at the contact of the San Andres Formation with the overlying Queen-Grayburg Formation. Chaotic mudstone-halite is interpreted as a result of introduction of mudstone and intense alteration and karstification of bedded halite under subaerial conditions. Remnant bedded textures in some chaotic mudstone and analogy to chaotic mudstone-halite textures in Recent playa lakes support this interpretation as well as facies relationships which show that the chaotic mudstone-halite is associated with zones of abundant mudstone beds in halite by lateral equivalence or by thick mudstone beds overlying chaotic mudstone-halite. Net mud maps reveal that many mudstone bodies have a crudely lobate geometry.

Study of diagenetic processes which modified San Andres bedded halite is not complete. A certain amount of recrystallization is clearly recognized where chevron fabrics have been destroyed along grain boundaries. More extensive recrystallization processes are postulated to destroy the millimeter scale floating hopper crystals which are sparsely preserved in the San Andres, but are very important in modern and experimental environments. Recrystallization has contributed to the absence of primary fabric in the equant muddy and anhydritic halite, but techniques to determine the extent to which the equant fabric and absence of bedding is

characteristic of some environmental conditions versus due to the loss of primary fabric through recrystallization have not been developed. Detailed understanding of the primary fabric developed in this study provides necessary background for diagenetic studies.

ACKNOWLEDGMENTS

George Donaldson and the crew of the Bureau of Economic Geology Core Research Center provided essential assistance transporting, cataloging, and slabbing the core used in this study. Thin sections and slabs of core were prepared by Ethel Butler. The manuscript was reviewed by S. C. Ruppel, E. G. Wermund, and T. C. Gustavson. Patti Granger assisted with compilation of maps and cross sections.

The research was funded by the U.S. Department of Energy, contract number DE-AC-97-83WM 46651.

Table 1. Composition of Unit 4 Halite

	<u>#1 J. Friemel</u>	<u>#1 G. Friemel</u>	<u>#1 Detten</u>	<u>#1 Harman</u>	<u>#1 Zeeck</u>	<u>#1 Grabbe</u>
Halite Thickness (feet)	165.5	152.5	172.7	169.7	176.0	183.7
Average Percent Halite	87	89	87	81	77	86
Average Percent Mudstone	9	7	8	10	10	8
Number of mudstone interbeds	91	116	112	129	101	136
Maximum mudstone bed thickness (mm)	470	310	640	310	920	450
Average mudstone bed thickness (mm)	30	15	19	29	52	28
Average percent mudstone in mudstone intervals	65	63	75	86	86	80
Cumulative thickness of chaotic mudstone-halite rock (feet)	27.5	19.5	12.3	13.6	20.0	29.6
Average percent anhydrite	4	4	5	9	13	6
Number of anhydrite interbeds	86	210	132	157	283	188
Maximum anhydrite bed thickness (mm)	10	180	120	990	1920	530

DRAFT

Table 2. Textural classification of halite with genetic significance.

Symbol	A	B	C	D	E	F	G	H	I
halite type	chevron halite rock	color banded, vertically oriented halite rock		chaotic mudstone-halite rock	equant muddy halite rock	equant anhydritic halite rock	displacive halite in other sediments	halite cavity-filling cement	fibrous fracture-filling halite cement
halite crystal size	0.5-5 cm tall	0.5-5 cm tall		0.3-3 cm	1-5 cm	1-5 cm	0.5-3 cm	1-20+ cm	0.3-1 cm
halite crystal shape	subvertical mosaic; L:W = 3:2 to 4:1	subvertical mosaic; L:W = 3:2 to 4:1		equant anhedral to euhedral crystals	equant mosaic	equant mosaic	euhedral cubes or hopper shapes	equant mosaic	fibrous
impurities	composition	anhydrite common; mudstone possible		mudstone, minor anhydrite	mudstone, minor anhydrite	anhydrite	mudstone; also dolomite, anhydrite	cavity-filling halite is clean but is associated with mudstone and anhydrite insoluble residues	trace of hematite present as coloring agent, otherwise pure halite
	percentage	<1-5%		10-50%	1-10%	1-25%	50-99%		
	location	anhydrite on grain boundaries, partings, mudstone only in pipe fills	within and between grains, along partings, in pipes		in masses between halite crystals, some also within grains	within grains, minor between grains	along partings, grain boundaries	matrix for halite	
fluid inclusions	abundant, small define relict growth facies	varied		few	varied	varied	few	large and abundant	?
associated with halite types	F along crystal boundaries and pipes, H and/or D in pipes	F & E, H and/or D in pipes		mudstone beds typically includes remnant B halite	may contain remnant A, B, possible H	may contain remnant A, B, possible H	non-halite rocks	all halite types	in non-halite rocks
identifying characteristics	minute fluid inclusions along relict halite growth faces	bedding and/or vertical orientation of crystals		10-50% mudstone in intercrystalline masses, chaotic texture	halite colored red brown or black by 1-10% impurities, no fabric, no bedding	halite with 1-25% anhydrite, no fabric, no bedding	euhedral to subhedral halite crystals in sediments	exceptionally coarse clear crystals, fill cavity in other salt type	fibrous halite in fracture, many examples red colored

C reserved for another primary fabric not yet recognized

DRAFT

sketch

Table 3. Weight percent clay size grains determined by pipette analysis in three samples from typical mudstone interbeds in San Andres halite from the DOE-Gruy Federal No. 1 Grabbe core. Analyses by Seay Nance, 1983.

Depth in Feet Below KB	Weight Percent Clay Grain Size
2,569.0	44
2,618.4	38
2,621.6	27

DRAFT

REFERENCES

- Adams, S. S., 1969, Bromine in the Salado Formation, Carlsbad potash district, New Mexico: New Mexico Bureau of Mines and Mineral Resources Bulletin 93, 122 p.
- Arthurton, R. S., 1973, Experimentally produced halite compared with Triassic layered halite-rock from Cheshire, England: *Sedimentology*, v. 20, p. 145-160.
- Baar, C. A., 1974, Geological problems in Saskatchewan potash mining due to peculiar conditions during deposition of potash beds, in Coogan, A. H., ed., Fourth Symposium on Salt, Northern Ohio Geological Society, v. 1, p. 101-118.
- Baars, D. L., 1962, Permian System of Colorado Plateau: American Association of Petroleum Geologists Bulletin, v. 46, p. 149-218.
- Bassett, R. L., and Palmer, D. P., 1981, Clay mineralogy of the Palo Duro Basin evaporite sequences, Randall County core, in Gustavson, T. C., and others, Geology and geo-hydrology of the Palo Duro Basin, Texas Panhandle, a report on the progress of nuclear waste isolation feasibility studies (1980): The University of Texas at Austin, Bureau of Economic Geology Geological Circular 81-3, p. 108-118.
- Bathurst, R. G. C., 1975, Carbonate sediments and their diagenesis, developments in sedimentology 12: New York, Elsevier, 658 p.
- Bein, A., and Land, L. S., 1982, San Andres carbonates in the Texas Panhandle: sedimentation and diagenesis associated with magnesium-calcium-chloride brines: The University of Texas at Austin, Bureau of Economic Geology Report of Investigations No. 121, 48 p.
- Bock, E., 1961, On the solubility of anhydrous calcium sulfate and gypsum in concentrated solutions of sodium chloride at 25°C, 30°C, 40°C, and 50°C: *Canadian Journal of Chemistry*, v. 39, p. 1746-1751.
- Brantley, S. L., Crerar, D. A., Møller, N. E., and Weare, J. H., 1984, Geochemistry of a modern marine evaporite, Bocana de Virrila, Peru: *Journal of Sedimentary Petrology*, v. 54, p. 447-462.

- Budnik, R. T., and Smith, Dale, 1982, Regional stratigraphic framework of the Texas Panhandle, in Gustavson, T. C., and others, Geology and geohydrology of the Palo Duro Basin, Texas Panhandle, a report on the progress of nuclear waste isolation feasibility studies (1981): The University of Texas at Austin, Bureau of Economic Geology Geological Circular 82-7, p. 38-86.
- Castens-Seidell, Barbara, 1984, Morphologies of gypsum on a modern sabkha: clues to depositional conditions (abs.): American Association of Petroleum Geologists, v. 68, p. 460.
- D'Appolonia Consulting Engineers, Inc., 1983, Geologic mapping of exploratory drift: WIPP-SPDV, Geotechnical Field Data Report No. 7, variously paginated.
- Dean, W. E., and Anderson, R. Y., 1982, Continuous subaqueous deposition of the Permian Castille evaporites, Delaware Basin, Texas and New Mexico, in Handford, C. R., Loucks, R. G., and Davies, G. R., eds., Depositional and diagenetic spectra of evaporites--a core workshop: Society of Economic Paleontologists and Mineralogists Core Workshop No. 3, p. 324-353.
- Dellwig, L. F., 1955, Origin of the Salina salt of Michigan: Journal of Sedimentary Petrology, v. 25, p. 83-110.
- Dutton, S. P., 1980, Petroleum source rock potential and thermal maturity, Palo Duro Basin, Texas: The University of Texas at Austin, Bureau of Economic Geology Geological Circular 80-10, 48 p.
- Fisher, R. S., and Hovorka, S. D., 1984, Textural and chemical zones in bedded halite, Permian lower San Andres Formation, Palo Duro Basin, Texas: The University of Texas at Austin, Bureau of Economic Geology Open-File Report OF-WTWI-1984-48 15 p..
- Folk, R. L., 1974, Petrology of sedimentary rocks: Austin, Hemphill, 182 p.
- Fracasso, M. A., and Hovorka, S. D., 1984, Cyclicity in the Middle Permian San Andres Formation, Palo Duro Basin, Texas Panhandle: The University of Texas at Austin, Bureau of Economic Geology Open-File Report OF-WTWI-1984-21, 42 p.

- Gavish, Eliezer, 1980, Recent sabkhas marginal to the southern coasts of Sinai, Red Sea, in Nissenbaum, A., ed., Hypersaline brines and evaporitic environments: New York, Elsevier, p. 233-251.
- Glennie, K. W., and Evans, G., 1976, A reconnaissance of the Recent sediments of the Ranns of Kutch, India: *Sedimentology*, v. 23, p. 625-647.
- Gornitz, V. M., and Schreiber, B. C., 1981, Displacive halite hoppers from the Dead Sea: some implications for ancient evaporite deposits: *Journal of Sedimentary Petrology*, v. 51, p. 787-794.
- Gustavson, T. C., Finley, R. J., and McGillis, K. A., 1980, Regional dissolution of Permian salt in the Andarko, Dalhart, and Palo Duro basins of the Texas Panhandle: BEG RI no. 106, 40 p.
- Handford, C. R., 1980, Lithofacies and depositional environments of evaporite-bearing strata based on Randall and Swisher County cores, in Gustavson, T. C., and others, *Geology and geohydrology of the Palo Duro Basin, Texas Panhandle, a report on the progress of nuclear waste isolation feasibility studies (1980)*: The University of Texas at Austin, Bureau of Economic Geology Geological Circular 80-7, p. 5-7.
- Handford, C. R., 1981, Bromide geochemistry of Permian halite in the Randall County core, in Gustavson, T. C., and others, *Geology and geohydrology of the Palo Duro Basin, Texas Panhandle, a report on the progress of nuclear waste isolation feasibility studies (1980)*: The University of Texas at Austin, Bureau of Economic Geology Geological Circular 81-3, p. 75-80.
- Handford, C. R., 1982, *Sedimentology and evaporite genesis in a Holocene continental-sabkha playa basin--Bristol Dry Lake, California*: *Sedimentology*, v. 29, p. 239-253.
- Handford, C. R., and Bassett, R. L., 1982, Permian facies sequences and evaporite depositional styles, Texas Panhandle, in Handford, C. R., Loucks, R. G., and Davies, G. R., eds., *Depositional and diagenetic spectra of evaporites--a core workshop*: Society of Economic Paleontologists and Mineralogists Core Workshop No. 3, p. 210-237.

- Hardie, L. A., and Eugster, H. P., 1971, The depositional environment of marine evaporites: a case for shallow clastic accumulations: *Sedimentology*, v. 16, p. 187-220.
- Hardie, L. A., Smoot, J. P., and Eugster, H. P., 1978, Saline lakes and their deposits: a sedimentological approach, *in* Matter, Albert, and Tucker, M. E., eds., *Modern and Ancient lake sediments: International Association of Sedimentologists Special Publication No. 2*, p. 7-41.
- Herrmann, A. G., Knake, Doris, Schneider, Jürgen, and Peters, Heide, 1973, Geochemistry of modern seawater and brines from salt pans: main components and bromine distribution: *Contributions to Mineralogy and Petrology*, v. 40, p. 1-24.
- Hite, R. J., 1968, Salt deposits of the Paradox Basin, southeast Utah and southwest Colorado: *Geological Society of America Special Paper 88*, p. 319-330.
- Holdaway, Katrine, 1978, Deposition of evaporites and red beds of the Nippewalla Group, Permian, western Kansas: *Kansas Geological Society Bulletin* 215 43 p.
- Hovorka, S. D., 1983, Sedimentary structures and diagenetic modifications in halite and anhydrite, Palo Duro Basin, *in* Gustavson, T. C., and others, *Geology and geohydrology of the Palo Duro Basin, Texas Panhandle, a report on the progress of nuclear waste isolation feasibility studies (1982): The University of Texas at Austin, Bureau of Economic Geology Geological Circular 83-4*, p. 49-57.
- Hovorka, S. D., 1982, Carbonate-anhydrite-halite cycles, San Andres Formation (Permian) Palo Duro Basin, Texas, *in* Shaw, R. L., and Pollan, B. J., eds., *Permian Basin cores--a workshop: Permian Basin Section, Society of Economic Paleontologists and Mineralogists Core Workshop No. 2*, p. 197-224.
- Hovorka, S. D., Naiman, E. R., and McGowen, J. H., 1982, Petrographic summary of Permian rocks from the DOE/Gruy Federal No. 1 Grabbe well, Swisher County, *in* Gustavson, T. C., and others, *Geology and geohydrology of the Palo Duro Basin, Texas Panhandle, a report on the progress of nuclear waste isolation feasibility studies (1981): The University of Texas at Austin, Bureau of Economic Geology Geological Circular 82-7*, p. 91-100.

Hovorka, S. D., Thomas, Sterling, Luneau, B. A., and Ruppel, S. C., in preparation a, Lithostratigraphic sections: Stone and Webster No. 1 Harman, and Stone and Webster No. 1 Zeeck, Swisher County, Texas, in Gustavson, T. C., and others, Geology and geohydrology of the Palo Duro Basin, Texas Panhandle, a report on the progress of nuclear waste isolation feasibility studies (1983): The University of Texas at Austin, Bureau of Economic Geology Geological Circular.

Hovorka, S. D., Thomas, Sterling, Luneau, B. A., and Noe, David, in preparation b, Stone and Webster No. 1 Detten core, Deaf Smith County, in Gustavson, T. C., and others, Geology and geohydrology of the Palo Duro Basin, Texas Panhandle, a report on the progress of nuclear waste isolation feasibility studies (1983): The University of Texas at Austin, Bureau of Economic Geology Geological Circular.

Hovorka, S. D., Thomas, Sterling, Luneau, B. A., and Johns, D. A., in preparation c, Stone and Webster No. 1 J. Friemel core, Deaf Smith County, in Gustavson, T. C., and others, Geology and geohydrology of the Palo Duro Basin, Texas Panhandle, a report on the progress of nuclear waste isolation feasibility studies (1983): The University of Texas at Austin, Bureau of Economic Geology Geological Circular.

Hunt, C. B., Robinson, T. W., Bowles, W. A., and Washburn, A. L., 1966, Hydrologic Basin, Death Valley, California: U.S. Geological Survey Professional Paper 494-B, 133 p.

Johnson, K. S., 1976, Evaluation of the Permian salt deposits in the Texas Panhandle and western Oklahoma for underground storage of radioactive wastes: The University of Oklahoma, School of Geology and Geophysics final report prepared for Union Carbide Corporation, subcontract no. 4494 (W-7405-ENG 26), 73 p.

Kolker, Allan, Hovorka, S. D., McGookey, D. A., and Nance, S. H., in preparation, Petrology and depositional environments of terrigenous clastic rocks, lower Clear Fork through Dewey Lake Formations, Palo Duro Basin, in Gustavson, T. C., and others, Geology and geohydrology of the Palo Duro Basin, Texas Panhandle, a report on the progress of nuclear waste isolation feasibility studies (1983): The University of Texas at Austin, Bureau of Economic Geology Geological Circular.

- Kukal, Zdenek, and Saadallah, Adnan, 1973, Aeolian admixtures in sediments of the northern Persian Gulf, in Purser, B. H., ed., *The Persian Gulf: Holocene carbonate sedimentation and diagenesis in a shallow epicontinental sea*: New York, Springer-Verlag, p. 115-121.
- Loucks, R. G., and Longman, M. W., 1982, Lower Cretaceous Ferry Lake anhydrite, Fairway field, East Texas: product of shallow-subtidal deposition, in Handford, C. R., Loucks, R. G., and Davies, G. R., *Depositional and diagenetic spectra of evaporites--a core workshop: Society of Economic Paleontologists and Mineralogists Core Workshop No. 3*, p. 130-173.
- Lowenstein, Tim, 1982, Primary features in a potash evaporite deposit, the Permian Salado Formation of West Texas and New Mexico, in Handford, C. R., Loucks, R. G., and Davies, G. R., eds., *Depositional and diagenetic spectra of evaporites--a core workshop: Society of Economic Paleontologists and Mineralogists Core Workshop No. 3*, p. 276-304.
- Luneau, B. A., in preparation, Halite veins and associated features in the halite-bearing formations, DOE cores, Palo Duro Basin, Texas Panhandle, in Gustavson, T. C., and others, *Geology and geohydrology of the Palo Duro Basin, Texas Panhandle, a report on the progress of nuclear waste isolation feasibility studies (1983)*: The University of Texas at Austin, Bureau of Economic Geology Geological Circular.
- McGookey, D. A., and Goldstein, A. G., 1982, Structural influence on deposition and deformation at the northwest margin of the Palo Duro Basin, in Gustavson, T. C., and others, *Geology and geohydrology of the Palo Duro Basin, Texas Panhandle, a report on the progress of nuclear waste isolation feasibility studies (1981)*: The University of Texas at Austin, Bureau of Economic Geology Geological Circular 82-7, p. 28-37.
- McGowen, J. H., 1981, Depositional sequences and associated sedimentary diagenetic facies: an ongoing investigation of salt-bearing core, Swisher County, Texas, in Gustavson, T. C., and others, *Geology and geohydrology of the Palo Duro Basin, Texas Panhandle, a report on the progress of nuclear waste isolation feasibility studies (1980)*: The University of Texas at Austin, Bureau of Economic Geology Geological Circular 81-3, p. 90-92.

- McKee, E. D., and Oriel, S. S., 1967, Paleotectonic maps of the Permian system: U.S. Geological Survey Miscellaneous Geologic Investigations Map I-450.
- Naiman, E. R., Bein, Amos, Folk, R. L., 1983, Complex polyhedral crystals of limpid dolomite associated with halite, Permian upper Clear Fork and Glorieta Formations, Texas: *Journal of Sedimentary Petrology*, v. 53, p. 549-555.
- ONWI, 1983, Geotechnical logs of San Andres Formation, Palo Duro Basin, Texas: unpublished data.
- Pettijohn, F. J., 1975, *Sedimentary rocks*, third edition: New York, San Francisco and London, Harper and Row, 628 p.
- Presley, M. W., 1979a, Upper Permian evaporites and red beds, in Dutton, S. P., and others, *Geology and geohydrology of the Palo Duro Basin, Texas Panhandle, a report on the progress of nuclear waste isolation feasibility studies (1978)*: The University of Texas at Austin, Bureau of Economic Geology Geological Circular 79-1, p. 39-49.
- Presley, M. W., 1979b, Salt deposits, in Dutton, S. P., and others, *Geology and geohydrology of the Palo Duro Basin, Texas Panhandle, a report on the progress of nuclear waste isolation feasibility studies (1978)*: The University of Texas at Austin, Bureau of Economic Geology Geological Circular 79-1, p. 50-56.
- Presley, M. W., 1981a, Permeable sheet sandstones of the Glorieta Formation intertonguing with salt-bearing rocks in the northwestern Texas Panhandle, in Gustavson, T. C., and others, *Geology and geohydrology of the Palo Duro Basin, Texas Panhandle, a report on the progress of nuclear waste isolation feasibility studies (1980)*: The University of Texas at Austin, Bureau of Economic Geology Geological Circular 81-3, p. 10-18.
- Presley, M. W., 1981b, San Andres salt stratigraphy and salt purity, in Gustavson, T. C., and others, *Geology and geohydrology of the Palo Duro Basin, Texas Panhandle, a report on the progress of nuclear waste isolation feasibility studies (1980)*: The University of Texas at Austin, Bureau of Economic Geology Geological Circular 81-3, p. 33-40.

- Presley, M. W., 1981c, Middle and upper Permian salt-bearing strata of the Texas Panhandle, lithologic and facies cross sections: The University of Texas at Austin, Bureau of Economic Geology Cross Sections.
- Reading, H. G., ed., 1978, Sedimentary environments and facies: New York, Elsevier, 557 p.
- Reineck, H. E., and Singh, I. B., 1980, Depositional sedimentary environments (2d ed.): New York, Springer-Verlag, 549 p.
- Reodder, Edwin, 1982, Possible Permian diurnal periodicity in NaCl precipitation, Palo Duro Basin, Texas, in Gustavson, T. C., and others, Geology and geohydrology of the Palo Duro Basin, Texas Panhandle, a report on the progress of nuclear waste isolation feasibility studies (1981): The University of Texas at Austin, Bureau of Economic Geology Geological Circular 82-7, p. 101-104.
- Ruppel, S. C., and Hovorka, S. D., 1983a, Stratigraphic section along the northeastern margin of the Palo Duro Basin: core analysis of DOE-Stone and Webster No. 1 Sawyer test well, Donley County, Texas, in Gustavson, T. C., and others, Geology and geohydrology of the Palo Duro Basin, Texas Panhandle, a report on the progress of nuclear waste isolation feasibility studies (1982): The University of Texas at Austin, Bureau of Economic Geology Geological Circular 83-4, p. 45-46.
- Ruppel, S. C., and Hovorka, S. D., 1983b, Stratigraphic section along the northwestern margin of the Palo Duro Basin: core analysis of DOE-Stone and Webster No. 1 Mansfield test well, Oldham County, Texas, in Gustavson, T. C., and others, Geology and geohydrology of the Palo Duro Basin, Texas Panhandle, a report on the progress of nuclear waste isolation feasibility studies (1982): The University of Texas at Austin, Bureau of Economic Geology Geological Circular 83-4, p. 47-48.
- Ruppel, S. C., and Ramondetta, P. J., 1982, Determination of salt purity using gamma-ray logs: San Andres Formation, Palo Duro Basin, in Gustavson, T. C., and others, Geology and geohydrology of the Palo Duro Basin, Texas Panhandle, a report on the progress of nuclear waste isolation feasibility studies (1981): The University of Texas at Austin, Bureau of Economic Geology Geological Circular 82-7, p. 183-199.

- Schreiber, B. C., 1978, Environments of subaqueous gypsum deposition, in Dean, W. E., and Schreiber, B. C., eds., Marine evaporites: Society of Economic Paleontologists and Mineralogists Short Course No. 4, p. 43-73.
- Schreiber, B. C., and Kinsman, D. J. J., 1975, New observations on the Pleistocene evaporites of Montallegro, Sicily and a modern analog: *Journal of Sedimentary Petrology*, v. 45, p. 469-479.
- Shearman, D. J., 1970, Recent halite rock, Baja California, Mexico: *Transactions of the Institute of Mining and Metallurgy*, v. 79, p. B155-B162.
- Smith, D. B., 1971, Possible displacive halite in the Permian Upper Evaporite Group of Northeast Yorkshire: *Sedimentology*, v. 17, p. 221-232.
- Smoot, J. P., 1983, Depositional subenvironments in an arid closed basin, the Wilkins Peak Member of the Green River Formation (Eocene), Wyoming, U.S.A: *Sedimentology*, v. 30, p. 801-827.
- Southgate, P. N., 1982, Cambrian skeletal halite crystals and experimental analogues: *Sedimentology*, v. 29, p. 391-407.
- Warren, J. K., in press, On the significance of evaporite lamination, in, Schreiber, B.C., ed., Sixth International Symposium on Salt: Salt Institute, Alexandria, Virginia.
- Wardlaw, N. C., and Schwerdtner, W. M., 1966, Halite-anhydrite seasonal layers in the Middle Devonian Prairie Evaporite Formation, Saskatchewan, Canada: *Geological Society of America Bulletin* 77, p. 331-342.
- Weiler, Y., Sass, E., and Zak, I., 1974, Halite oolites and ripples in the Dead Sea, Israel: *Sedimentology*, v. 21, p. 623-632.

Plates

Plate 1 Stone and Webster No. 1 J. Friemel core, San Andres unit 5

Plate 2 Stone and Webster No. 1 J. Friemel core, San Andres unit 4

Plate 3 Stone and Webster No. 1 Detten core, San Andres unit 5

Plate 4 Stone and Webster No. 1 Detten core, San Andres unit 4

Plate 5 Stone and Webster No. 1 G. Friemel core, San Andres unit 5

Plate 6 Stone and Webster No. 1 G. Friemel core, San Andres unit 4

Plate 7 Stone and Webster No. 1 Harman core, San Andres unit 5

Plate 8 Stone and Webster No. 1 Harman core, San Andres unit 4

Plate 9 Stone and Webster No. 1 Zeeck core, San Andres unit 5

Plate 10 Stone and Webster No. 1 Zeeck core, San Andres unit 4

Plate 11 DOE-Gruy Federal No. 1 Grabbe core, San Andres unit 5

Plate 12 DOE-Gruy Federal No. 1 Grabbe core, San Andres unit 4

Plate 13 DOE-Gruy Federal No. 1 Rex White core, San Andres unit 5

Plate 14 DOE-Gruy Federal No. 1 Rex White core, San Andres unit 4

Plate 15 Correlation of San Andres unit 5 through seven cored wells. The techniques used to produce this correlation are described in the text.

Plate 16 Correlation of San Andres unit 4 through seven cored wells. The techniques used to produce this correlation are described in the text.

22 11

Table 1 Composition of unit 4 in the seven cores studied, based on the visually estimated percent mineralogy shown in Plates 1 through 14. Limitations of the methods of visual estimates are discussed in the text.

Table 2 Textural classification of halite with genetic significance.

Table 3 Weight percent clay size grains determined by pipette analysis in three samples from typical mudstone interbeds in San Andres halite from the DOE-Gruy Federal No. 1 Grabbe core. Analyses by Seay Nance.

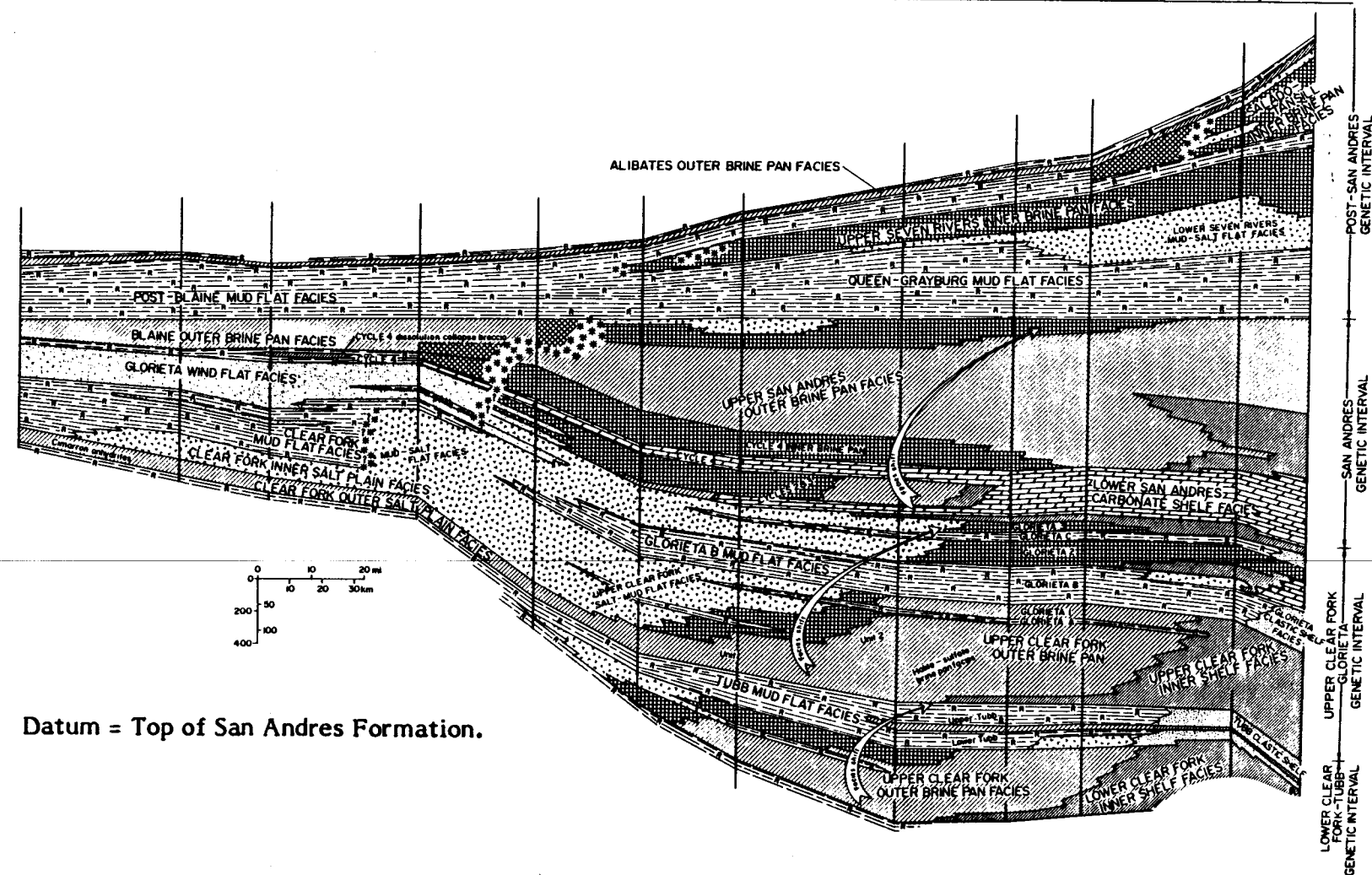
DRAFT

			Palo Duro Basin	Dalhart Basin	General Lithology and depositional setting	
SYSTEM	SERIES	GROUP	FORMATION	FORMATION		
QUATERNARY	HOLOCENE		alluvium, dune sand Playa	alluvium, dune sand Playa		
	PLEISTOCENE		Tahoka "cover sands" Tule Blanco	"cover sands"	Lacustrine clastics and windblown deposits	
TERTIARY	NEOGENE		Ogallala	Ogallala	Fluvial and lacustrine clastics	
CRETACEOUS			undifferentiated	undifferentiated	Marine shales and limestone	
TRIASSIC		DOCKUM			Fluvial-deltaic and lacustrine clastics	
PERMIAN	OCHOA		Dewey Lake	Dewey Lake	Cyclic sequences: shallow-marine carbonates; hypersaline-shelf anhydrite, halite; continental red beds	
			Alibates	Alibates		
	GUADALUPE	ARTESIA		Salado/Tansill		Artesia Group undifferentiated
				Yates		
				Seven Rivers		
				Queen/Grayburg		
	LEONARD	CLEAR FORK		San Andres		Blaine
				Glorieta		Glorieta
				Upper Clear Fork		Clear Fork
				Tubb		undifferentiated Tubb-Wichita Red Beds
			Lower Clear Fork			
			Red Cave			
		WICHITA				
		WOLFCAMP				
PENNSYLVANIAN	VIRGIL	CISCO			Shelf and shelf-margin carbonate, basinal shale, and deltaic sandstone	
	MISSOURI	CANYON				
	DES MOINES	STRAWN				
	ATOKA	BEND				
	MORROW					
MISSISSIPPIAN	CHESTER				Shelf carbonate and chert	
	MERAMEC					
	OSAGE					
ORDOVICIAN		ELLEN-BURGER			Shelf dolomite	
CAMBRIAN ?					Shallow marine(?) sandstone	
PRECAMBRIAN					Igneous and metamorphic	

Figure 1. Generalized stratigraphic column, Palo Duro Basin, modified from Budnik and Smith (1982).

DRAFT

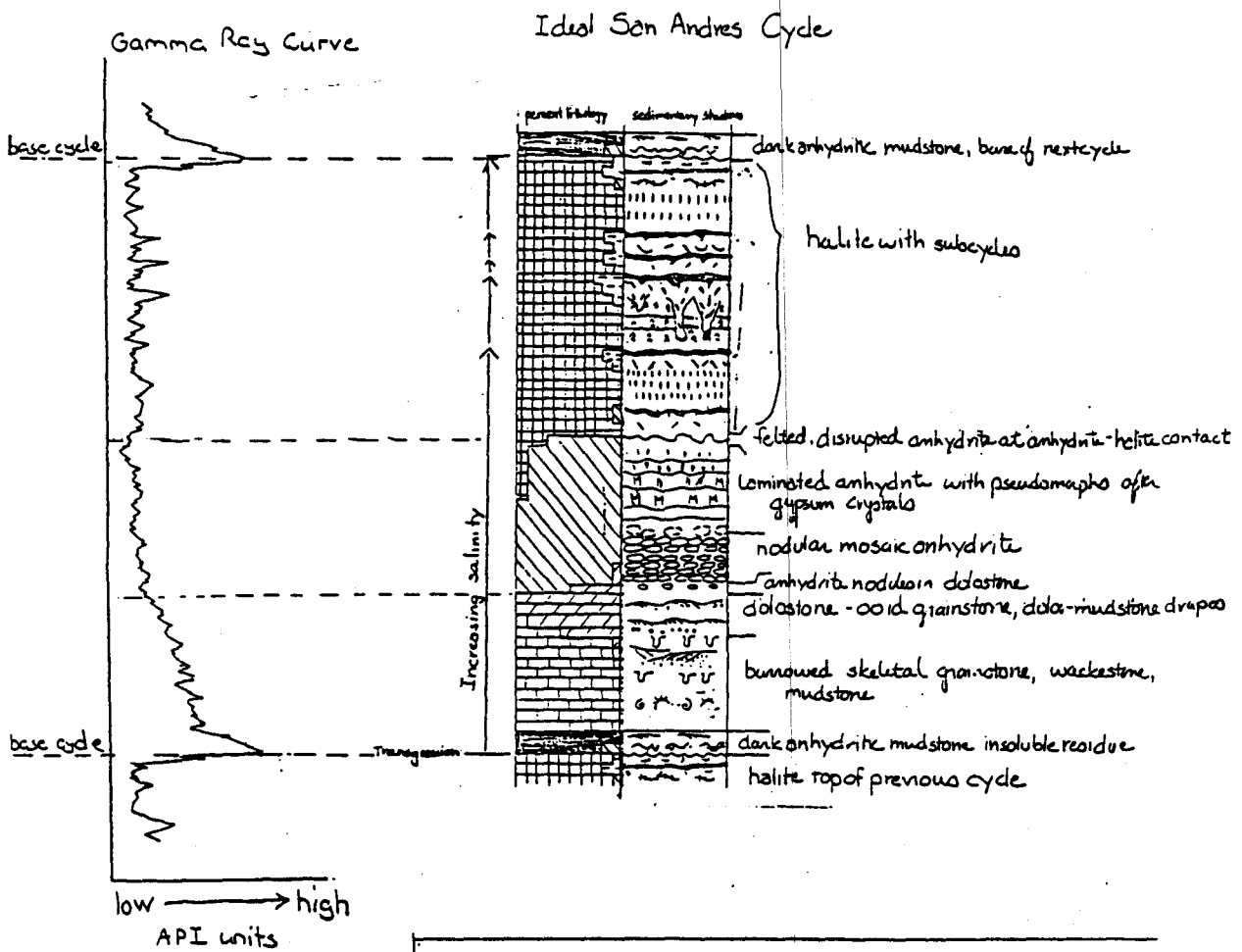
NORTH
 TEXAS 10 OKLA. TEXAS SHERMAN 31 39 HARTLEY 33 5 OLDHAM 45 DEAF SMITH 2 CASTRO 13 LAMB 92 HOCKLEY 8
 DALHART BASIN AMARILLO UPLIFT PALO DURO BASIN MATADOR ARCH SOUTH



DRAFT

Datum = Top of San Andres Formation.

Figure 2. Regional north-south cross section of salt-bearing rocks in the Texas Panhandle. From Presley (1981).



Key

Lithology	limestone	anhydrite	halite	red mudstone
	dolomite			black mud
structures	skeletal grain	nodules	voided crystals	disrupted
	skeletal sand	lamina	chevron	ripple
	ooids	pseudomorph after gypsum crystals	mudstone-halite with chaotic fabric	
	cross beds		red mudstone interbed	
	ripples		anhydrite interbed	
	burrows		pit	

Figure 3. San Andres cycles are composed of a sequence (base to top) of dark mudstone, carbonate, anhydrite, and halite. Many cycles are incomplete or vary from this idealized pattern, but recognition of this pattern and corresponding pattern shown on gamma-ray logs allows identification of over twenty regionally traceable cycles within the San Andres Formation. From Fracasso and Hovorka (1984).

DRAFT

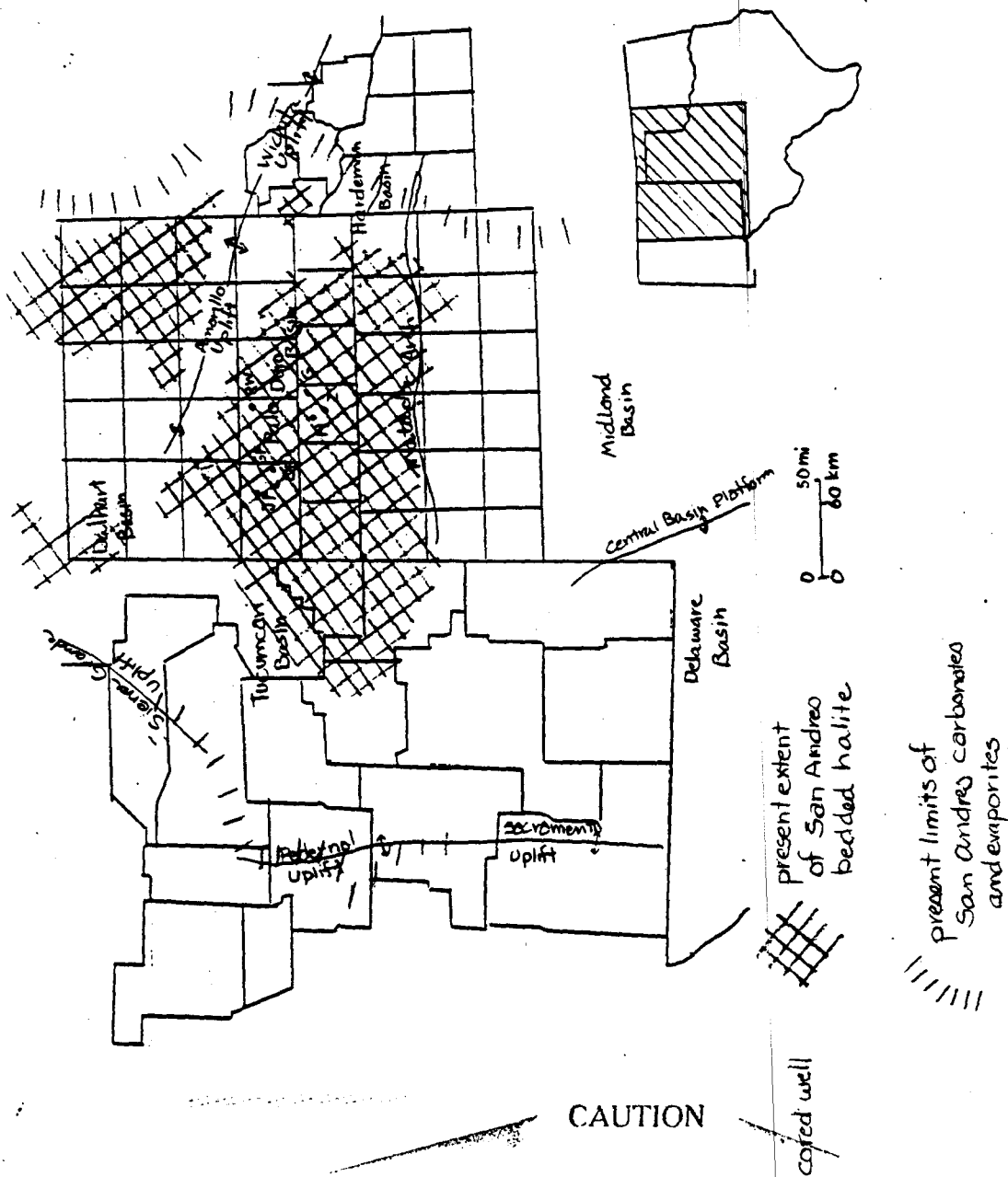


Figure 4. Index map of the Texas Panhandle and southeastern New Mexico showing the locations of the cored wells used in this study, structural elements, and generalized distribution of San Andres facies rocks. Distribution of San Andres facies is compiled from McKee, Oriol, and others (1967), Johnson (1976), and M. A. Fracasso (work map, 1984).

This report describes research carried out by staff members of the Bureau of Economic Geology that addresses the feasibility of the Palo Duro Basin for isolation of high-level nuclear wastes. The report describes the progress and current status of research and tentative conclusions reached. Interpretations and conclusions are based on available data and state-of-the-art concepts, and hence, may be modified by more information and further application of the involved sciences.

DRAFT

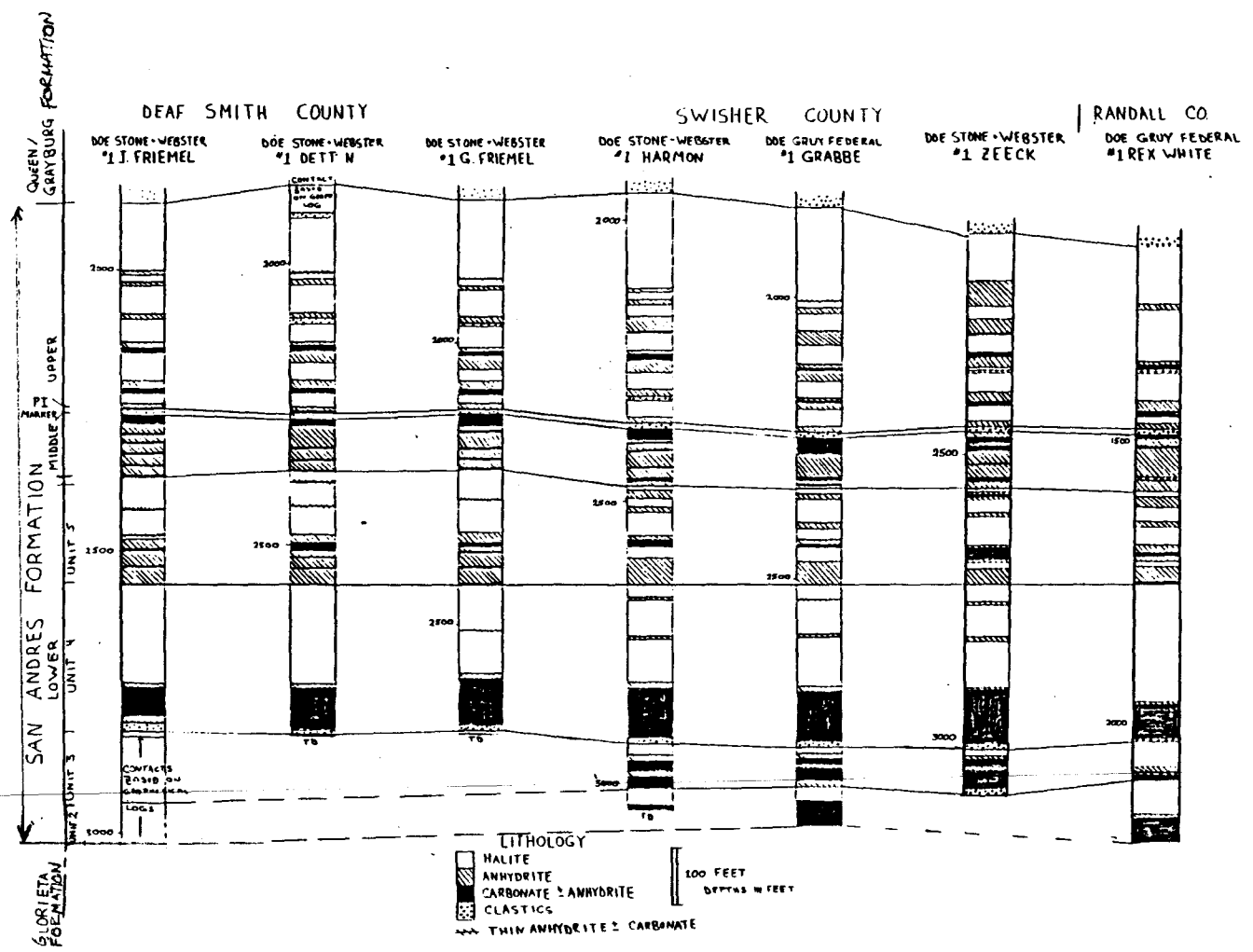


Figure 5. Cross section of the San Andres Formation through the cores used in this study, showing the stratigraphy and the intervals cored.

DRAFT

Key to detailed logs, San Andres units 4 and 5 halite

Column 1 Depths in feet below kelly bushing

PC indicates point count of 100 points over 1 foot interval of slabbed core to check estimated percent lithology.

+ and * indicate sampled interval, core not available during detailed logging and checking.

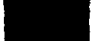
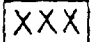




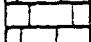
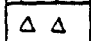

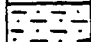
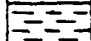

* indicates sample logged by BEG and a detailed description available in BEG files.

+ indicates sample logged, but no detailed description.

Intervals sampled before BEG logging are labeled as "sampled" in column 2

Column 2 Estimated percent lithology

Mineral Composition

	Porosity
	Potash Salt
	Halite
	Anhydrite
	Gypsum
	Dolostone
	Limestone
	Chert
	Sandstone
	Siltstone
	Mudstone
	Claystone

Carbonate Components

G	Grainstone
P	Packstone
W	Wackestone
M	Mudstone

Figure 6. Key to the symbols used in detailed logs of unit 4 and 5 halite.

DRAFT

Carbonate Components (continued)

- oolites or coated grains
- intraclasts
- ⊖ fossiliferous (general)
- molluscs
- crinoids
- ⊖ forams
- ⊖ brachiopods
- A phylloid algae
- ⊖ coral

Column 3 Structures

Sketch of structures in left half of column; interbeds of one lithology in another extend 3/4 of column width; boundaries between lithologies drawn across entire column width.

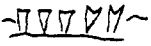
Halite


- ^ ^ ^ chevrons
- ||||| vertically oriented crystals
- ////// dark bands
- ⊖ ⊖ pipe, pits (show residue at bottom)
- ⊖ anhydrite
- ⊖ chaotic mud salt
- ⊖ recrystallized halite
- ⊖ exceptionally coarse halite
- mudstone interbed
- +++++ anhydrite interbed
- discontinuous mudstone interbed
- +++++ discontinuous anhydrite interbed
- // nonhorizontal bedding


DRAFT

Column 3 Structures (continued)

Anhydrite

 gypsum pseudomorphs


 bedding (schematic)


 contorted bedding

 nodular

* crystallotopic

Carbonates

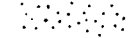
 bedding, scour surface

 wispy lamination

 ripple lamination

 cross beds

 intraclasts

 coarse grainstone

 burrows


 stylolites

Clastics


 lamination

 burrows

 ripple lamination

 disturbed intraclastic fabric

 more disturbed

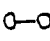







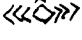

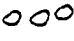

 cross bedding

 dissipation structures

DRAFT

Column 3 Structures (continued)

General

	boudinage
	mudcracks
	clasts
	faulting
	fractures
	birdseye-fabric
	contorted alminae.
	displacive halite hoppers
	skeletal displacive halite
	filled fracture
	nodules (note composition)
	crystallographic anhydrite in other lithologies

Column 4 Comments

A. At left edge letters A through F indicate halite rock types.

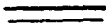
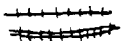


Halite Types

- A bedded halite with chevron fluid inclusions
- B bedded halite with vertically oriented crystals
- D chaotic mudsalt
- E recrystallized muddy halite
- F recrystallized halite with interstitial anhydrite
- G displacive halite in sediment
- H coarse recrystallized cavity fill halite
- I fibrous fracture fill

See table and text for description of halite classification.

DRAFT

B. Location, irregularity and estimated continuity of mudstone and anhydrite interbeds in halite.

 mudstone
 anhydrite
 irregular base, flat top
 discontinuous beds

C. Comments on interbeds

M indicates mudstone

A indicates anhydrite Z indicates siltstone

bed thickness shown

5A indicates 5 anhydrite interbeds too closely spaced to show individually, estimated percent impurities shown.

DRAFT

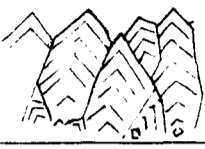
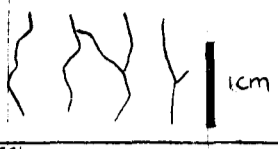
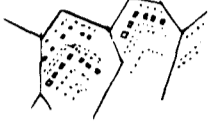
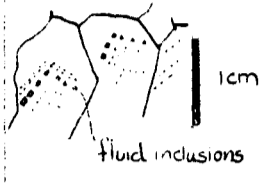
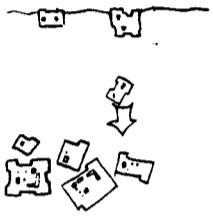

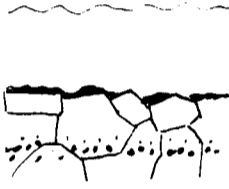
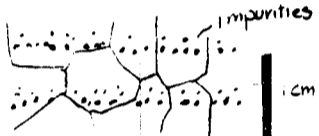

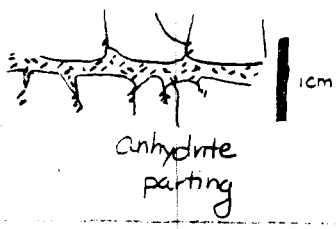
Depositional Processes	Description	Resulting Fabrics	Described by
	VERTICALLY-ORIENTED CRYSTALS Competition for space among crystals growing on a brine pool floor		Arthurton, 1973 Holdaway, 1978 Shearman, 1970 Wardlaw and Schwerdtner, 1966
	CHEVRON STRUCTURES Fluid inclusions trapped during crystal growth reflect variation in crystal growth rate		Wardlaw and Schwerdtner Shearman, 1970 Roedder, 1982
	CUMULATES Crystals form rapidly at the air/brine interface. When capillary forces holding them at the surface are broken, they fall to the brine pool floor		Arthurton, 1973 Dellwig, 1955
	COLOR-BANDED HALITE Impurities including gypsum, organic material, and argillaceous material deposited within halite		Dellwig, 1955
	DISSOLUTION SURFACE Flooding with brine not saturated with halite causes truncation of halite crystals. Gypsum may be precipitated before halite precipitation resumes		Wardlaw and Schwerdtner 1966 Adams, 1969, p 102 Arthurton, 1973 Dellwig, 1955 Holdaway, 1978 Shearman, 1970

Figure 7. Summary of halite fabrics in the San Andres Formation comparing the fabrics seen in the San Andres with fabrics produced by modern or experimental halite precipitation. Papers discussing origins of ancient and modern halite fabrics are cited.

DRAFT



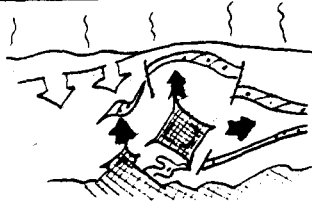
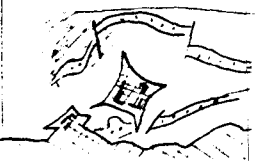


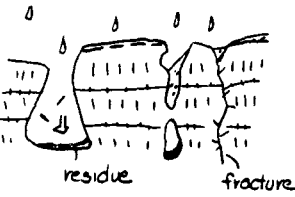
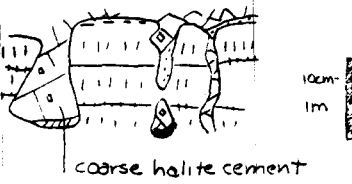

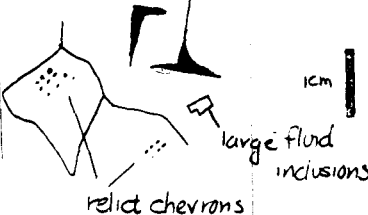
Depositional Processes	Description	Resulting Fabrics	Described by
	<p>MUDSTONE INTERBEDS</p> <p>Influx of mudstone may occur when the halite flat is either dry or flooded. Transporting process may be eolian, fluvial or subaqueous.</p>		<p>Hordie and others, 1978 Adams, 1969, p96 Handford, 1981</p>
	<p>DISPLACIVE HALITE</p> <p>As salinity of interstitial brine increases, skeletal mud inclusive halite crystals precipitate.</p>		<p>Gornitz and Schreiber, 1981 Handford, 1981 Holdaway, 1978 Southgate, 1982</p>
	<p>HALOTURBATION</p> <p>During salinity drops, halite is dissolved. Alternating growth and dissolution of halite disturbs fabric in mudstones.</p>		<p>Smith, 1971 Holdaway, 1978 Handford, 1981</p>
 <p>residue fracture</p>	<p>HALITE KARST</p> <p>Low salinity water dissolves vertical pits and pipes.</p>	 <p>coarse halite cement</p>	<p>Hunt and others, 1966, p82 Shearman, 1970 Weiler and others 1974</p>
	<p>RECRYSTALLIZATION</p> <p>Small crystals aggrade, grain boundary migration.</p>	 <p>relict chevrons large fluid inclusions</p>	<p>Adams, 1969, p39</p>

Figure 7. (continued)

DRAFT

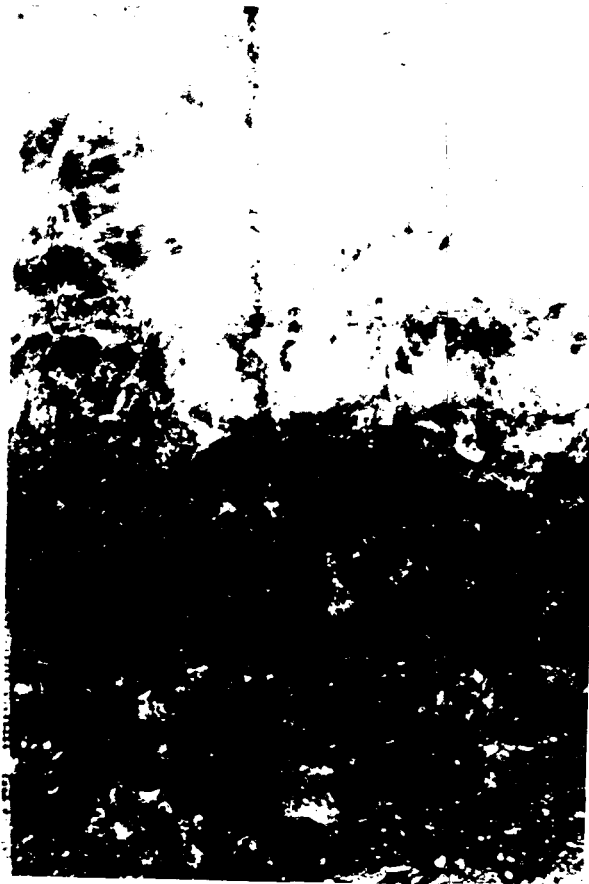


Figure 8. Elongated, vertically oriented halite crystals are visible in an etched slab because they are rimmed by anhydrite (white). Slab from San Andres unit 4, Stone and Webster No. 1 J. Friemel core, 2,673 feet, width 7.5 cm.

DRAFT

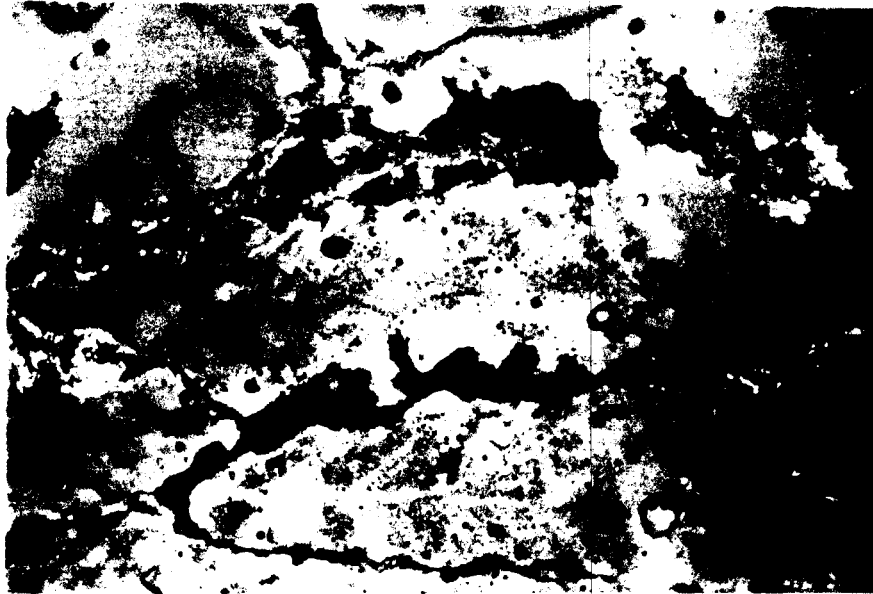


Figure 9. Elongated, vertically oriented halite crystals (gray) with abundant, weakly zoned fluid inclusions are rimmed with anhydrite (dark). Thin section from San Andres unit 4, Stone and Webster No. 1 G. Friemel core, 2,546.6 feet, width 5 mm, partly crossed nicols.

DRAFT



Figure 10. Cubic halite crystals less than a millimeter across are preserved only within an anhydrite matrix. Fluid inclusions within the crystals define poorly formed lamination. These small, randomly oriented crystals may have formed at the sediment/water interface and foundered when they became too heavy to be suspended by capillary forces. Thin section from San Andres unit 4, Stone and Webster No. 1 G. Friemel core, 2,325.2 feet, width 3.25 mm, partly crossed nicols.



Figure 11. Small halite cubes in anhydrite matrix are aligned and may have formed as floating rafts of cubes at the air-brine interface. Thin section from San Andres unit 4, Stone and Webster No. 1 G. Friemel core, 2,512.3 feet, width 7.7 mm, partly crossed nicols.



Figure 12. Equant mosaic halite with small, randomly scattered fluid inclusions within crystals and minor anhydrite along grain boundaries. Note that grain boundaries are triple junctions, suggesting, by analogy with similar fabrics in carbonates, that some recrystallization has taken place. Thin section from San Andres unit 4, Stone and Webster No. 1 G. Friemel core, 2,466 feet, width 7.7 mm, partly crossed nicols.



Figure 13. Fluid inclusions concentrated along regularly-spaced relict growth faces of bottom nucleated crystals are called chevron structures when the crystals oriented with the cube corners upward grew in preference to those in other orientations. Thin section from San Andres unit 5, Stone and Webster No. 1 Mansfield core, 1,377.0 feet, width 7.7 mm, plane light.

2247



Figure 14. Coronets are similar to chevrons, but crystals with cube faces upward are growing preferentially to other orientations. In this example, the coronets are nucleated on detrital halite cubes or foundered rafts which were deposited with cube faces on the brine pool floor. Thin section from San Andres unit 4, Stone and Webster No. 1 G. Friemel core, 2,512.3 feet, width 7.7 mm, partly crossed nicols.

DRAFT

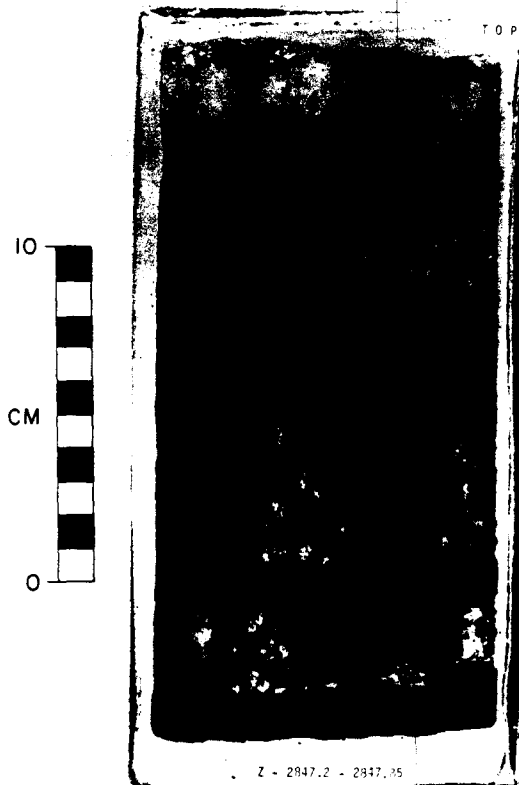


Figure 15. Color banding due to alteration of anhydritic, fluid inclusion-rich, white halite with dark halite pigmented by clay, organic matter, and anhydrite. The dark bed at the base of the slab is an anhydritic mudstone bed. The 1 cm thick slab is 10 cm wide and is mounted on plexiglass so that the photograph could be taken in both transmitted and reflected light. Core from Stone and Webster No. 1 Zeck well, depth 2,847.2 to 2,847.8 feet.

CAUTION

This report describes research carried out by staff members of the Bureau of Economic Geology that addresses the feasibility of the Palo Duro Basin for isolation of high-level nuclear wastes. The report describes the progress and current status of research and tentative conclusions reached. Interpretations and conclusions are based on available data and state-of-the-art concepts, and hence, may be modified by more information and further application of the involved sciences.

DRAFT



Figure 16. Chevron structures have been truncated by a corrosion surface. Anhydrite, probably deposited from the lower salinity water which caused the corrosion forms a parting along the truncation surface and along zones of permeability or former open spaces between halite crystals. Thin section from San Andres unit 4, Stone and Webster No. 1 G. Friemel core, 2,522.0 feet, width 7.7 mm, partly crossed nicols.

DRAFT

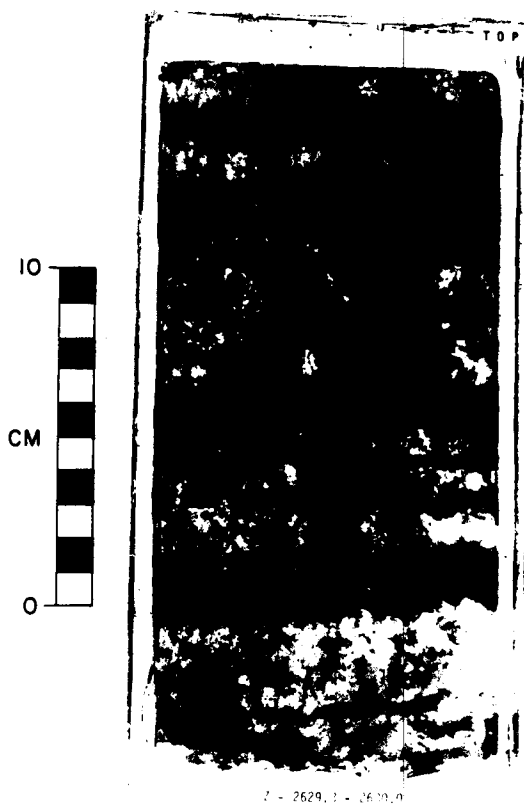


Figure 17. Vertical features visible as lighter recrystallized halite in banded chevron halite are known as pipes. Slab mounted on plexiglass from San Andres unit 4, Stone and Webster No. 1 Zeeck core, 2,629.3 to 2,630.3 feet is 10 cm wide.

DRAFT

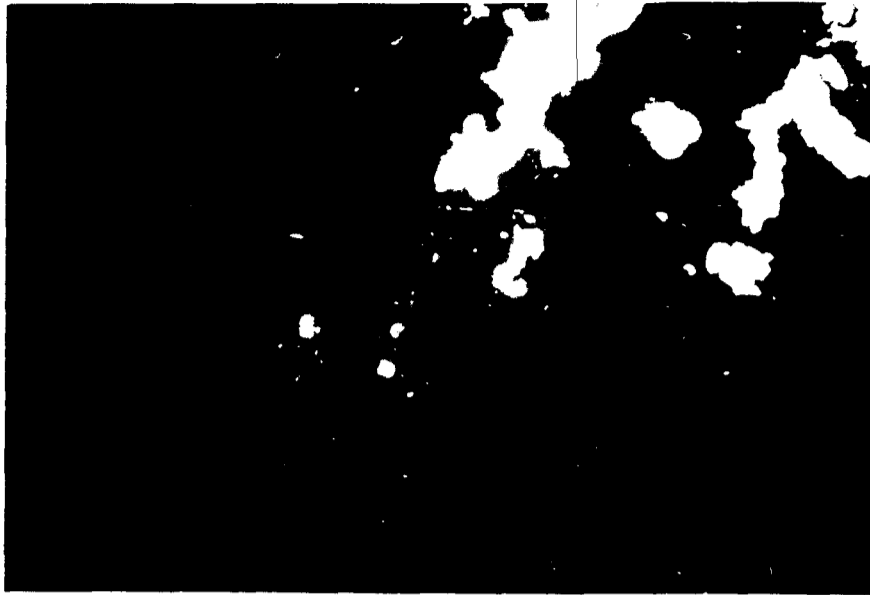


Figure 18. Anhydritic, fluid inclusion rich host halite on the right of the photograph has been truncated by a pipe filled with clear halite with sparse, large fluid inclusions on the left. Thin section from San Andres unit 5, Stone and Webster No. 1 G. Friemel core, 2,222.9 feet, width 7.7 mm, partly crossed nicols.

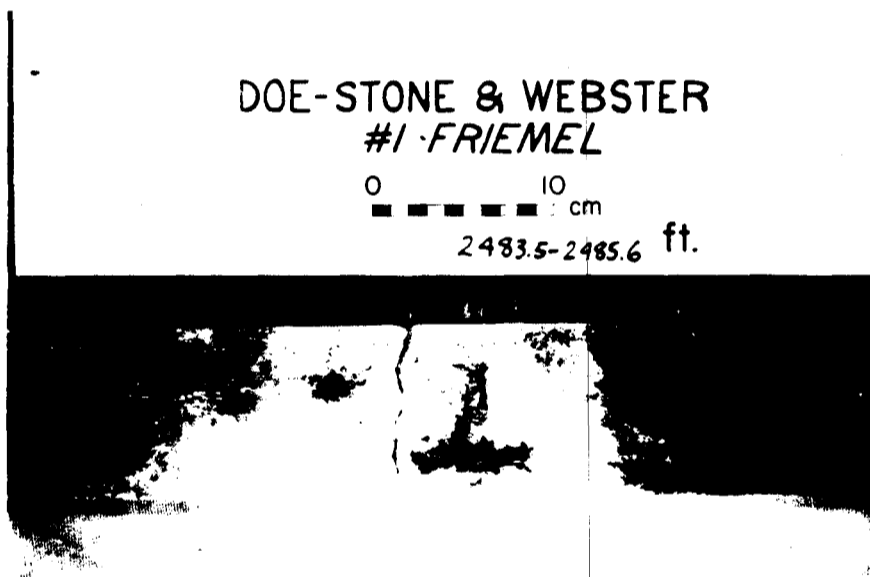


Figure 19. Mudstone (dark) fills several pipes in white chevron halite. The pipes are slightly sinuous tubes which cut across the slabbed face of the core, making them appear to be discontinuous. A dark bed of muddy halite is overlain by a mudstone bed at the top of the core. The pipes are truncated at this bed, suggesting that the mudstone in the pipes may have been supplied during deposition of the mudstone bed. San Andres unit 4 from the Stone and Webster No. 1 J. Friemel core, 2,483.5 to 2,485.6 feet. Core is 10 mm wide.

DRAFT



Figure 20. A large pit in muddy halite has a dark anhydritic mudstone (M) on its floor and is filled with coarse, clear halite. The slab from the Stone and Webster No. 1 Mansfield core, 1,726.0 to 1,726.4 feet is mounted on plexiglass and shown in partly transmitted, partly reflected light. The core is 10 cm wide.

DRAFT

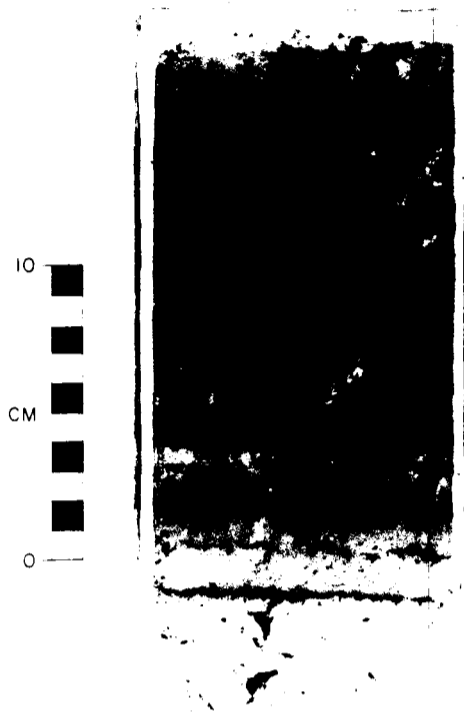


Figure 21. A pit with a complex shape in banded, chevron halite is partly filled with dark, anhydritic mudstone and partly filled with clear halite. The slab from the Stone and Webster No. 1 Detten core, 2,713.5 to 2,714.2 feet is mounted on plexiglass and shown in partly transmitted, partly reflected light. The core is 10 cm wide.

DRAFT

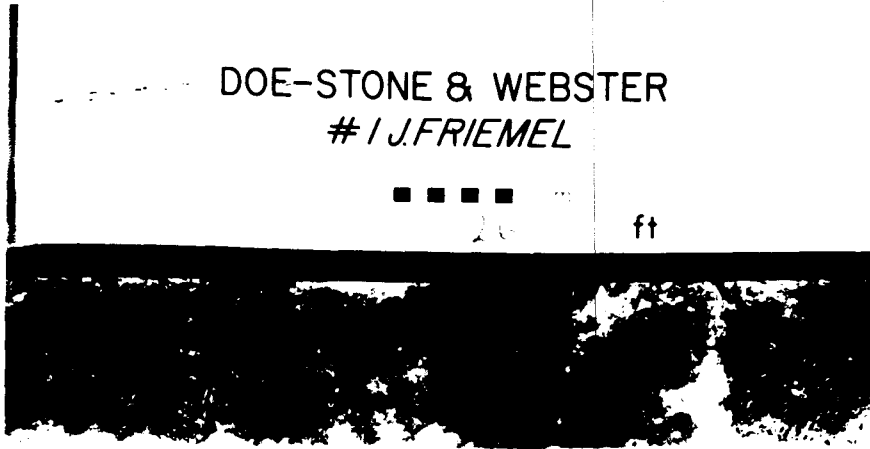


Figure 22. Color bands in halite are tilted at an angle of 16 degrees from horizontal. This deformation influences only about 20 cm of core with overlying and underlying beds undeformed and is interpreted as an early karst collapse block. The pit into which collapse occurred is not visible in core. The core from the Stone and Webster No. 1 J. Friemel well, 2,611.0 feet is 10 cm wide.



Figure 23. Halite along grain boundaries lacks chevron structures. This absence of this primary fabric along most grain boundaries is attributed to recrystallization during diagenesis. Thin section from San Andres unit 5, Stone and Webster No. 1 G. Friemel core, 2,243.6 feet, width 3.25 mm, partly crossed nicols.

DRAFT



Figure 24. The acicular shape and random orientation of crystals of anhydrite within halite are evidence that the anhydrite is a diagenetic rather than a detrital phase. Thin section from San Andres unit 4, Stone and Webster No. 1 G. Friemel core, 2,504.3 feet, width 0.85 mm, crossed nicols.



Figure 25. Crystals of limpid dolomite along grain boundaries in halite are diagenetic phases. Note the unusual, stumpy crystal shape due to the expression of many crystal faces. Thin section from San Andres unit 5, Stone and Webster No. 1 G. Friemel core, 2,294.6 feet, width 0.85 mm, crossed nicols.

DRAFT



Figure 26. Zones of dense fluid inclusions alternate with zones lacking in fluid inclusions to define chevron structures. Thin section from San Andres unit 5, Stone and Webster No. 1 G. Friemel core, 2,312.0 feet, width 3.25 mm, partly crossed nicols.



Figure 27. Vertical orientation of chevron crystals is interpreted as a result of the most rapid growth of the crystals which are oriented with corners upward. The chevrons have been recrystallized along grain boundaries. Thin section from San Andres unit 4, Stone and Webster No. 1 G. Friemel core, 2,467.8 feet, width 5 mm, partly crossed nicols.

DRAFT



Figure 28. Halite crystals with chevron structures are oriented with long axes and chevron corners oblique to vertical. This may reflect growth as rosettes, probably nucleated on detrital halite crystals which were deposited with cube faces on the brine pool floor. The dark material is the anhydrite matrix. Thin section from San Andres unit 4, DOE - Gruy Federal No. 1 Rex White core, 1,880 feet, width 7.7 mm, plane light.

DRAFT

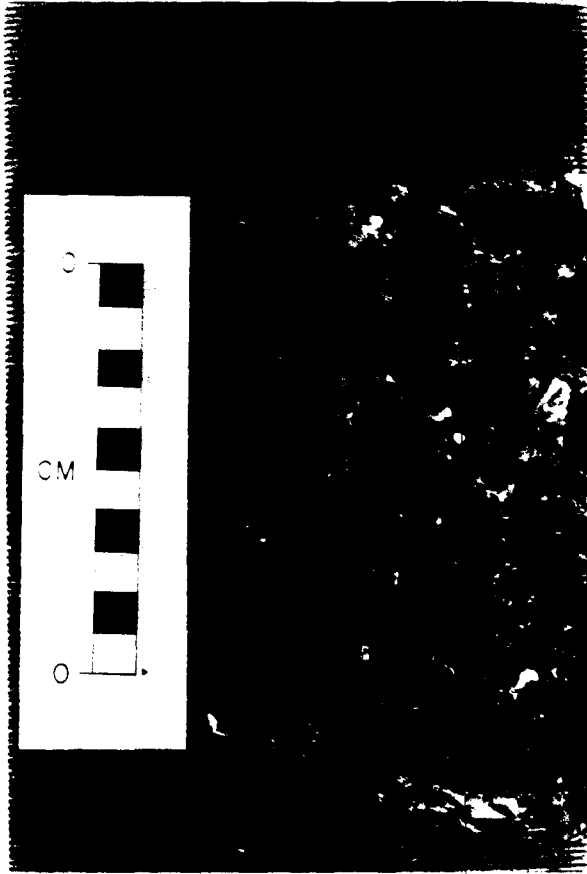


Figure 29. Mudstone and halite mixed without any definition of bedding is called chaotic mudstone-halite. In this example, the halite crystals are dark and anhedral, and the mudstone is structureless with abundant small, white anhydrite modules. Core is from San Andres unit 4 in the Stone and Webster No. 1 Zeek well, depth 2,802 feet.

DRAFT



Figure 30. Typical chaotic mudstone-halite with euhedral halite crystals (gray). Minor amounts of white anhydrite and dolomite rim some mudstone masses. Thin section from San Andres unit 4, Stone and Webster No. 1 G. Friemel core, 2,513.4, width 7.7 mm, partly crossed nicols.

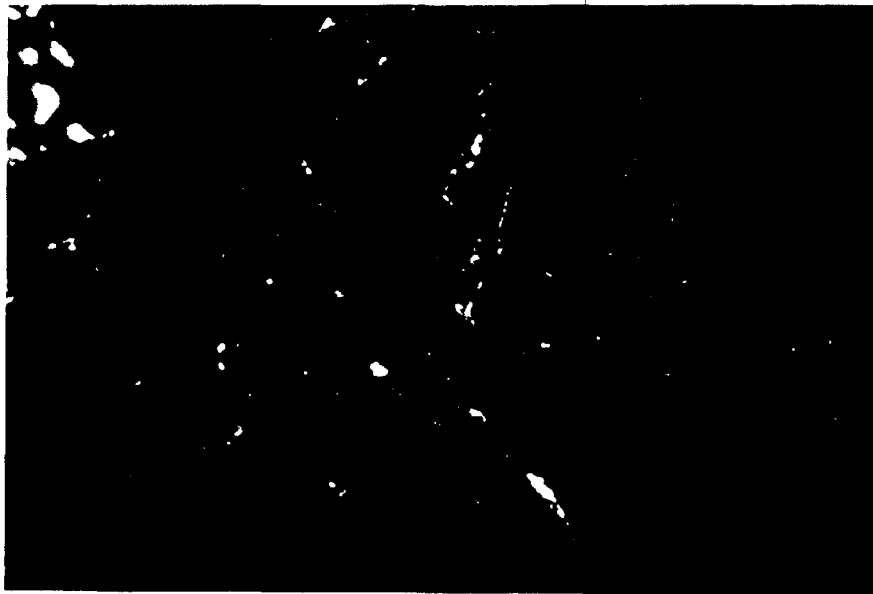


Figure 31. Typical chaotic mudstone-halite texture with anhedral, corroded-looking halite crystals. Thin section from San Andres unit 5, Stone and Webster No. 1 G. Friemel core, 2,317.6 feet, width 7.7 mm, partly crossed nicols.

DRAFT

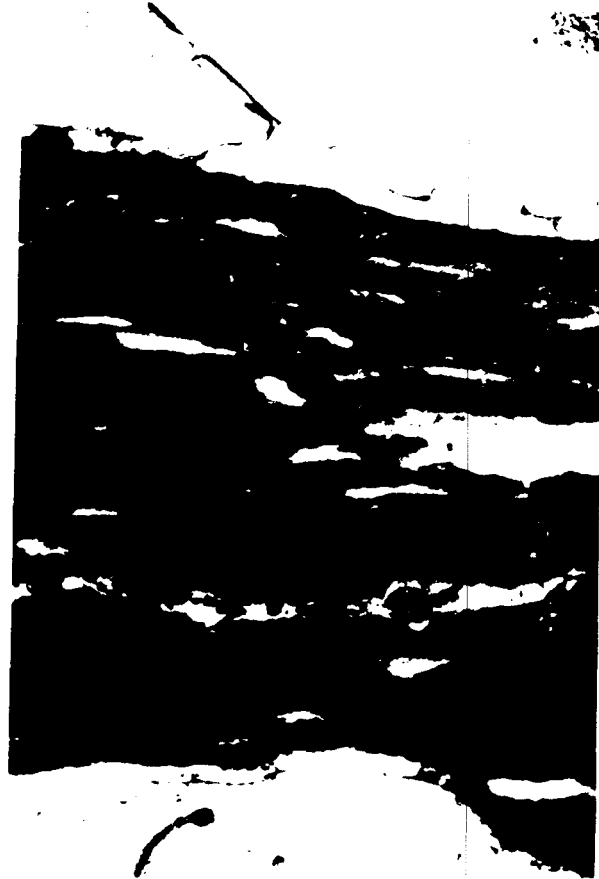


Figure 32. Mudstone mass (dark) in chaotic mudstone-halite contains elongated anhydrite nodules (A) showing the deformed character of mudstone. Thin section from San Andres unit 4, Stone and Webster No. 1 Mansfield core, 1,545 feet, width 3.25 mm, plane light.

DRAFT

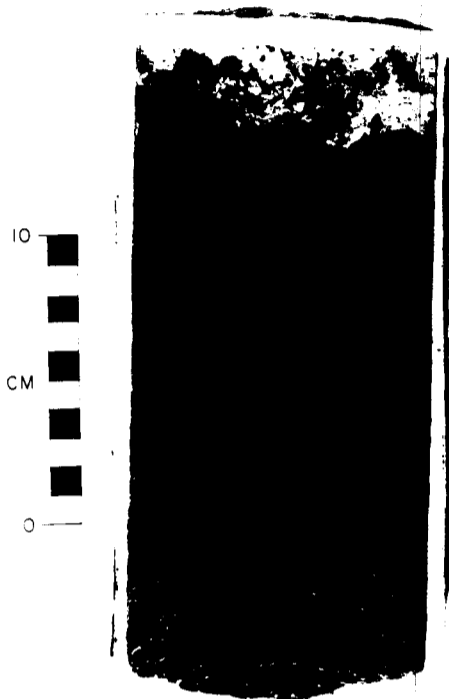


Figure 33. Finely crystalline halite and mudstone evenly mixed in subequal amounts is an unusual texture in the San Andres Formation. Slab, 10 cm wide from San Andres unit 4, DOE - Gruy Federal No. 1 Grabbe core, depth 2,578.3 to 2,579.1 feet.

DRAFT

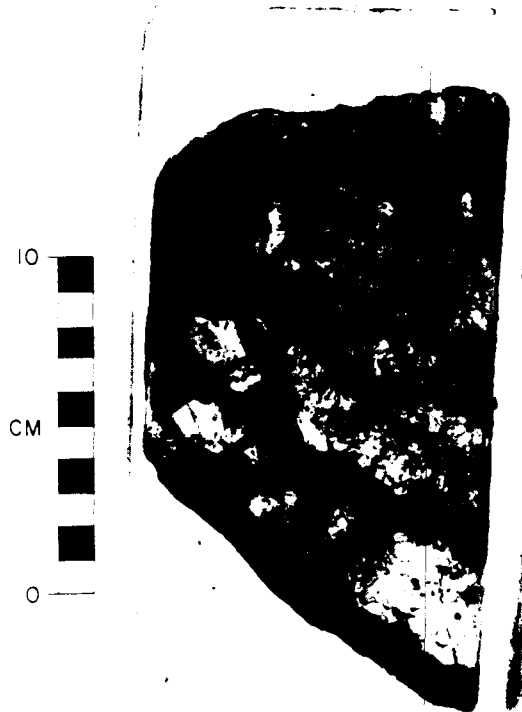


Figure 34. Chaotic mudstone-halite has areas with partly preserved primary fabric. Note the light-colored anhydritic areas in the upper and lower part of the slab where primary fabric is preserved. The slab is from San Andres unit 5 of the Stone and Webster No. 1 Mansfield core, 1,726.5 to 1,726.9 feet and is mounted on plexiglass and shown in partly transmitted, partly reflected light. The core is 10 cm wide.

DRAFT

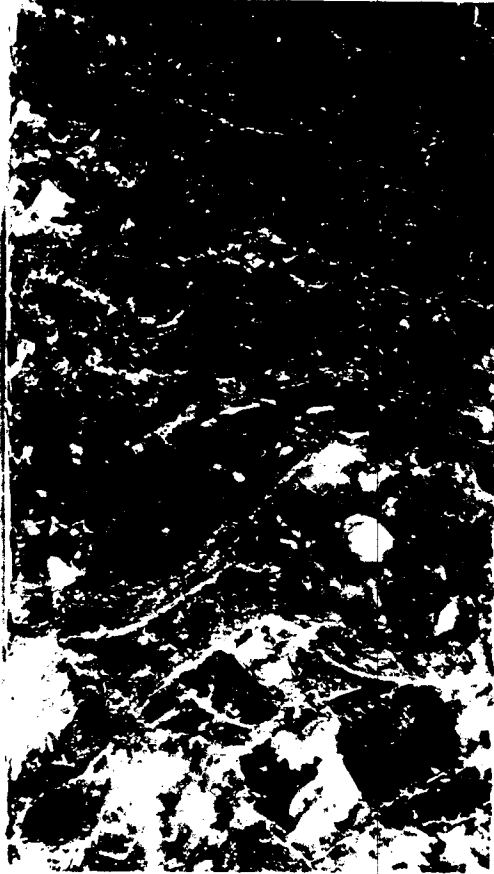


Figure 35. Dish shaped mudstone masses in chaotic mudstone halite are interpreted as former karst pit floors where the host halite has been recrystallized and lost all of its primary fabric. Core from San Andres unit 5 in the Stone and Webster No. 1 G. Friemel core, 2,229 to 2,230.8 feet.

DRAFT

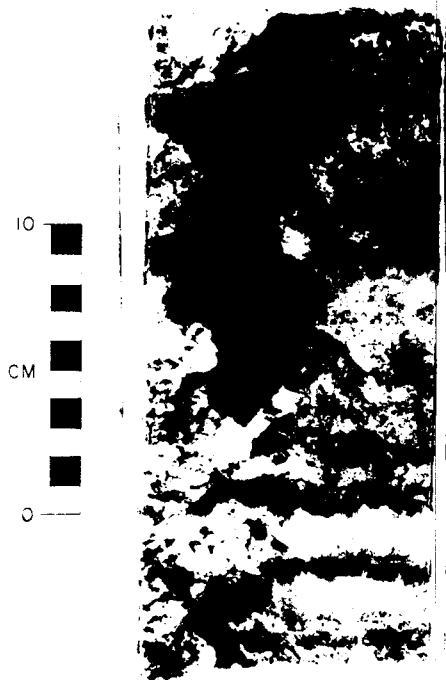


Figure 36. A pit in bedded chevron halite has been filled with a first generation of clear halite cement (1), a second generation of anhydritic mudstone (2), and a third generation of euhedral displacive halite crystals within the mudstone (3). The slab is from the upper San Andres of the Stone and Webster No. 1 Zeack core, 2,039.4 to 2,040.1 feet and is mounted on plexiglass and shown in partly transmitted, partly reflected light. The core is 10 cm wide.

DRAFT

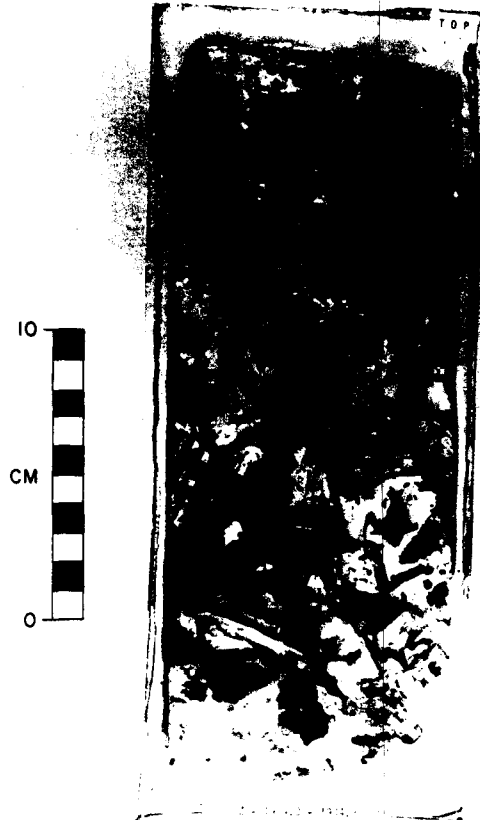


Figure 37. Equant, muddy halite rock is composed of coarse clear halite with impurities of mudstone, and in this sample, anhydrite. Large fluid inclusions (I) are abundant. The largest inclusion was breached when the slab was cut and has been filled with dark epoxy. The slab from the upper San Andres of the Stone and Webster No. 1 Zeack core, depth 1,904.0 to 1,904.8 feet is mounted on plexiglass and is shown in transmitted and reflected light.

DRAFT

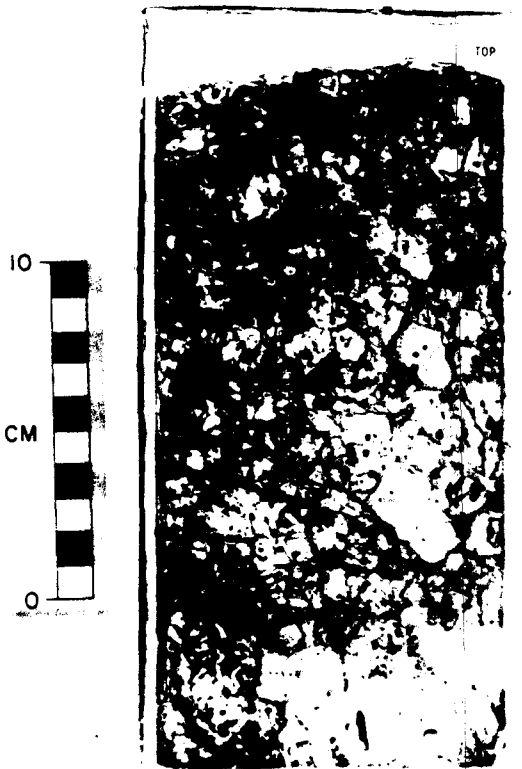


Figure 38. Equant, anhydritic halite rock is composed of equant crystals of halite. Compare the right side of the core, where anhydrite (white) is the dominant impurity, to the left side of the core where the dark areas are mudstone masses within and between crystals forming equant muddy halite rock. Most of the dark areas in the anhydritic part of the slab were fluid inclusions which were breached and filled with grit during slab preparation. The slab from San Andres unit 4 of the DOE-Gruy Federal No. 1 Grabbe core, depth 2,587.0 to 2,787.7 feet is mounted on plexiglass and is shown in transmitted and reflected light.

DRAFT

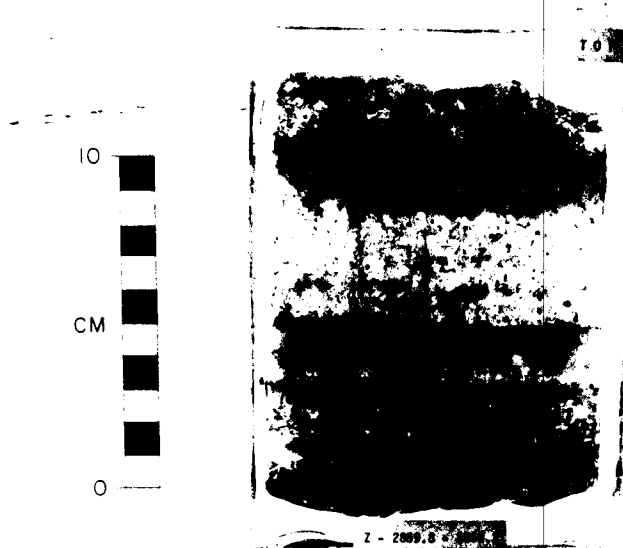


Figure 39. Bedding in chevron halite is defined by partings marked by anhydrite and dark impurities. The initial layer of halite above the parting is clear, equant halite, which becomes cloudy with fluid inclusions defining chevrons toward the top of the layer. The slab from San Andres unit 4 of the Stone and Webster No. 1 Zeck core, depth 2,859.8 to 2,860.2 feet is mounted on plexiglass and is shown in transmitted and reflected light.



Figure 40. Displacive cubes of halite in a muddy siltstone bed have inclusions of muddy siltstone within them. The zonation within the muddy siltstone indicate that episodes of displacive growth of halite alternated with episodes of non-displacive cementation. Thin section from the San Andres unit 4 in the DOE-Gruy Federal No. 1 Rex White core, 1,879 feet, plane light, width 7.7 mm.

DRA



Figure 41. Slightly skeletal halite crystals (dark) in a silty mudstone bed with highly disturbed to intraclastic bedding have elongated corners relative to cube centers. Slab from the San Andres unit 4 in the DOE-Gruy Federal No. 1 Rex White core, depth 1,807 feet. Photograph by Laura Elliott.



Figure 42. Skeletal halite growing preferentially in a clayey laminae within a lens of mudstone in an anhydrite bed. Thin section from the San Andres unit 4 in the Stone and Webster No. 1 G. Freimel core, 2,583.6 feet plane light, width 7.7 mm.

DRAFT



Figure 43. Coarse, clear halite is interpreted as cement filling a large karst cavity. In this example, the cavity is larger than the core width, allowing precipitation of very coarse crystals. The core is from the San Andres unit 4 of the Stone and Webster No. 1 Mansfield well, depth 1,689 to 1,686 feet.

CAUTION

This report describes research carried out by staff members of the Bureau of Economic Geology that addresses the feasibility of the Palo Duro Basin for isolation of high-level nuclear wastes. The report describes the progress and current status of research and tentative conclusions reached. Interpretations and conclusions are based on available data and state-of-the-art concepts, and hence, may be modified by more information and further application of the involved sciences.

DRAFT

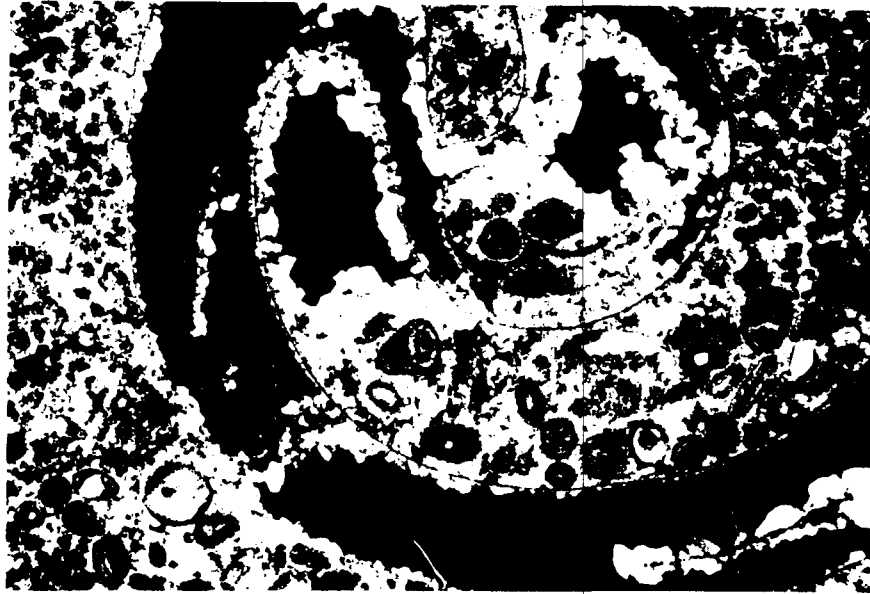


Figure 44. Halite cement (black) fills a gastropod mold. Thin section from the San Andres unit 4 carbonate in the DOE-Gruy Federal No. 1 Grabbe core, 2,854.3 feet, crossed nicols, width 7.7 mm.

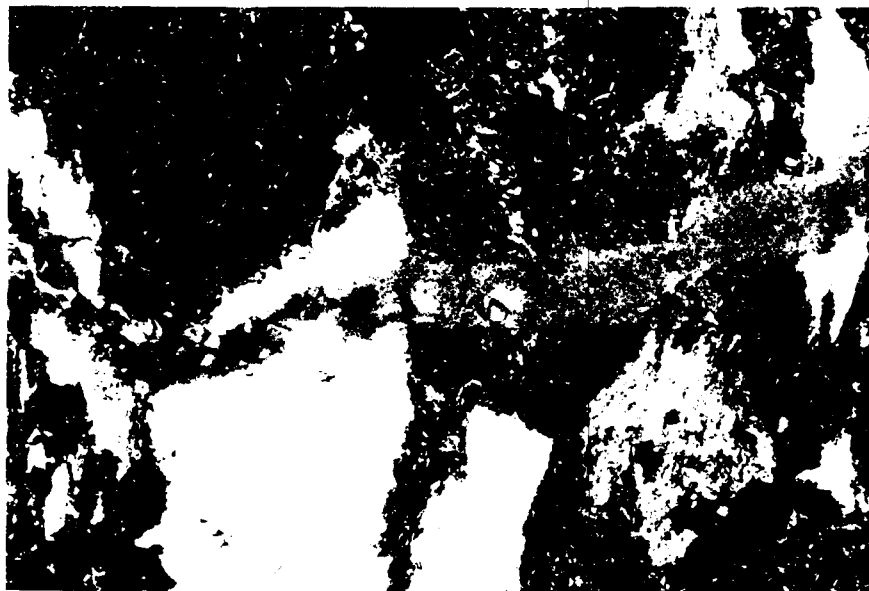


Figure 45. A halite-filled fracture (gray) cutting mudstone (dark) and anhydrite nodules (white). Thin section from the San Andres unit 5 in the Stone and Webster No. 1 G. Friemel core, 2,283.0 feet, partly crossed nicols, width 5 mm.

DRAFT

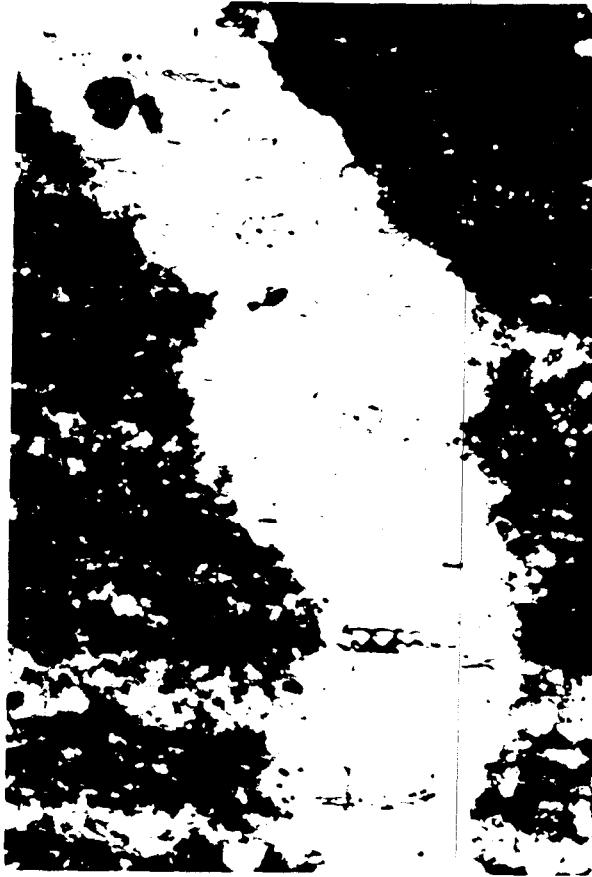


Figure 46. The halite in the halite-filled fracture is composed of horizontal fibers. Blades of anhydrite project from the walls and are oriented parallel to the halite fibers. Thin section from the Stone and Webster No. 1 Mansfield core, 1,582.4 is 0.85 mm wide and shown in partly crossed nicols.

DRAFT

DOE-STONE & WEBSTER

#1 HARMON



2483

ft.



Figure 47. Halite has pseudomorphously replaced large gypsum crystals in ripple laminated, dolomitic anhydrite. Lamination marking relict growth surfaces are preserved within the halite crystals. Core from the uppermost anhydrite bed in the San Andres unit 5 in the Stone and Webster No. 1 Harman core, 2,483 feet, core width 10 cm.

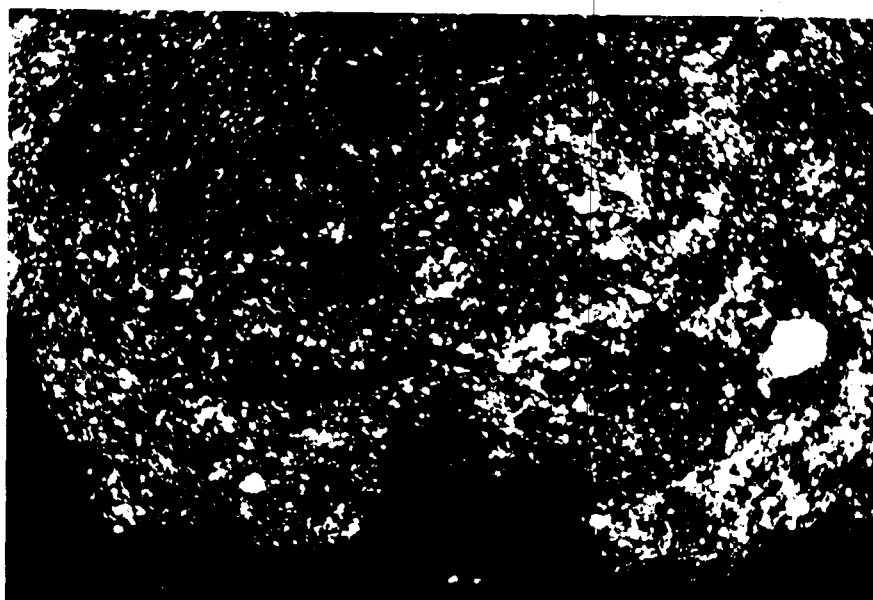


Figure 48. Typical red-brown mudstone composed of angular, silt-sized quartz and feldspar, red-brown clay, anhydrite, and minor silt-sized dolomite. Irregular contact at the base of the slide is between the mudstone and the underlying halite. Thin section from the San Andres unit 4 in the Stone and Webster No. 1 G. Friemel core, 2,548.2 feet, crossed nicols, width 7.7 mm.

DRA



Figure 49. Fine ripple lamination in siltstone with mudstone drapes. Mudcracks or possible molds of halite crystals (M) truncate lamination in the middle mudstone bed. Fabric in the upper mudstone bed has been disturbed by soft sediment microfolding and faulting. Core from San Andres unit 4 in the Stone and Webster No. 1 Mansfield well, depth 1,583 feet. Core is 10 cm wide.

DRAFT



Figure 50. Photomicrograph of fine ripple lamination in the same interval as shown in Figure 46. Silty ripples are separated by thick clay drapes. White cracks are artifacts of drying and sampling of the core. Thin section from the San Andres unit 4 in the Stone and Webster No. 1 Mansfield core, 1,582.4 feet, plane light, width 7.7 mm.

DR



Figure 51. Two slightly deformed ripple-laminated siltstone beds are within halite with fairly well-preserved primary fabric, including chevrons and vertically-oriented crystals. Slab from San Andres unit 4 from the Stone and Webster No. 1 J. Friemel core, depth 2,673.3 to 2,673.8 feet. Core is 10 cm wide.

DRAFT



Figure 52. A mudstone interbedded in halite has disturbed fabric and abundant small anhydrite nodules (white) in the lower centimeter of the bed, overlain by ripple-laminated siltstone and clay drapes. The base of the bed has been deformed and enriched in anhydrite by the dissolution of a minor amount of the underlying halite during deposition of the bed. Note the silt-filled mold of a cubic halite crystal (M) within the clay drape. Thin section from the San Andres unit 4 in the Stone and Webster No. 1 G. Friemel core, 2,500.6 feet, partly crossed nicols, width 0.85 mm.



Figure 53. Intraclastic siltstone (light color) fills a mold of a halite crystal in rippled clayey siltstone. The fabric of siltstone and the overlying clayey layer have both been disrupted by dissolution of the halite. Thin section from the San Andres unit 4 in the Stone and Webster No. 1 Mansfield core, 1,583.9 feet, plane light, width 7.7 mm.

DRAFT

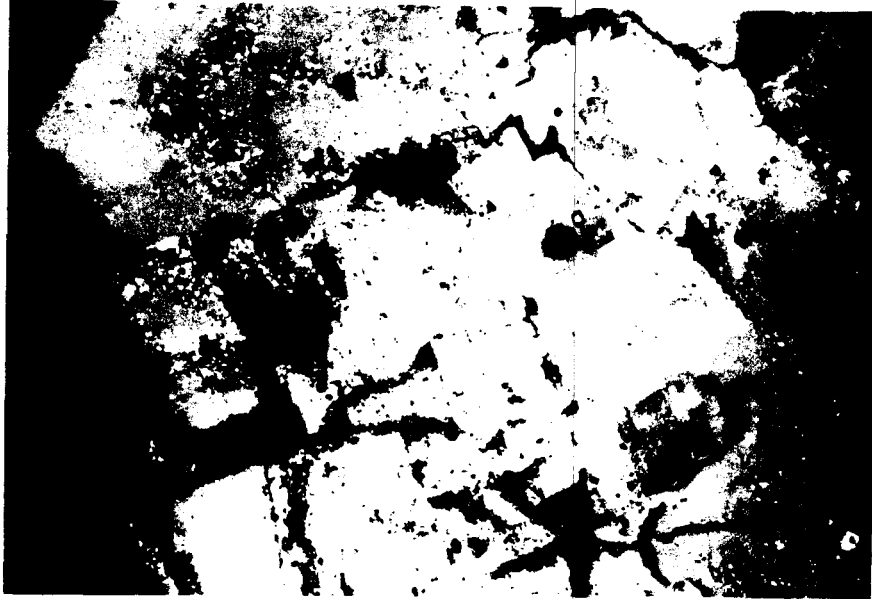


Figure 54. The contact between halite (gray) and a muddy siltstone interbed is gradational. In the lower part of the photo fluid inclusions chevron structures in anhydritic halite indicate deposition on the brine-pool floor. The upper part of the halite, however, has inclusions of muddy siltstone indicating that this halite may have grown displacively into the overlying mudstone bed. Thin section from the San Andres unit 4 in the Stone and Webster No. 1 G. Friemel core, 2,556.4 feet, partly crossed nicols, width 7.7 mm.

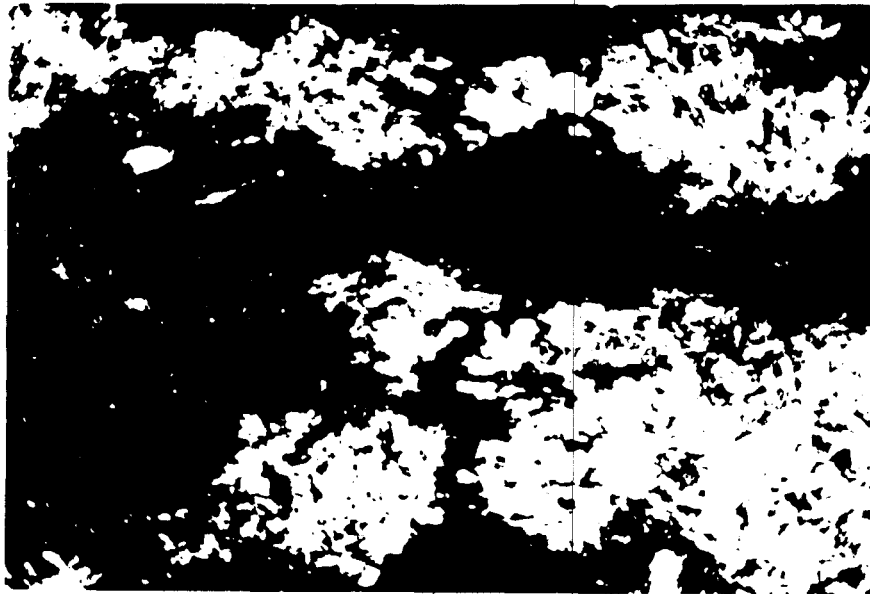


Figure 55. A fracture in mudstone has cut several anhydrite nodules, but the anhydrite nodules have partly healed themselves. Dark areas are fibrous halite filling the fracture. Thin section from the San Andres unit 4 in the Stone and Webster No. 1 G. Friemel core, 2,431.9 feet, crossed nicols, width 3.25 mm.

DRAFT



Figure 56. Well-formed load cast structures in dark, dolomite-siliciclastic mudstone at the base of San Andres unit 4 in the Stone and Webster No. 1 G. Friemel well. Width of the unslabbed core is 10 cm.

DRAFT

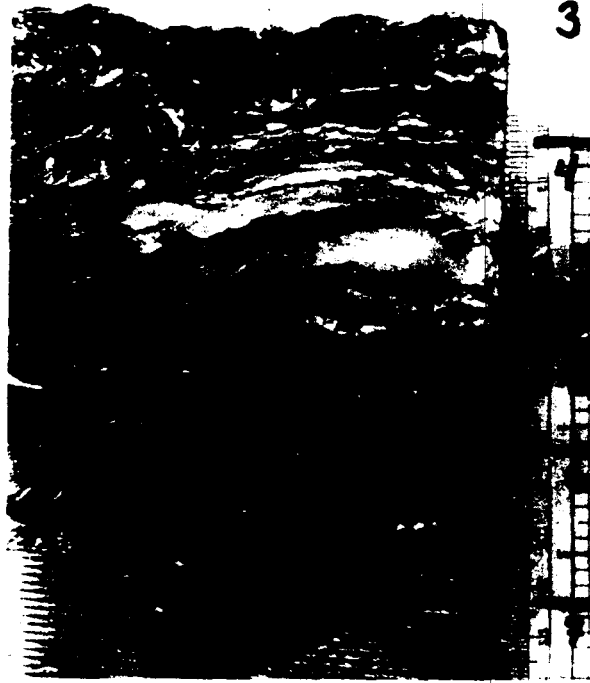


Figure 57. Small scale, soft sediment microfaults deform a thin siltstone residue beneath an anhydrite bed within San Andres unit 4 halite. Slabbed core from the Stone and Webster No. 1 Zeeck well, depth 2,563 feet is 10 cm wide.

DRAFT

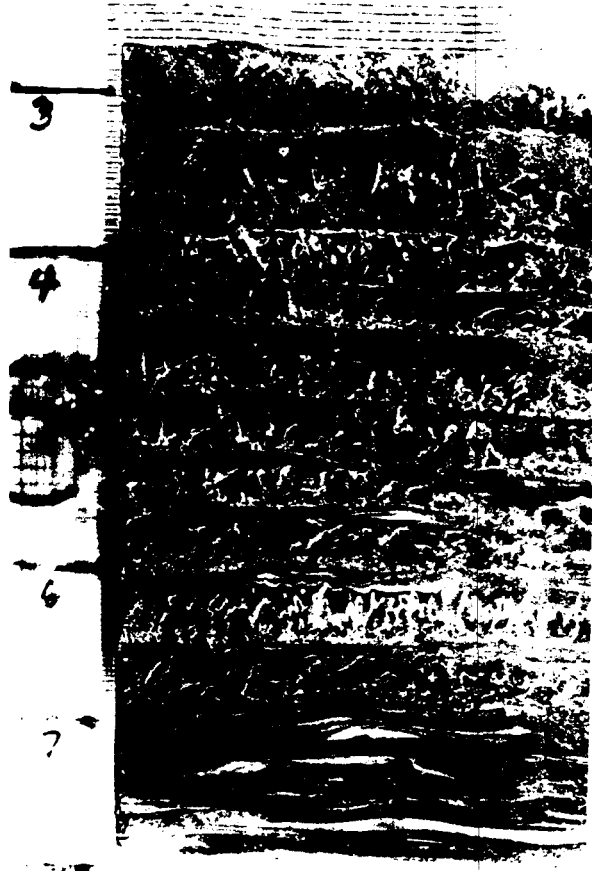


Figure 58. Starved ripple-laminated dark mudstone at the base of an anhydrite bed. The anhydrite contains halite pseudomorphs after bottom nucleated gypsum crystals as well as starved ripple lamination. Slabbed core from San Andres unit 4 in the Stone and Webster No. 1 Zeeck well, depth 2,826 feet.

DRAFT

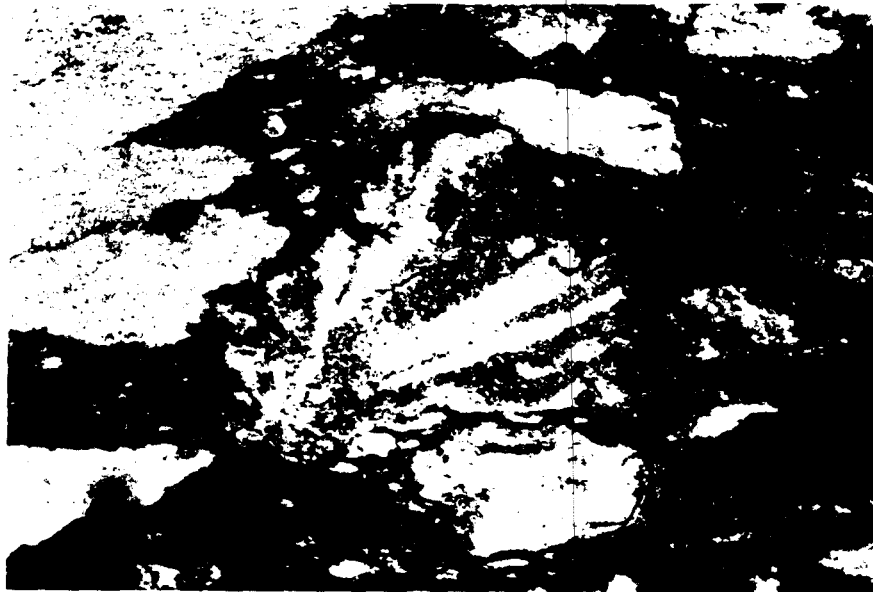


Figure 59. Anhydrite nodules within dark mudstones at the base of the lowest cycle in unit 5 contain relict pseudomorphs after gypsum crystals, suggesting that they originated by fragmentation of thin anhydrite beds. Compare the fabric in this residue to the unaltered anhydrite bed in figure 61. Thin section from the Stone and Webster No. 1 Mansfield core, 1,543.0 feet, plane light, width 3.25 mm.

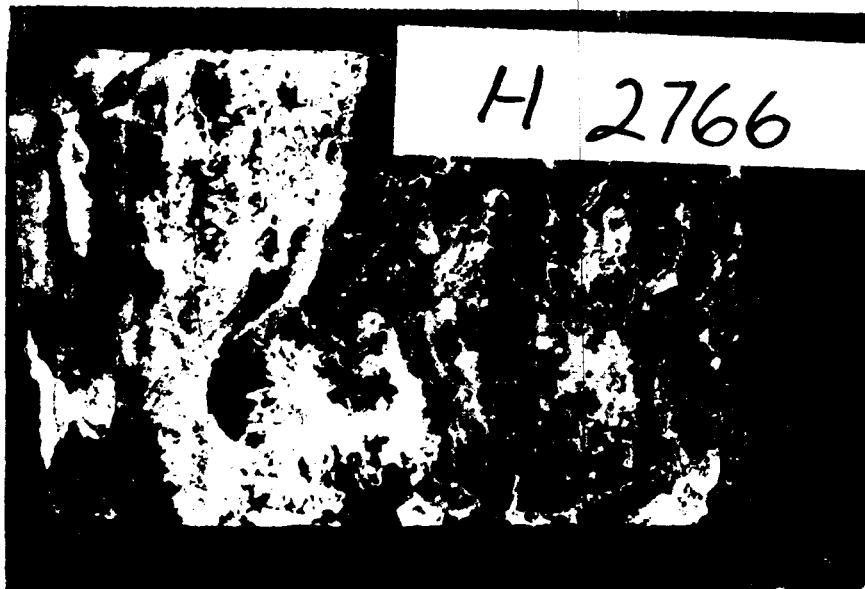


Figure 60. A thin anhydrite bed within halite has been extensively replaced by halite. The irregular bedding surfaces, small pseudomorphs after gypsum, and eyes of halite within the bed are typical of these interbeds. Slabbed core from San Andres unit 4 of the Stone and Webster No. 1 Harman well, depth 2,766 feet.

DRAFT

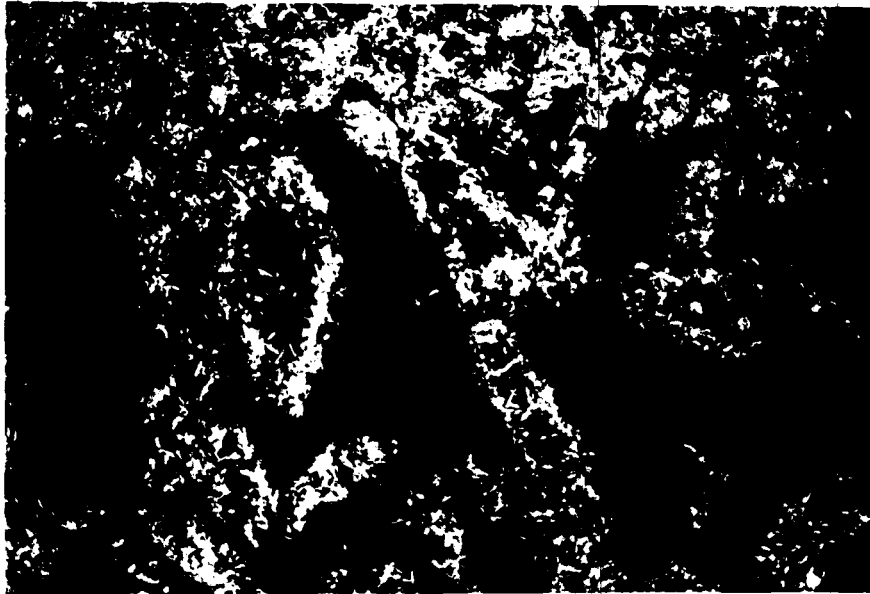


Figure 61. Anhydrite (white) and halite (gray) pseudomorphs after gypsum in a thin anhydrite bed. The centers of many of the pseudomorphs have been replaced by halite. Thin section from the San Andres unit 5 in the Stone and Webster No. 1 G. Friemel core, 2,284.6 feet, partly crossed nicols, width 7.7 mm.

DOE-STONE & WEBSTER
#1 MANSFIELD

0 10 cm

1451 ft.



Figure 62. The upper surface of this anhydrite bed is highly irregular, with what appears to be a pit filled with halite on the left side of the core truncating the laminated anhydrite host. Slabbed core from San Andres unit 5, Stone and Webster No. 1 Mansfield core depth 1,451 feet.

DRAFT



Figure 63. An anhydrite bed (A) has collapsed into the underlying bedded halite (Stone and Webster No. 1 Harman). At the base of the anhydrite is an anhydritic mudstone residue. Lamination within the anhydrite is steeply dipping at the base of the bed and becomes horizontal at the top, indicating that the collapse occurred during deposition of the bed. Slabbed core from top of San Andres unit 5 in the Stone and Webster No. 1 Detten well, depth 2,389 to 2,393 feet.

DRAFT

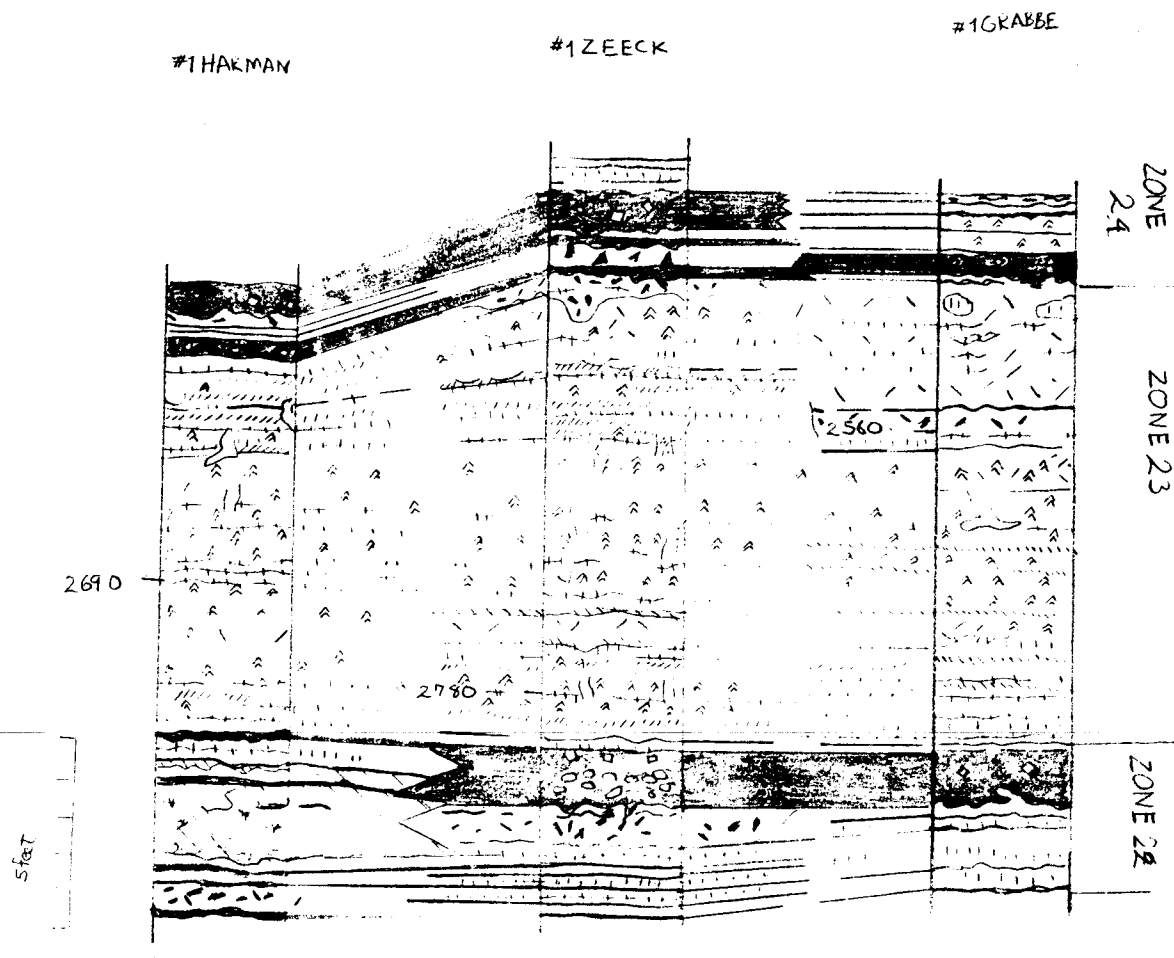
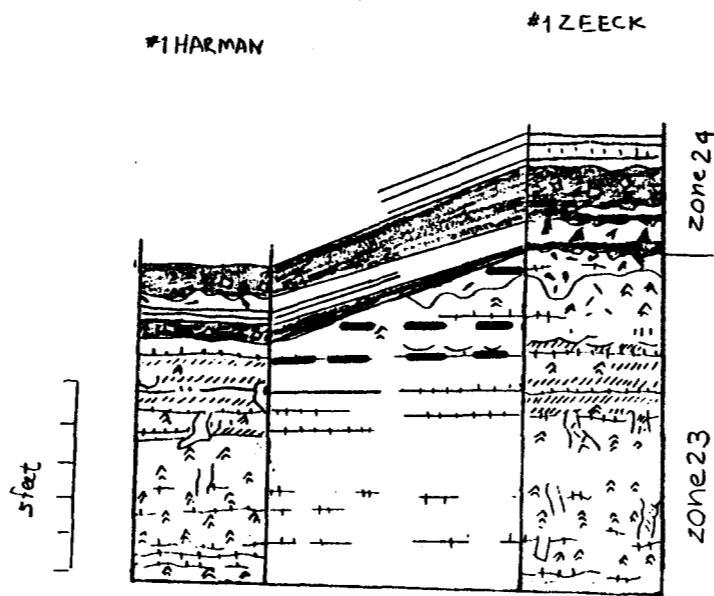


Figure 64. Details of correlation of zone 23 and over and underlying zones in the three cores from Swisher County. Note that zone 23 is chevron halite truncated by abundant anhydrite partings throughout the area. The key to the symbols is shown in Figure 6.

DRAFT

CORRELATION A



CORRELATION B

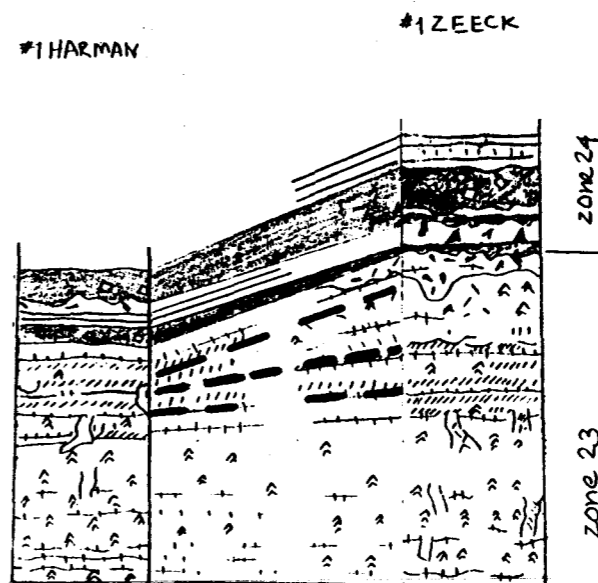


Figure 65. The variation in thickness of the chevron halite in San Andres unit 4, zone 23 in Swisher County could be due either to erosion or dissolution of halite during deposition of the mudstone beds of zone 24, as shown in correlation A, or to deposition of a thinner sequence of halite in the upper part of zone 23, as shown in correlation B. The key to the symbols is shown in figure 6.

DRAFT

#1 HARMAN

#1 ZEECK

#1 GRABBE

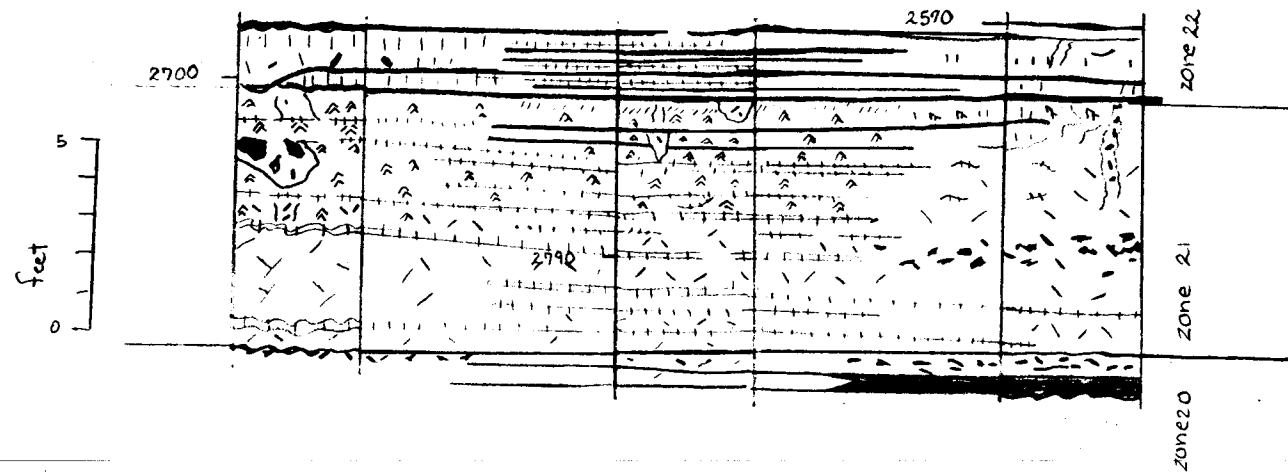


Figure 66. Correlation of zone 21 of San Andres unit 4 in Swisher County demonstrates the kind of variability in a typical zone of anhydritic halite. The key to the symbols is shown in figure 6.

DRAFT

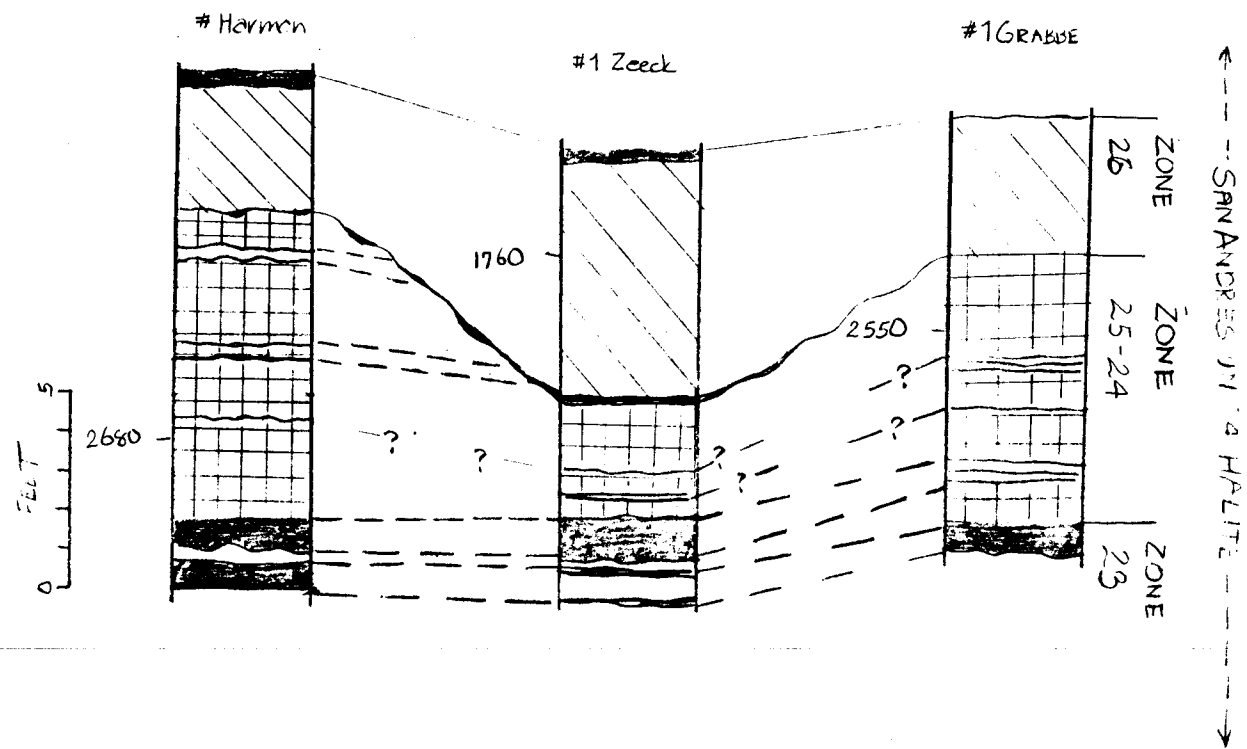


Figure 67. The anhydrite bed of San Andres unit 4, zone 26 is thickest in the No. 1 Zeck well, and the underlying halite is correspondingly thin. A mudstone insoluble residue underlies the anhydrite only in the No. 1 Zeck well. This relationship is interpreted as a result of dissolution of halite in the Zeck well during the transgression which deposited the anhydrite. The key to the symbols is shown in figure 6.

DRAFT

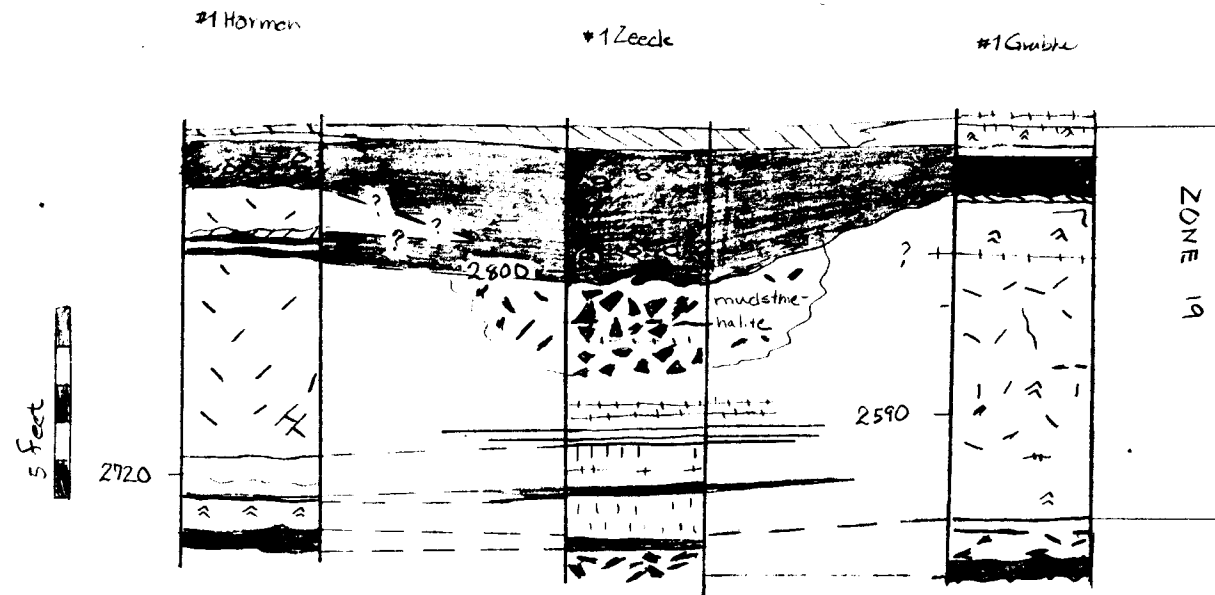


Figure 68. Zone 19 of San Andres unit 4 is muddier in the No. 1 Zeack core than in the other cores from Swisher County. The extra thick mudstone bed and the underlying mudstone-halite indicates deposition of more mudstone in the area of the No. 1 Zeack well, but the geometry of this mudstone thick cannot be defined with the core spacing available. The key to the symbols is shown in figure 6.

DRAFT

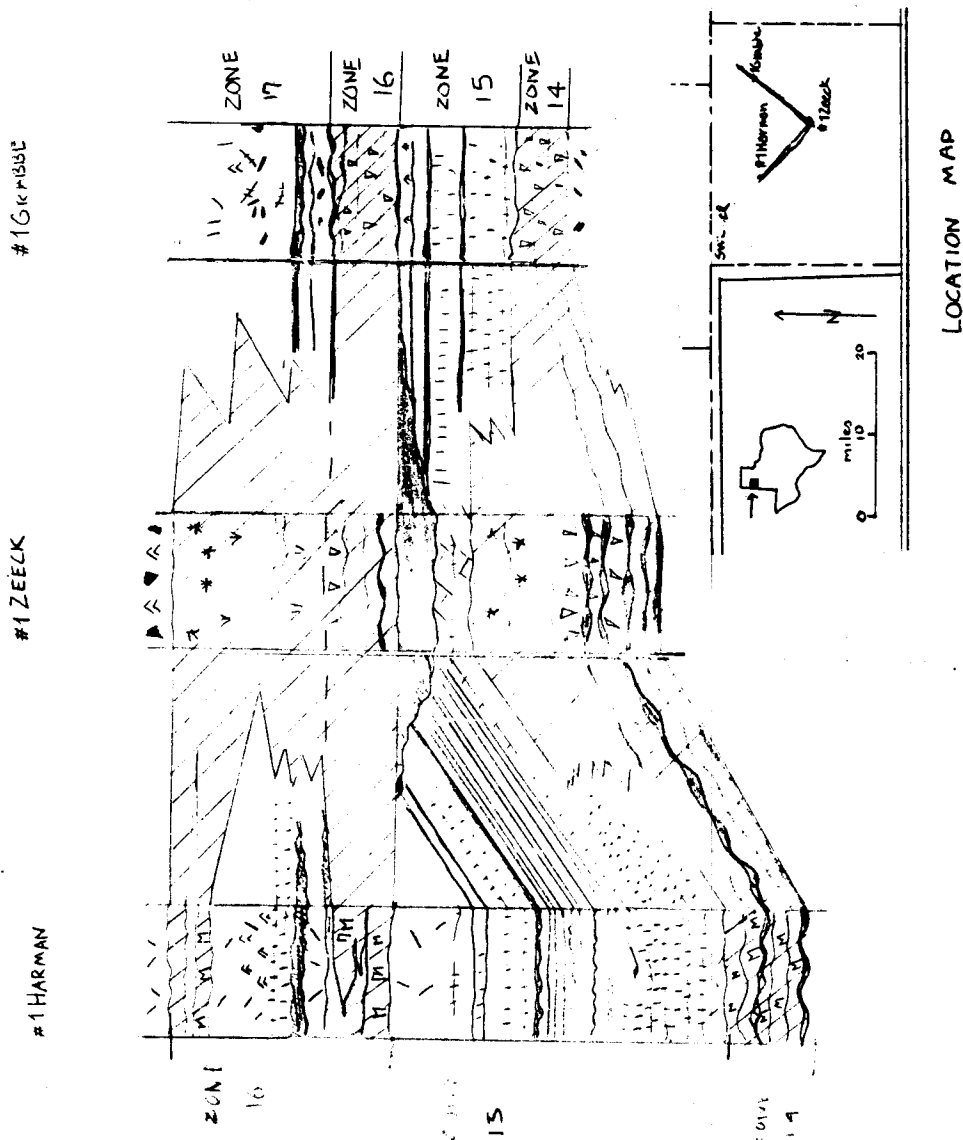


Figure 69. Zones 14 through 17 of San Andres unit 4 show complex variations in Swisher county. Both anhydrite beds are thickest in the No. 1 Zeack core. The halite of zone 15 thins in this well and exhibits recrystallized textures, interpreted as a result of dissolution beneath the anhydrite. The key to the symbols is shown in figure 6.

This report describes research carried out by staff members of the Bureau of Economic Geology that addresses the feasibility of the Palo Duro Basin for isolation of high-level nuclear wastes. The report describes the progress and current status of research and tentative conclusions reached. Interpretations and conclusions are based on available data and state-of-the-art concepts, and hence, may be modified by more information and further application of the involved sciences.

DRAFT

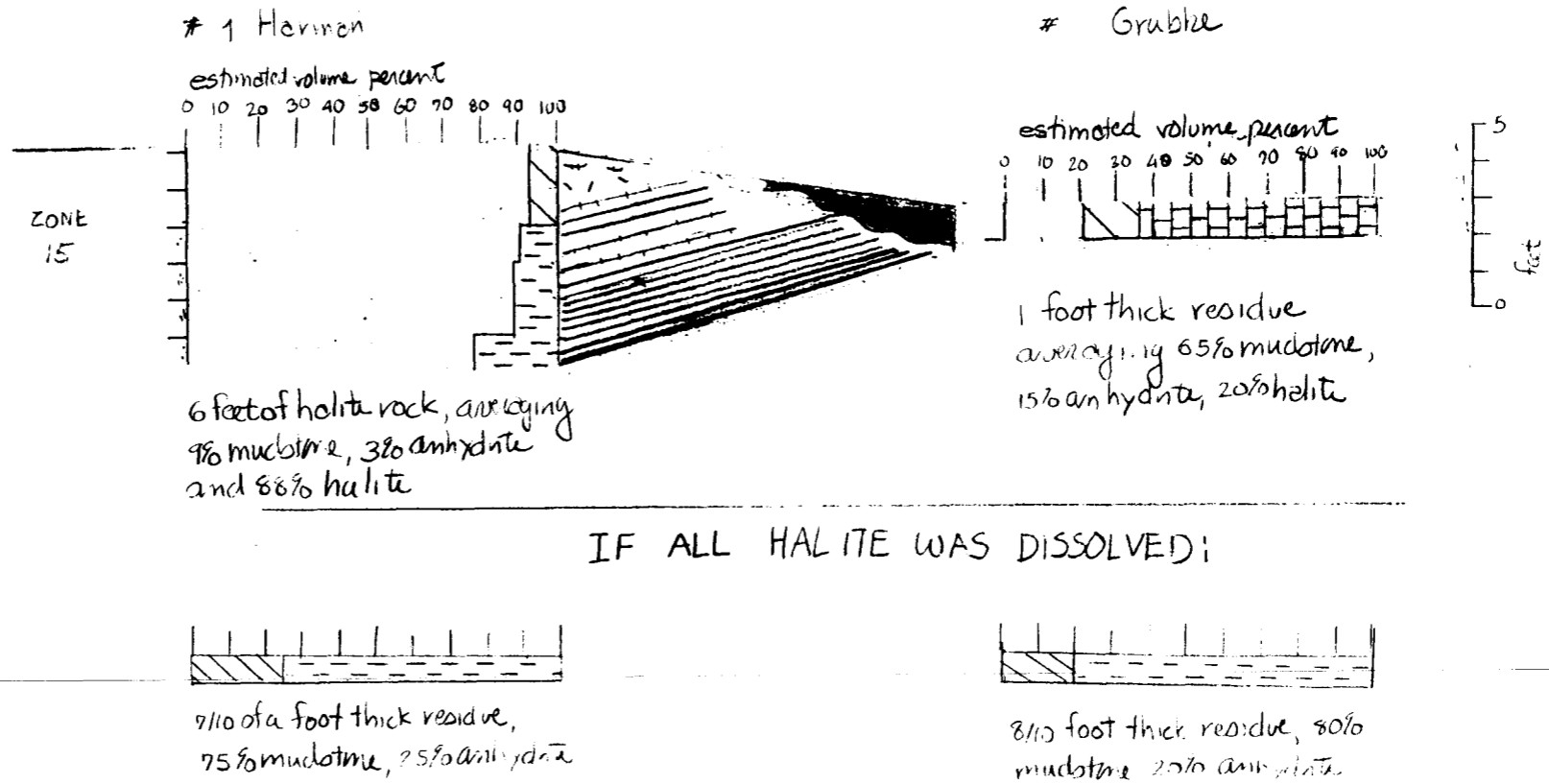


Figure 70. The amount and composition of impurities in the halite of zone 15 in the No. 1 Harman core is approximately equal to the amount and composition of impurities in the residue of the No. 1 Grabbe core. The method of calculation is discussed in the text.

DRAFT

STONEWEBSTER #1 MANSFIELD STONEWEBSTER #1 J. FRIEMEL STONEWEBSTER #1 DETTEN STONEWEBSTER #1 G. FRIEMEL STONEWEBSTER #1 HARMAN STONEWEBSTER #1 ZEECK DOE-GRUYFEDER #1 GRABSE DOE-GRUYFEDER #1 REXWHITE

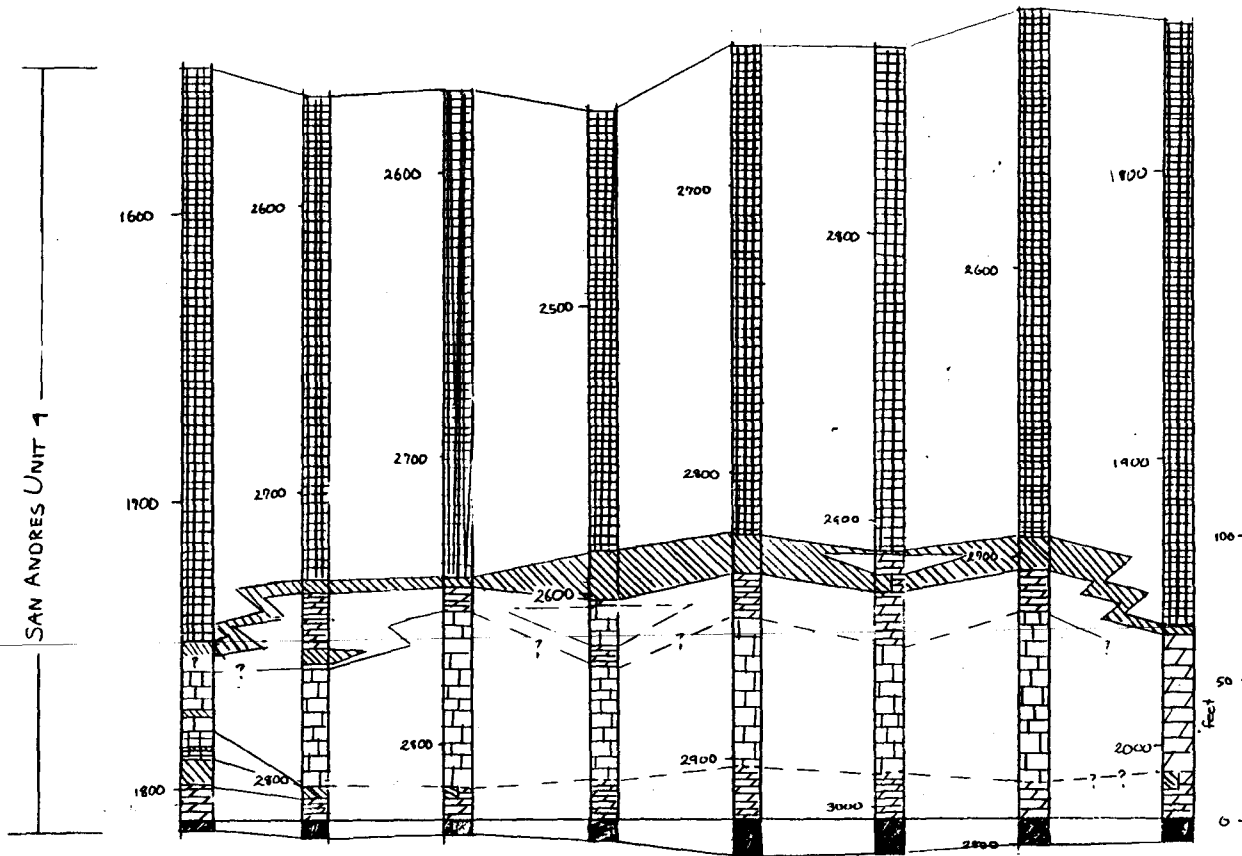


Figure 71. Distribution of facies in the entire San Andres unit 4 shows that while the thickness of the entire unit 4 is fairly constant in the north-central part of the Palo Duro Basin where wells were cored, the halite thickens toward the north (No. 1 Mansfield and No. 7 Rex White cores) at the expense of carbonate.

DRAFT

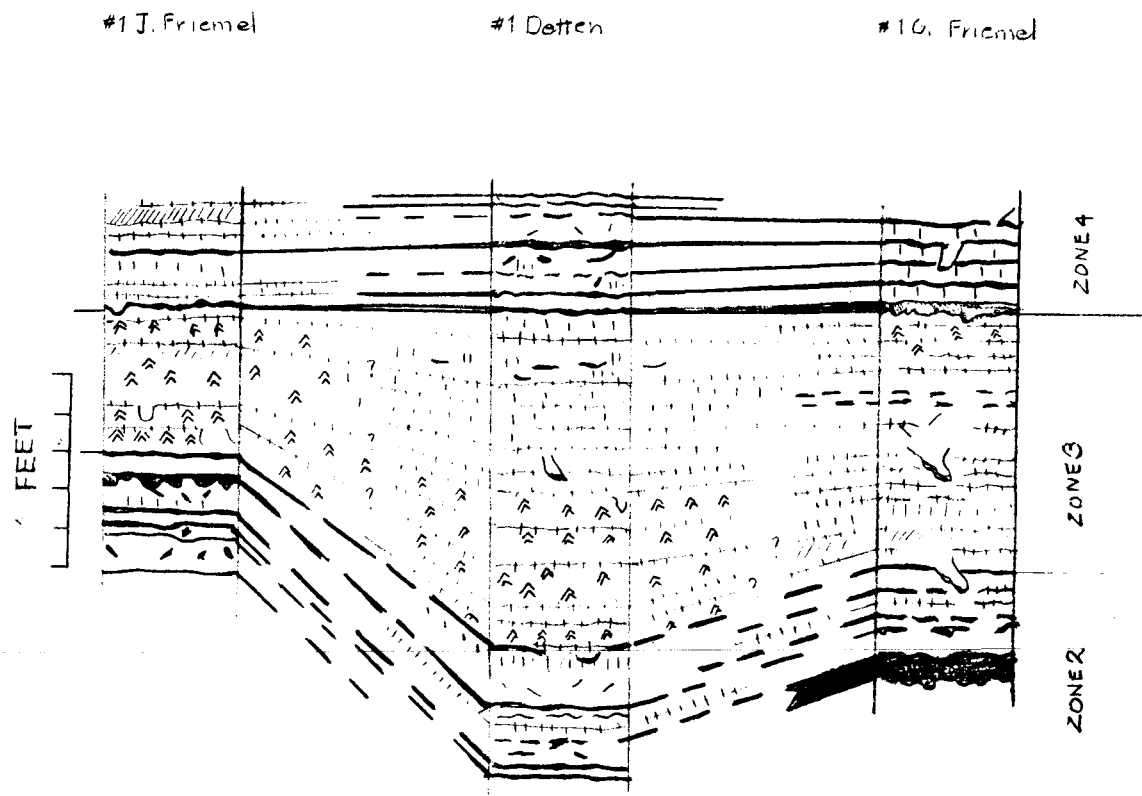
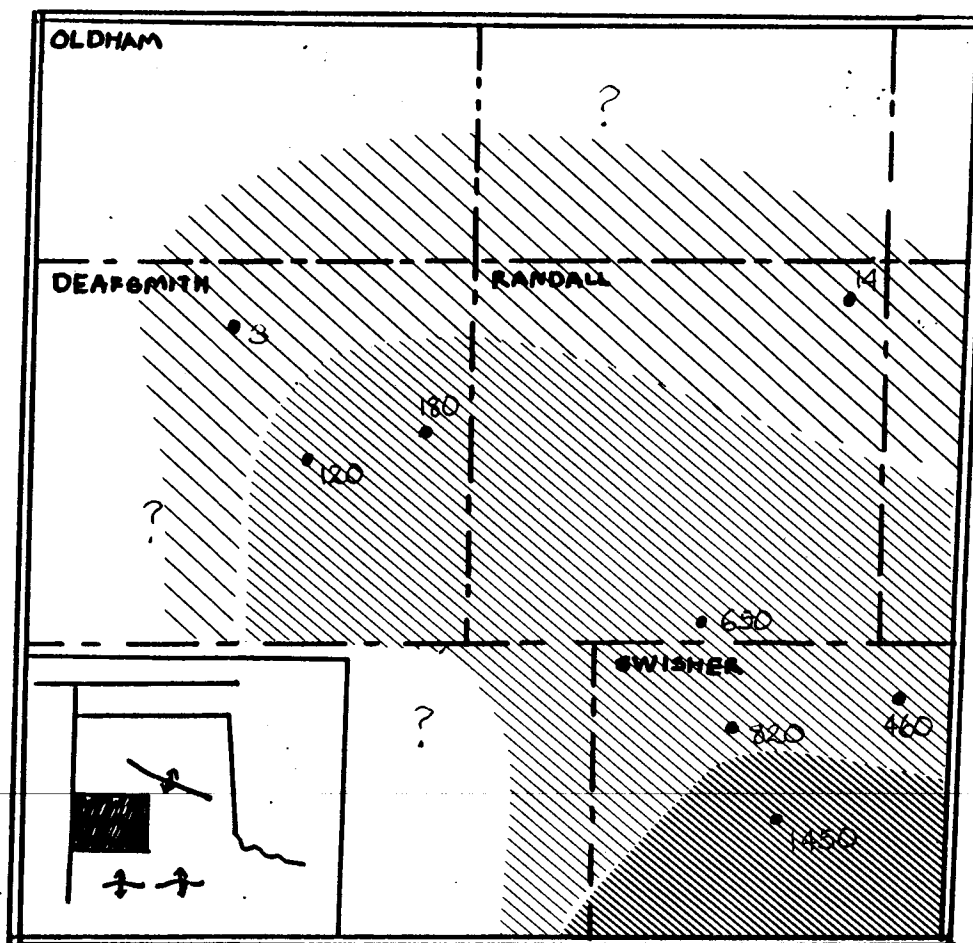


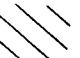


Figure 72. The anhydritic halite of zone 3 is thicker in the No. 1 Detten core than in the other cores in Deaf Smith County. The variation in thickness does not appear to be due to dissolution in the area of the other wells, but to greater sediment accumulation in the area of the No. 1 Detten well. The key to the symbols is shown in figure 6.

DRAFT



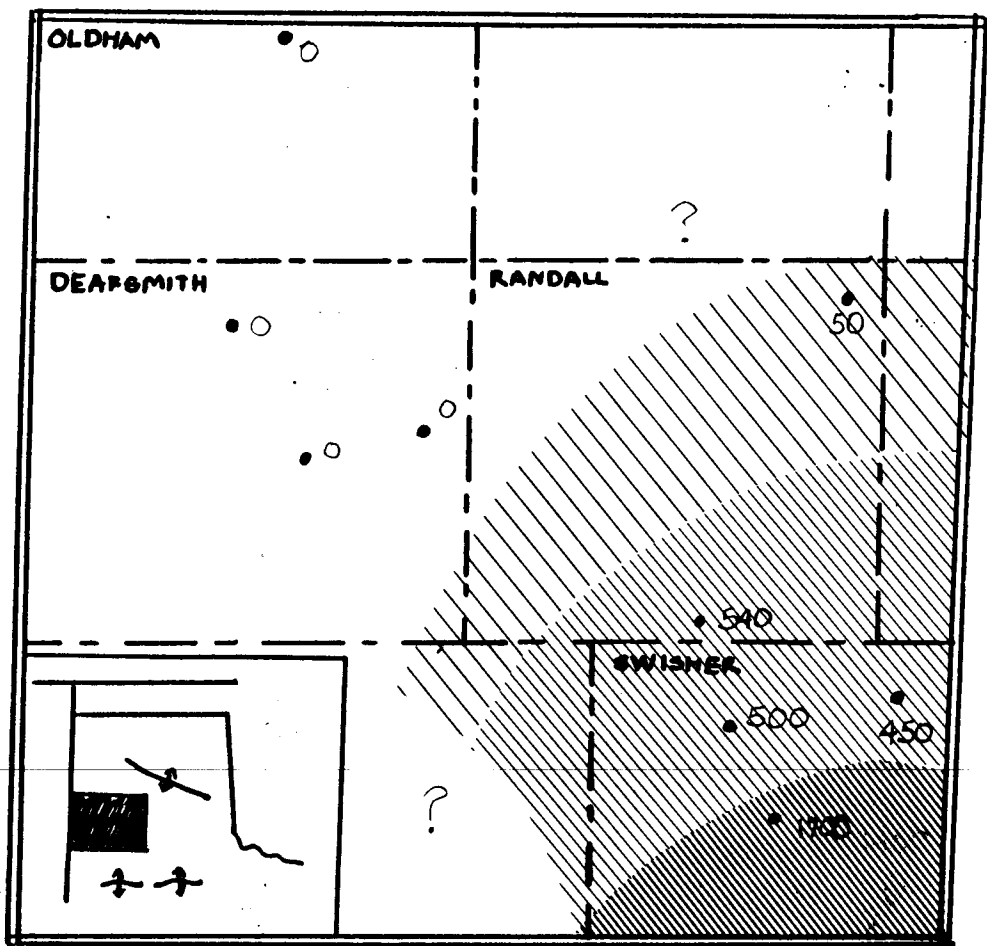
-  Anhydrite thickness > 1 m
-  Anhydrite thickness > 10 cm
-  Anhydrite < 10 cm, > 1 cm




Thickness of anhydrite bed
given in millimeters

Distribution of anhydrite in San Andres unit 4, zone 14

Figure 73. The anhydrite beds in San Andres unit 4, zone 14, 16, and 26 thicken toward the south in the area of Swisher County. Note that these figures are based on only seven data points provided by cored wells.

DRAFT



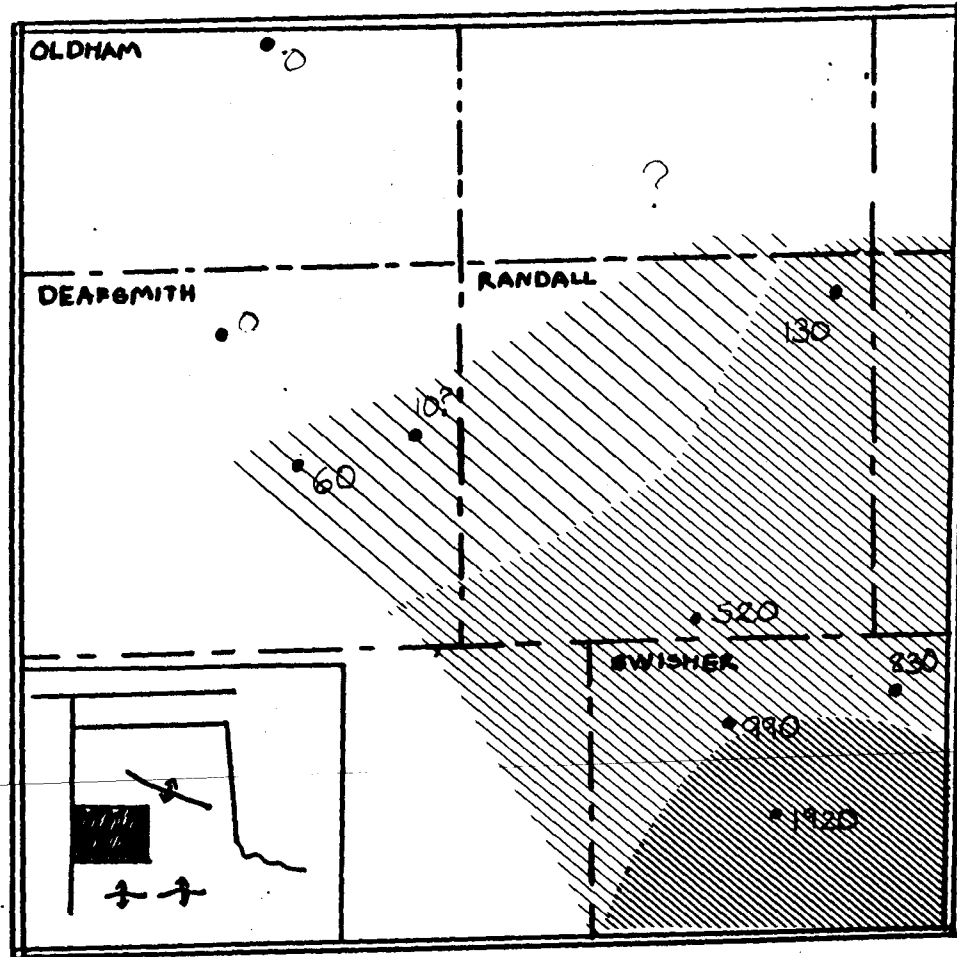
-  Anhydrite thickness > 1 m
-  Anhydrite thickness < 1 m > 10 cm
-  Anhydrite present



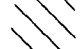
Thickness of anhydrite bed - given in millimeters

Distribution of anhydrite in San Andres unit 4, zone 16

Figure 73 (continued)

DRAFT



-  Anhydrite thickness >1m
-  Anhydrite thickness <1m >10cm
-  Anhydrite present

Distribution of anhydrite in San Andres unit 4, zone 26

Figure 73 (continued)

DRAFT

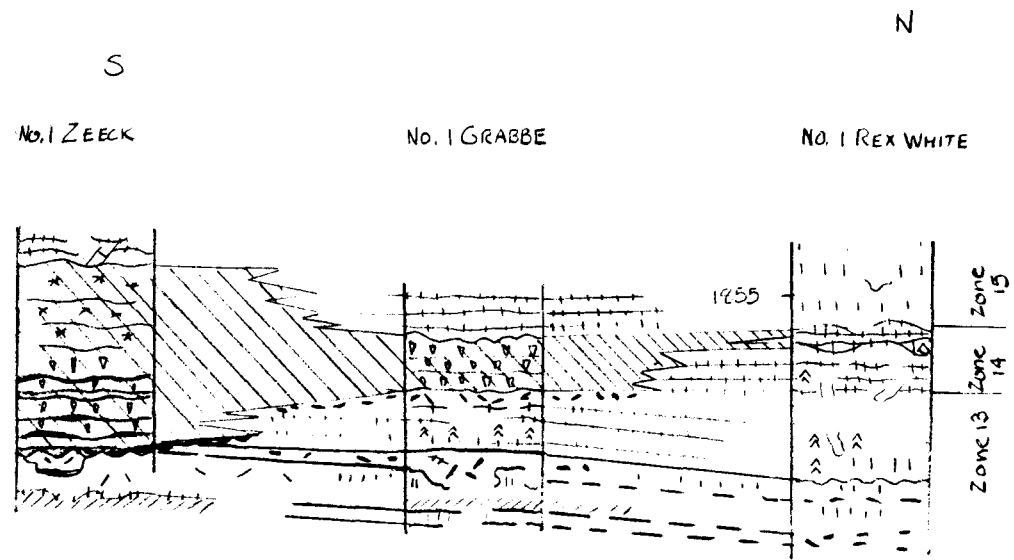


Figure 74. The anhydrite bed of zone 14 pinches out to the north (No. 1 Rex White core) into chevron halite with abundant anhydrite partings and thin interbeds. A thin mudstone residue underlies the anhydrite in the south (No. 1 Zeck core). The key to the symbols is shown in figure 6.

DRAFT

DRAFT

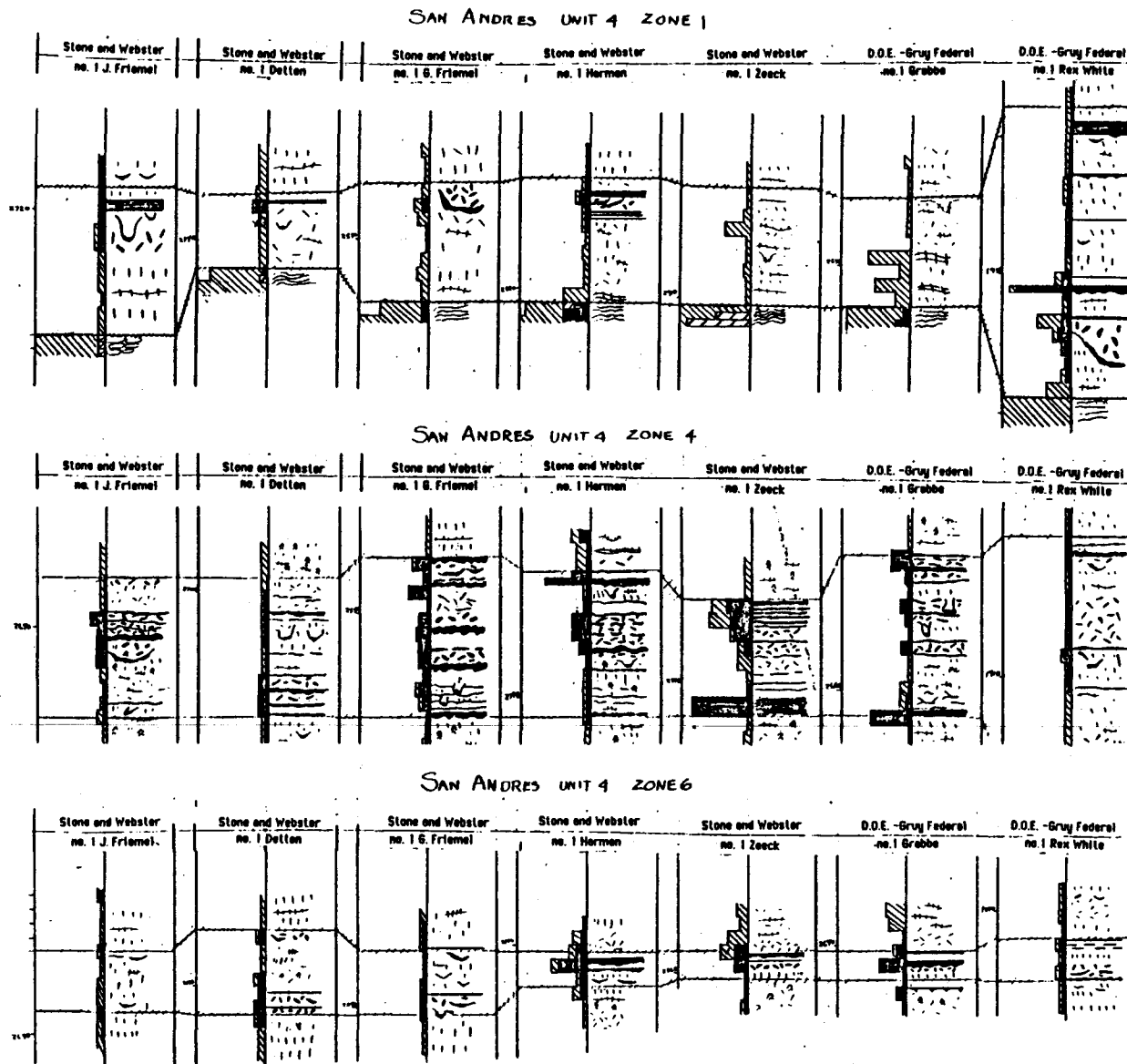
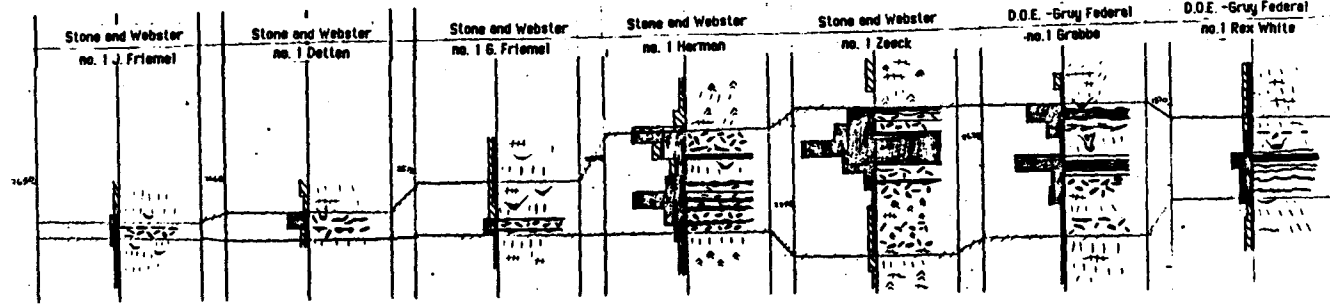
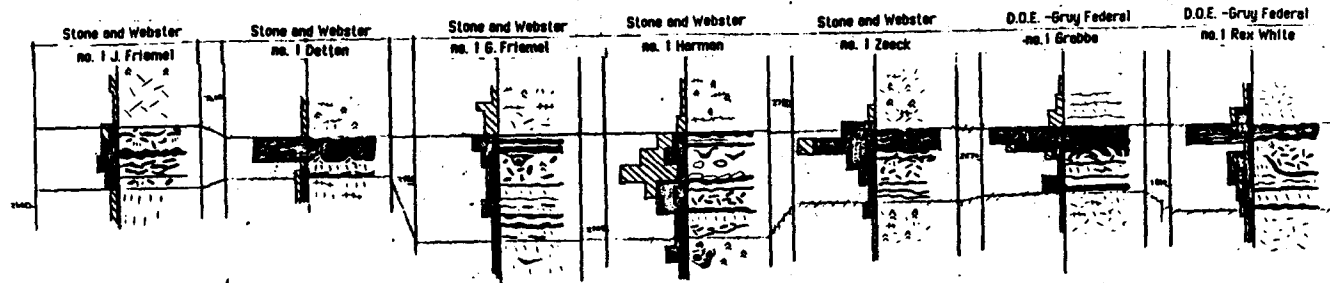


Figure 75. Cross sections through zones with abundant mudstone beds can be used with conventional techniques of net clastic mapping to show the geometry of mudstone bodies within San Andres unit 4, zones 1, 4, 6, 12, 22, and 24.

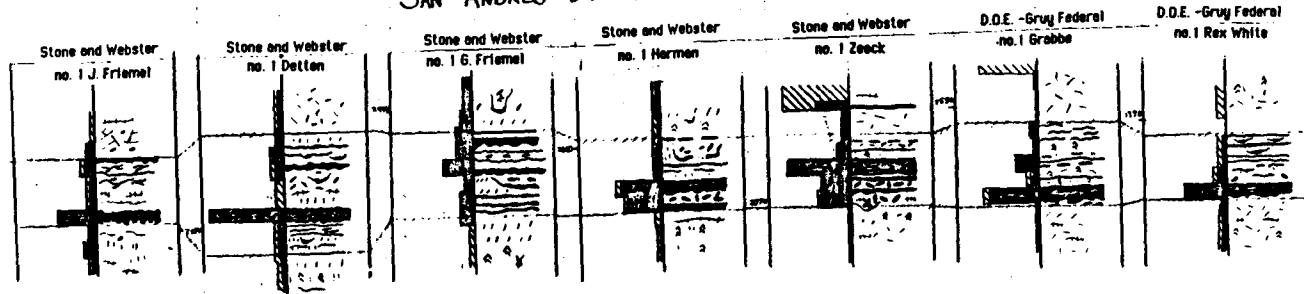
SAN ANDRES UNIT 4 ZONE 12



SAN ANDRES UNIT 4 ZONE 22

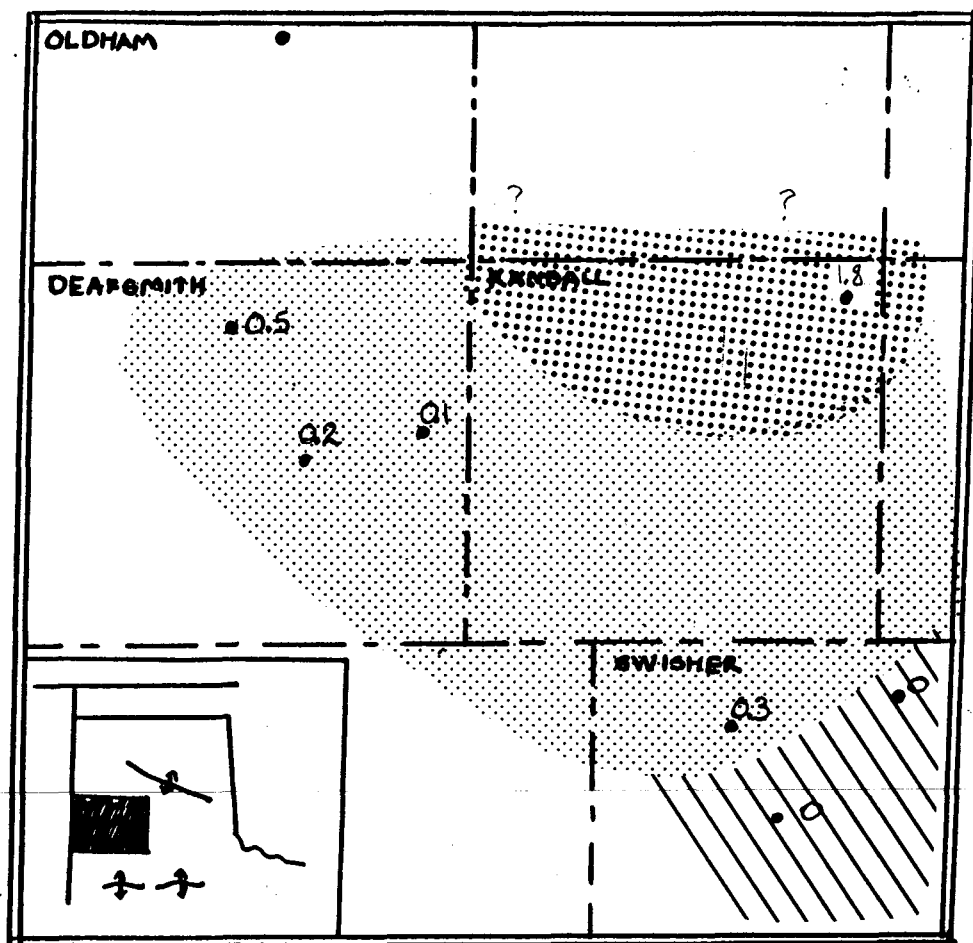


SAN ANDRES UNIT 4 ZONE 24



DRAFT

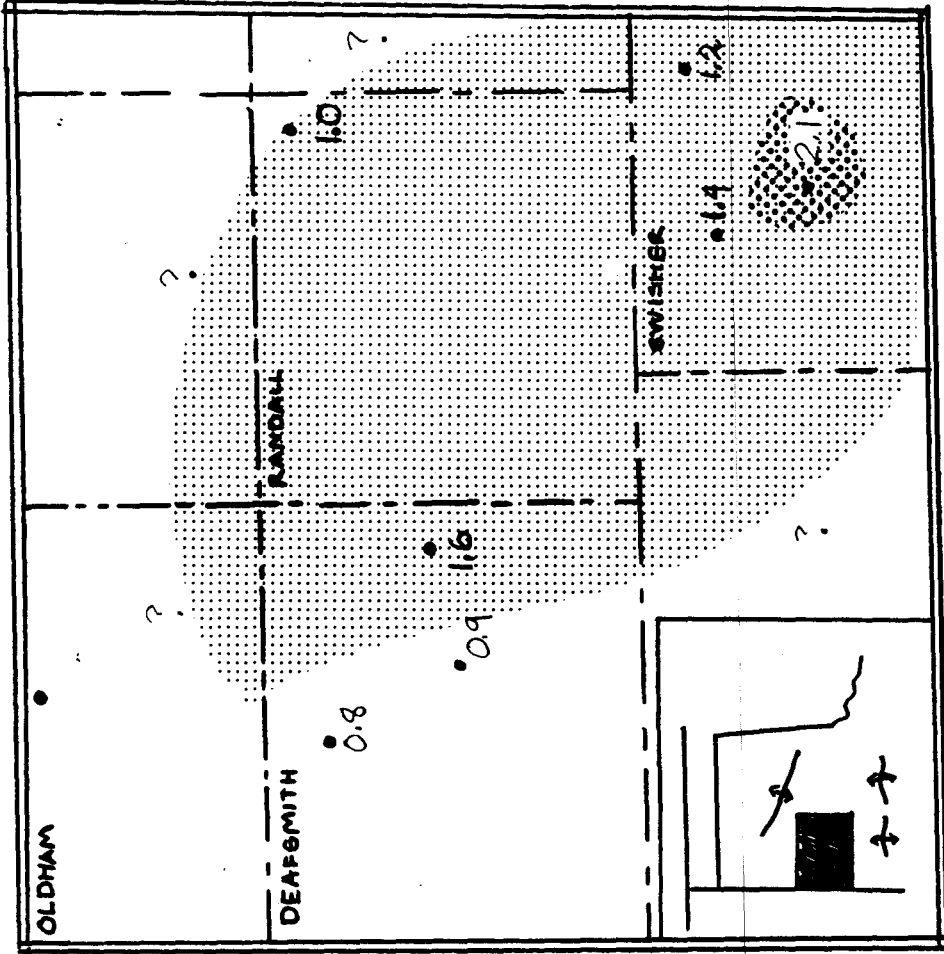
Figure 75 (continued)



Net mud, San Andres unit 4, zone 1

Figure 76. The geometry of mudstone bodies are mapped by preparing net mudstone maps within San Andres unit 4, zones 1, 4, 6, 12, 22, and 24. The thickness of the mudstone shown is the summation of the amount of mudstone as both minor and dominant lithologies within the interval. Note that these maps are based on only seven data points, and show general trends but lack detail.

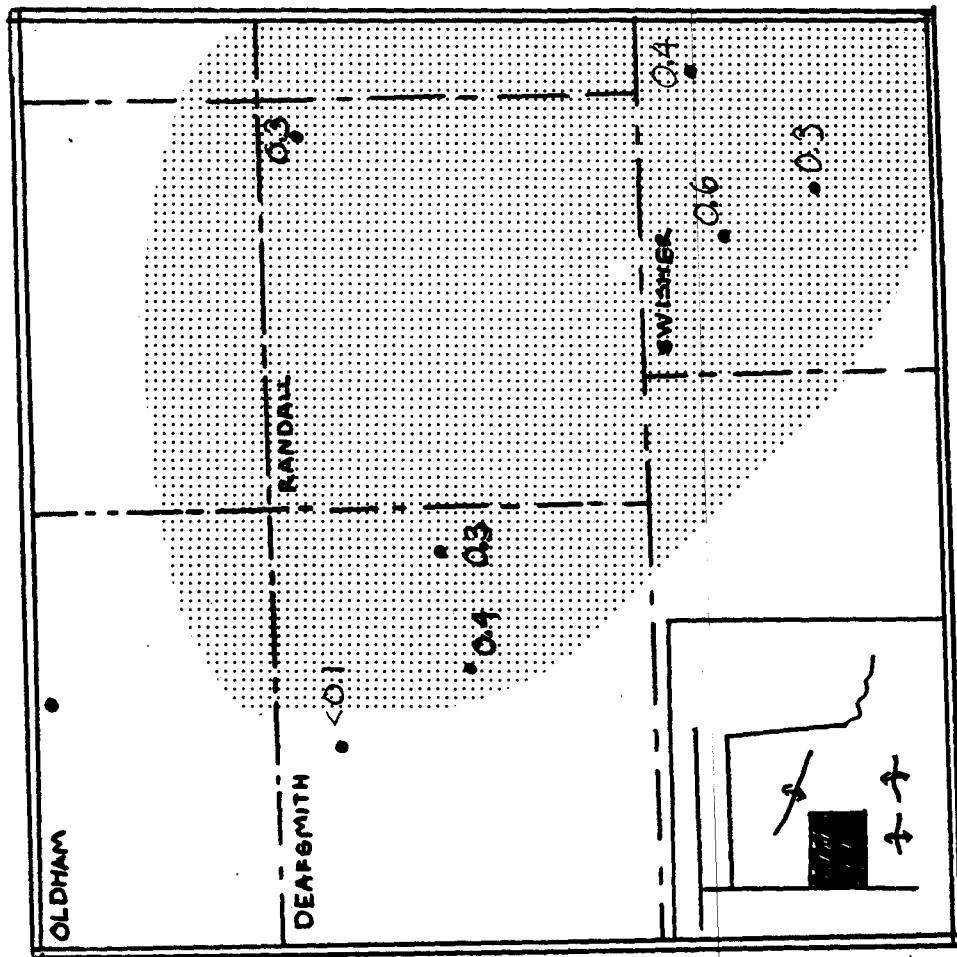
DRAFT



Net mudstone, San Andres unit 4, zone 4

Figure 76 (continued)

DRAFT



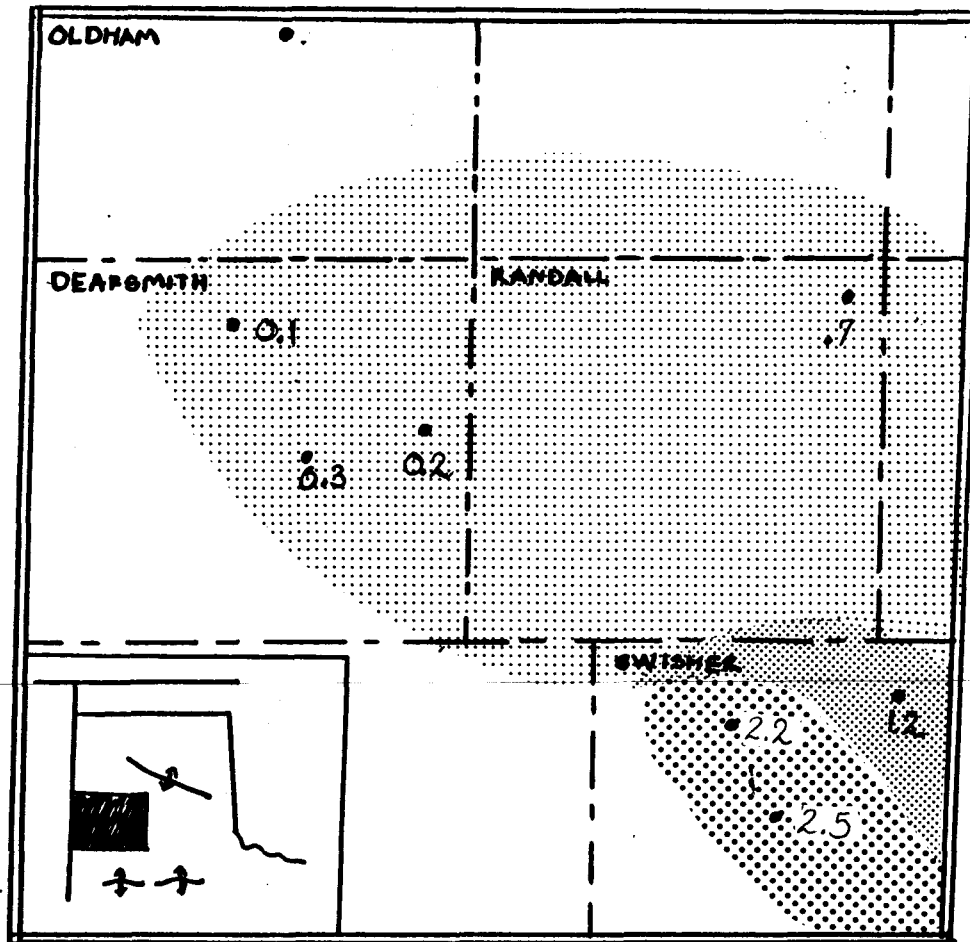
mudstone $>0.1 < 1.0$ feet
 mudstone thickness given
 in feet

DRAFT

Net mud, San Andres unit 4, zone 6

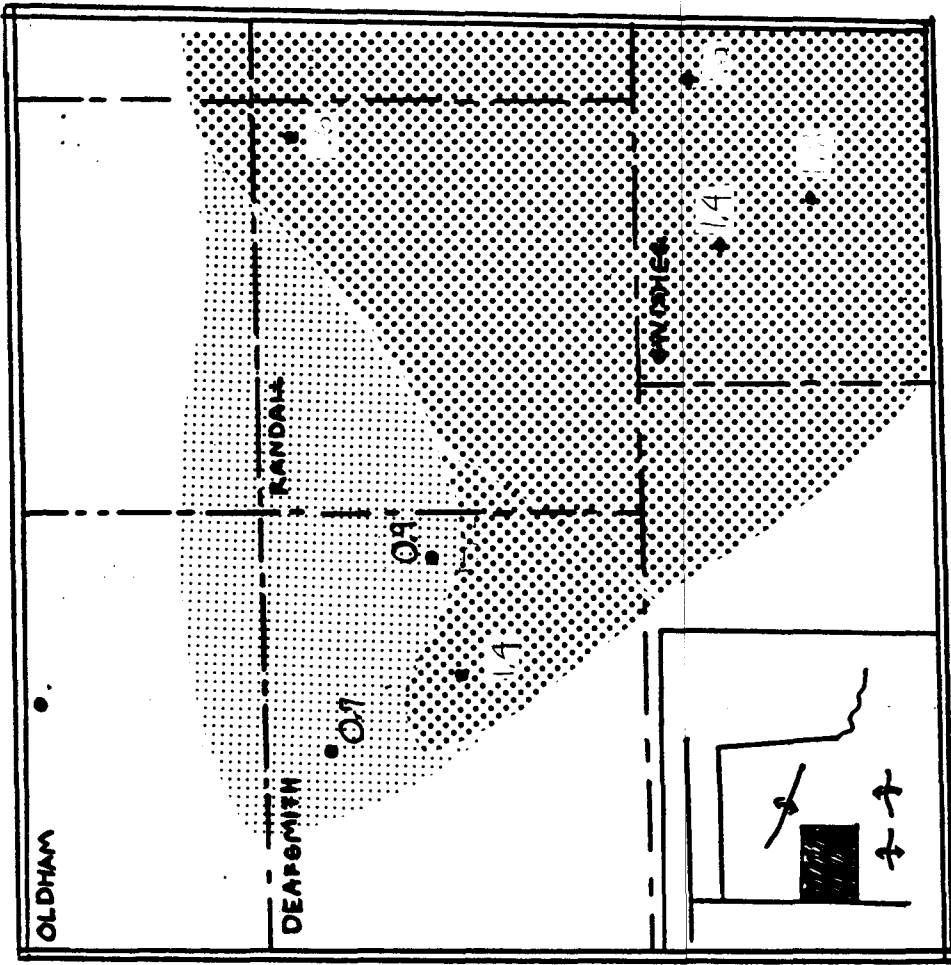
Figure 76 (continued)

DRAFT



Net mud, San Andres Unit 4, zone 12

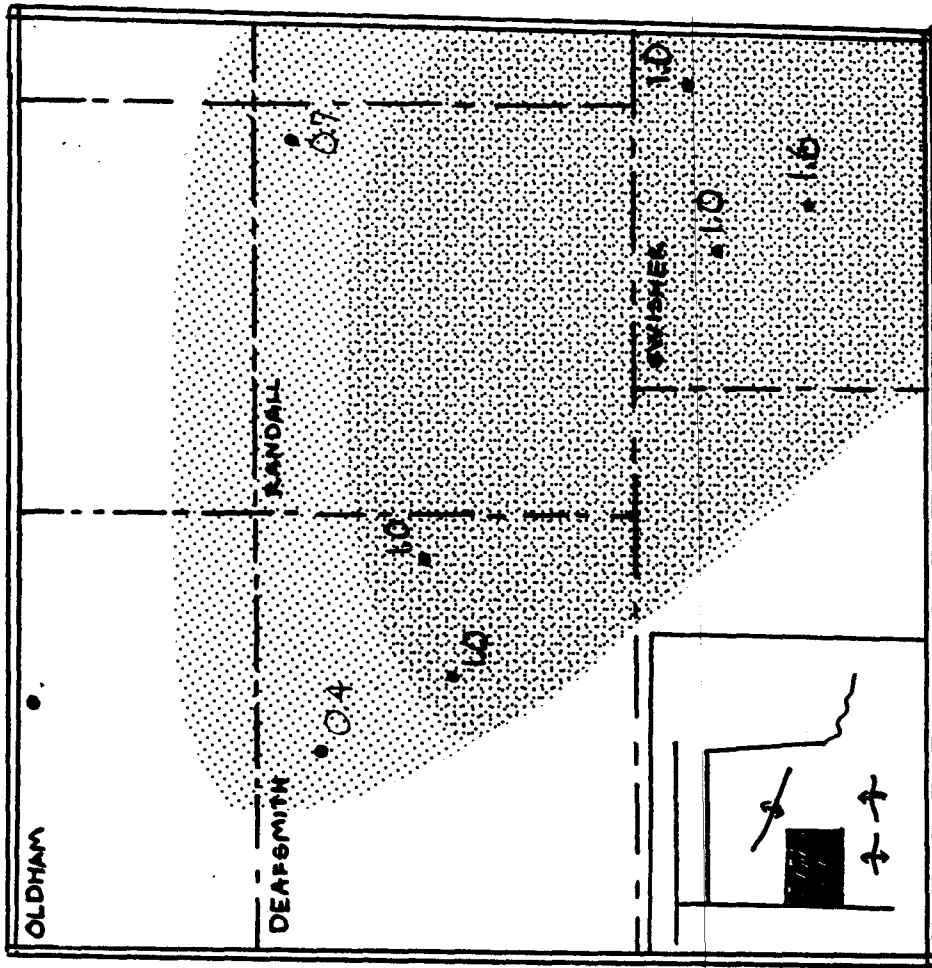
Figure 76 (continued)



Net mud, San Andres unit 4, zone 22

Figure 76 (continued)

DRAFT



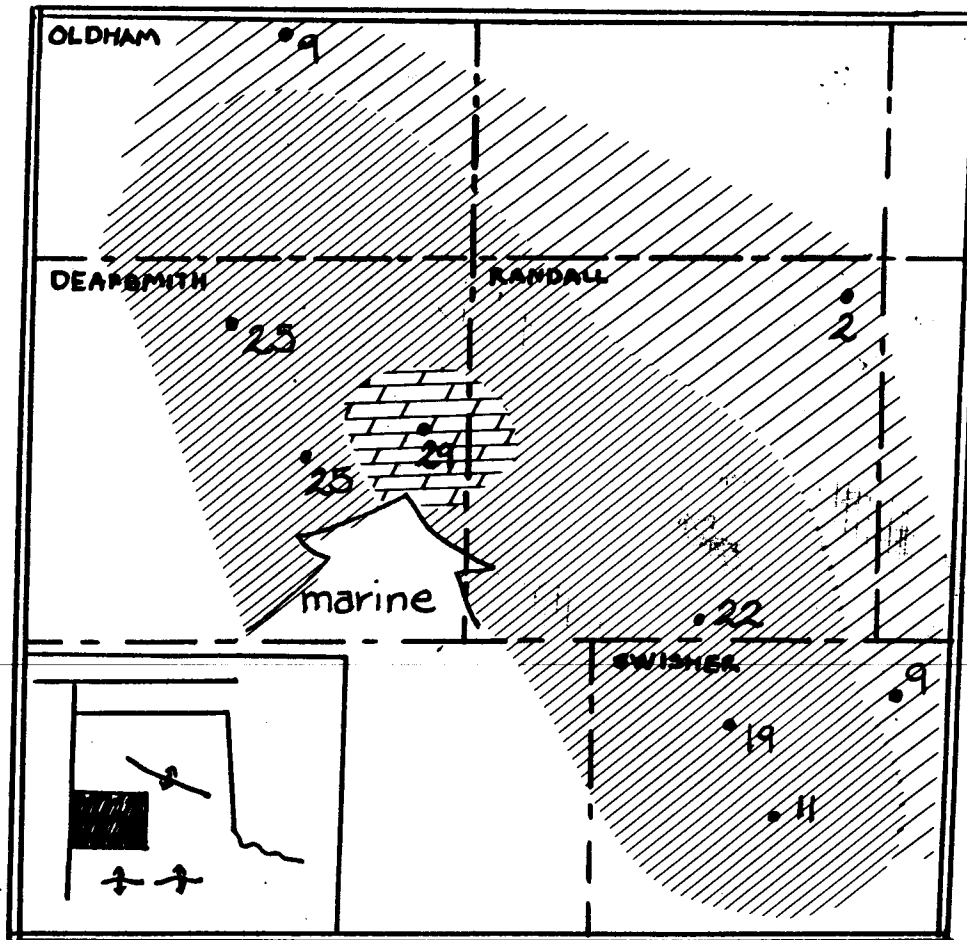
mudstone > 1 foot thick
 mudstone < 1 foot thick
 mudstone thickness given in feet

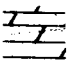
DRAFT


Net mud, San Andres unit 9, zone 24

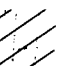
Figure 76 (continued)

DRAFT



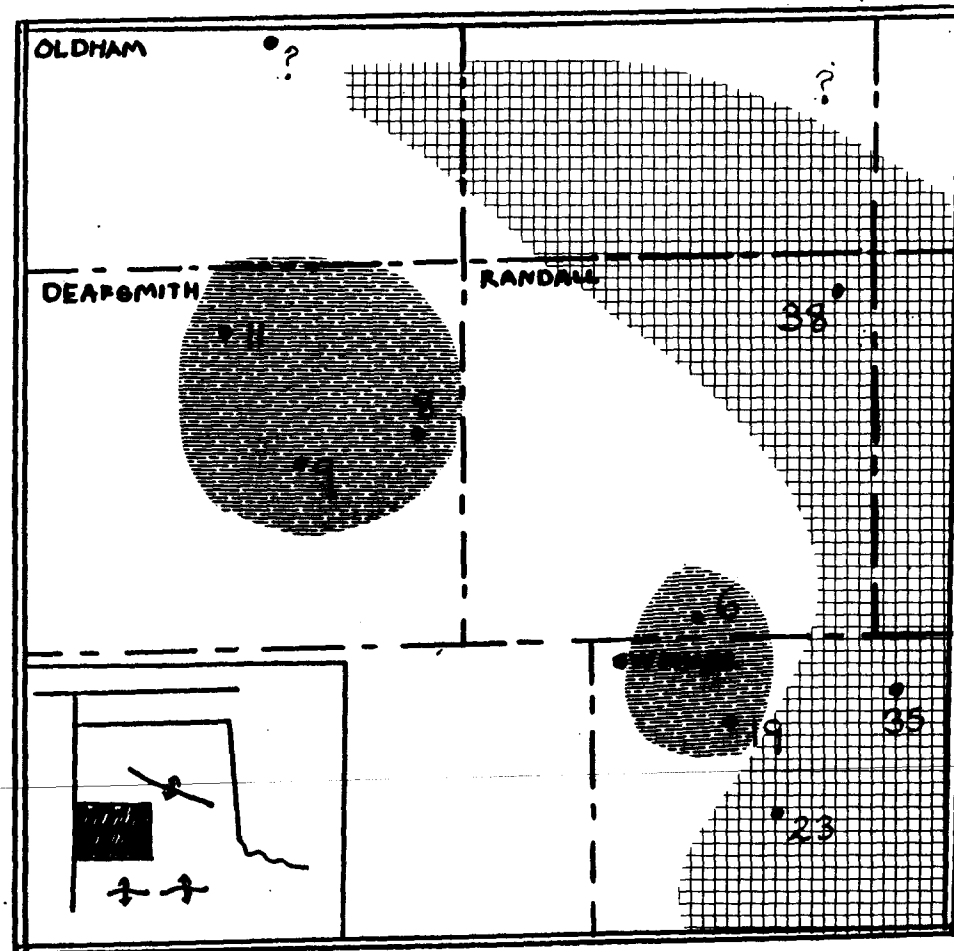
 Dolomitic anhydrite present


 Anhydrite thicker than 10 feet


 Anhydrite present

Thickness of zone 2 anhydrite given in feet

Figure 77. Isopach and composition of zone 2 San Andres unit 5 showing distribution of the thickest, most marine facies in Deaf Smith County.



 Thickness of zones 27 to 31, unit 4
 > 20 feet

 Dark insoluble residue
 at the base of unit 5

DRAFT

Figure 78. Isopach of units 27 through 31 in San Andres unit 4 compared to distribution of the dark anhydritic mudstone residue at the base of unit 5. Note the inverse relationship between the thickness of the salt interval and the presence of residue. Note the correspondence between the distribution of residue and the most marine facies in the overlying cycle shown in Figure 77.

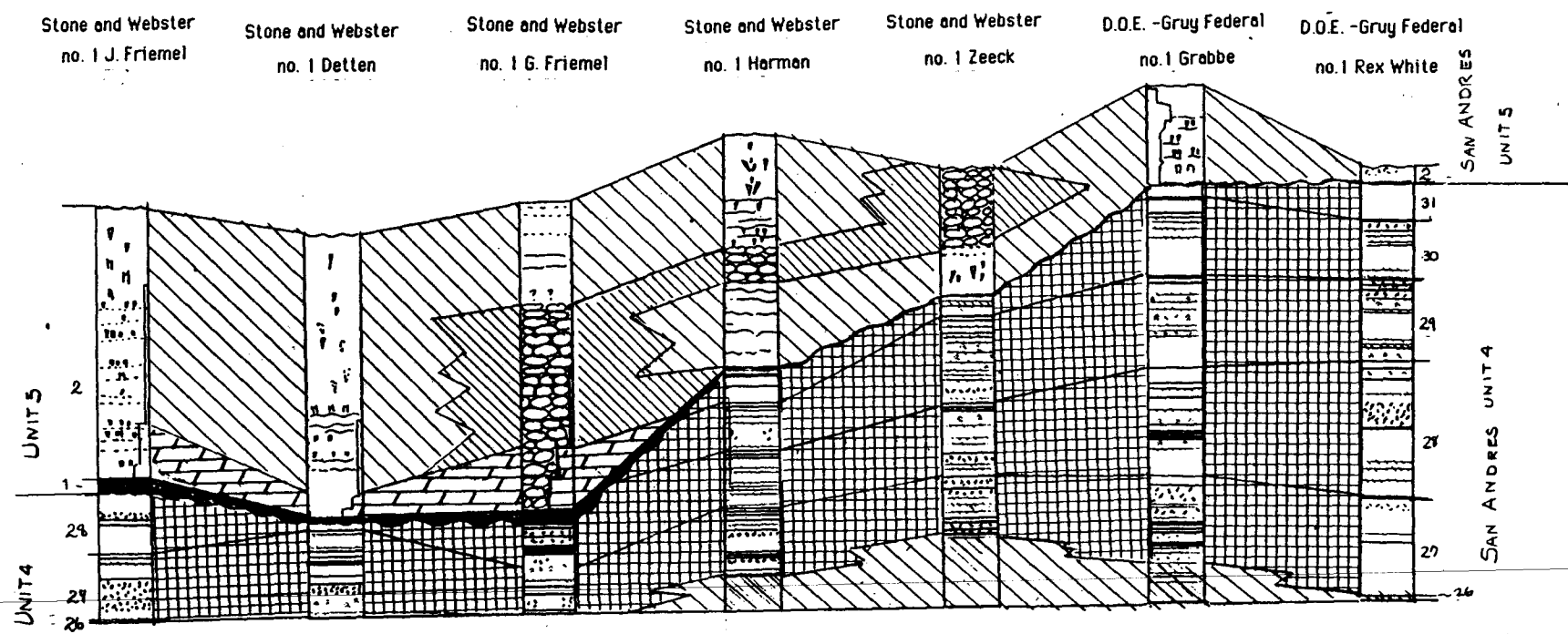
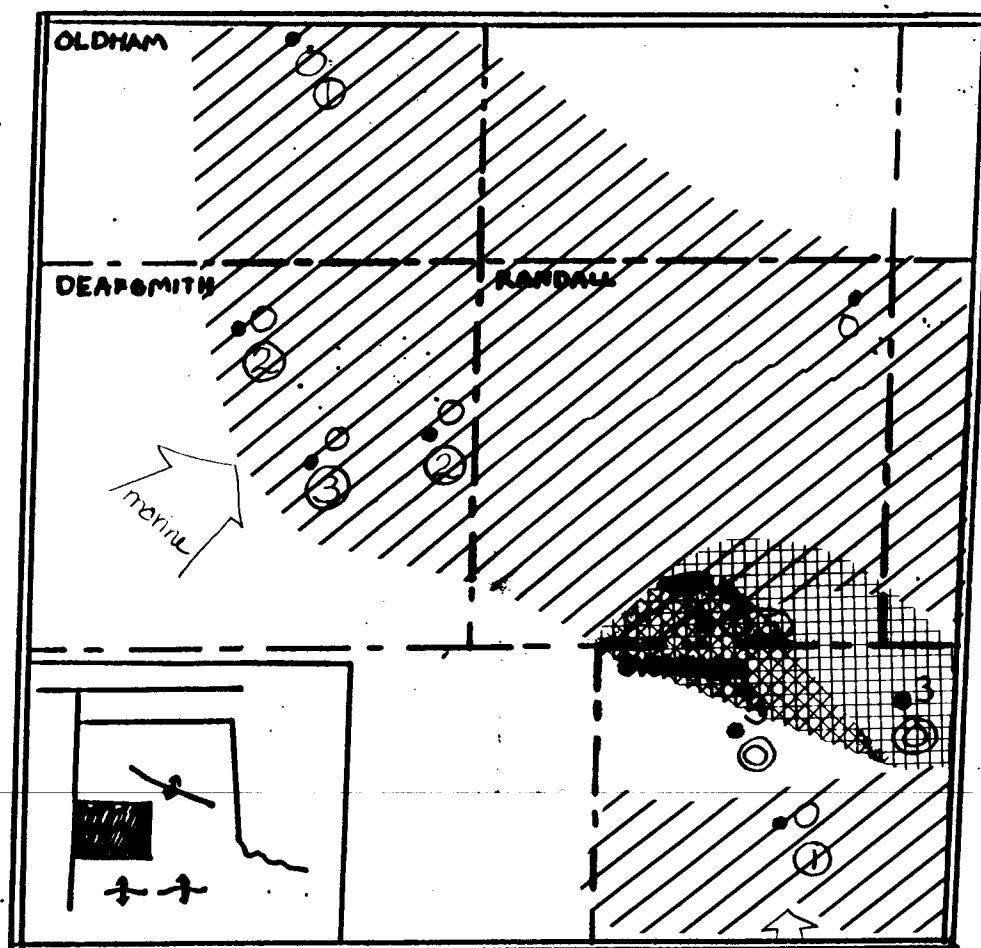


Figure 79. Cross section of the relationship between the uppermost bedded halite interval of unit 4 and the lowest cycle of unit 5. The upper anhydrite marker of unit 4, zone 26 is used as a datum. The key to the symbols is shown in figure 6.

DRAFT



▣ Presence of zone 3 halite

▨ Dolomite present within zone 3 anhydrite

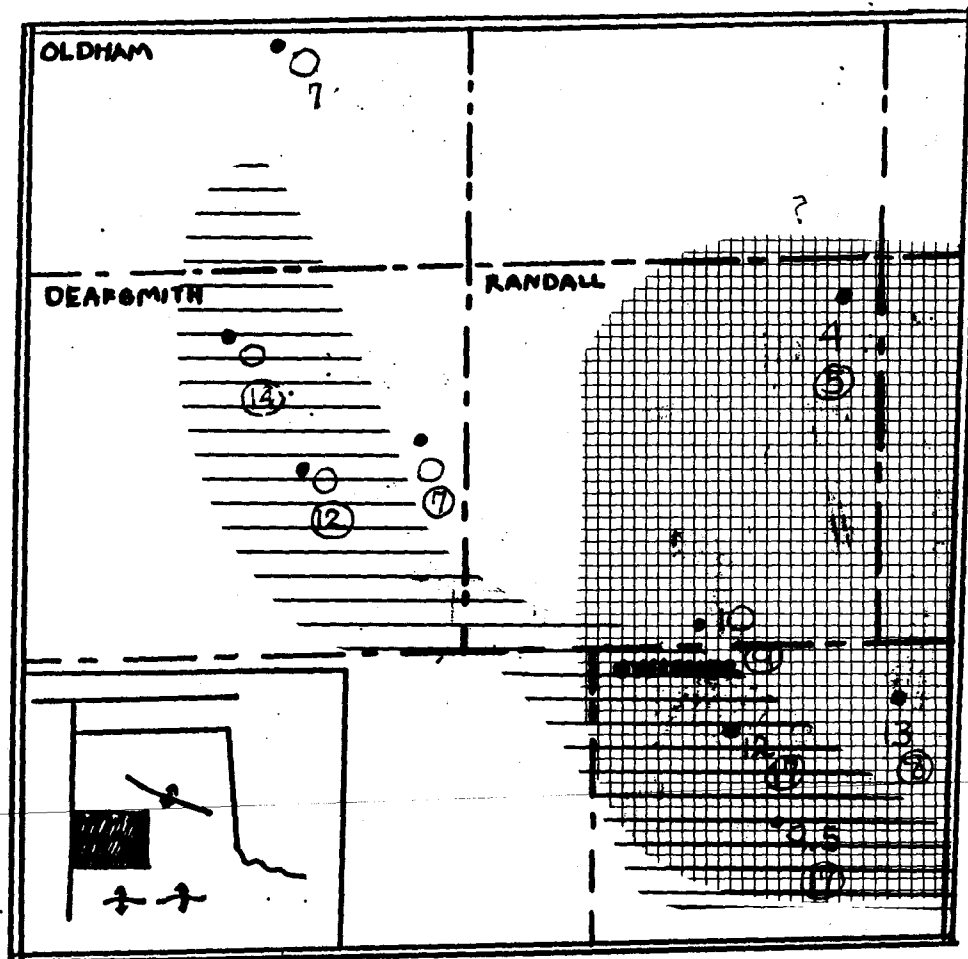
Thick ness of zone 3 halite
in feet


Thick ness of zone 5 dolomite
circled, in feet

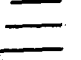
Distribution of halite in San Andres unit 5, zone 3
and dolomite in San Andres unit 5, zone 5

Figure 80. Distribution of halite in San Andres unit 5, zone 3 and dolomite in zone 5, again showing an inverse relationship between preservation of halite at the top of one cycle and lower salinity facies in the overlying cycle.

DRAFT



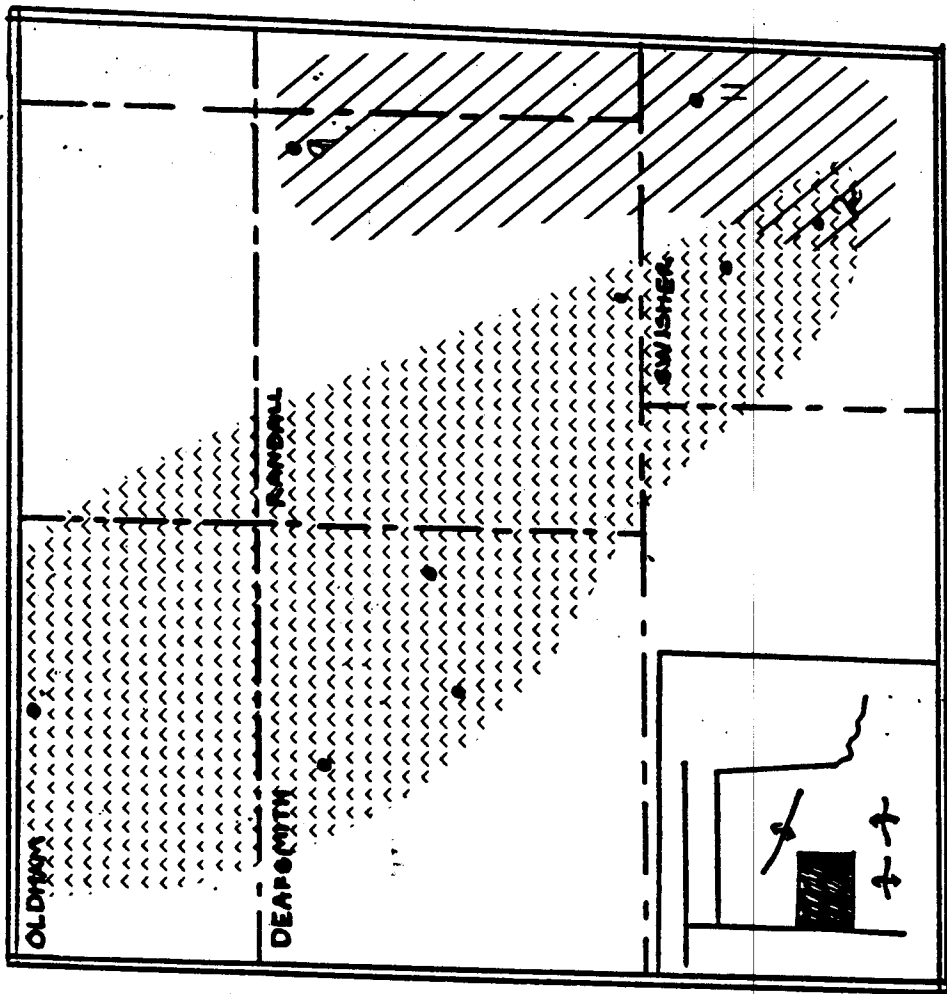
 halite present in San Andres unit 5, zone 6
 thickness of halite given in feet.

 dolomite in San Andres unit 5, zone 8 thicker than 10 feet
 thickness of dolomite (circled) given in feet

Distribution of halite in San Andres unit 5; zone 6 and dolomite in San Andres unit 5; zone 8

Figure 81. Distribution of halite in San Andres unit 5, zone 6 and dolomite in zone 8. The inverse relationship between preservation of halite at the top of one cycle and lower salinity facies in the overlying cycle is not clearly developed in this interval.

DRAFT



// Presence of anhydrite in zone 15
 ~~~ Chevron halite with anhydrite partings in zone 15

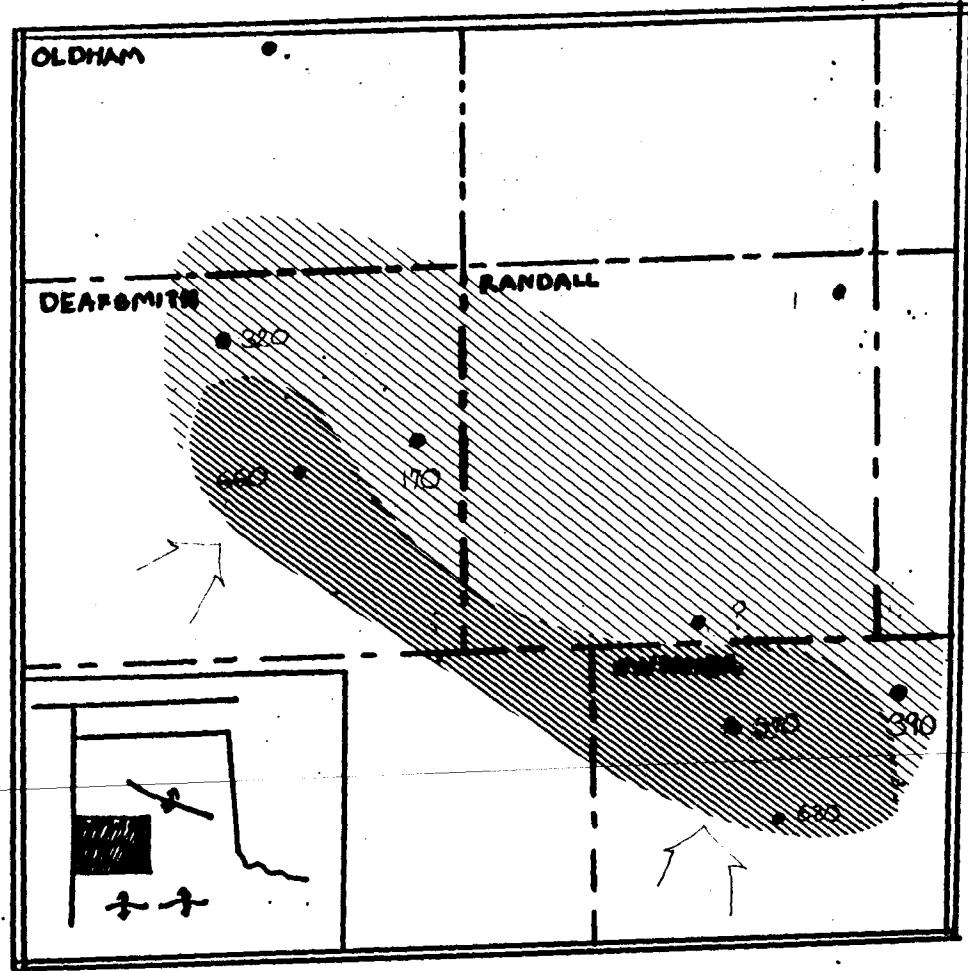
Thickness of anhydrite in zone 15 in feet

DRAFT

Distribution of anhydrite in San Andres unit 5, zone 15

Figure 82. Distribution of anhydrite and anhydritic chevron halite in San Andres unit 5, zone 15. This cycle is unusual in that the lowest salinity facies are in the east.



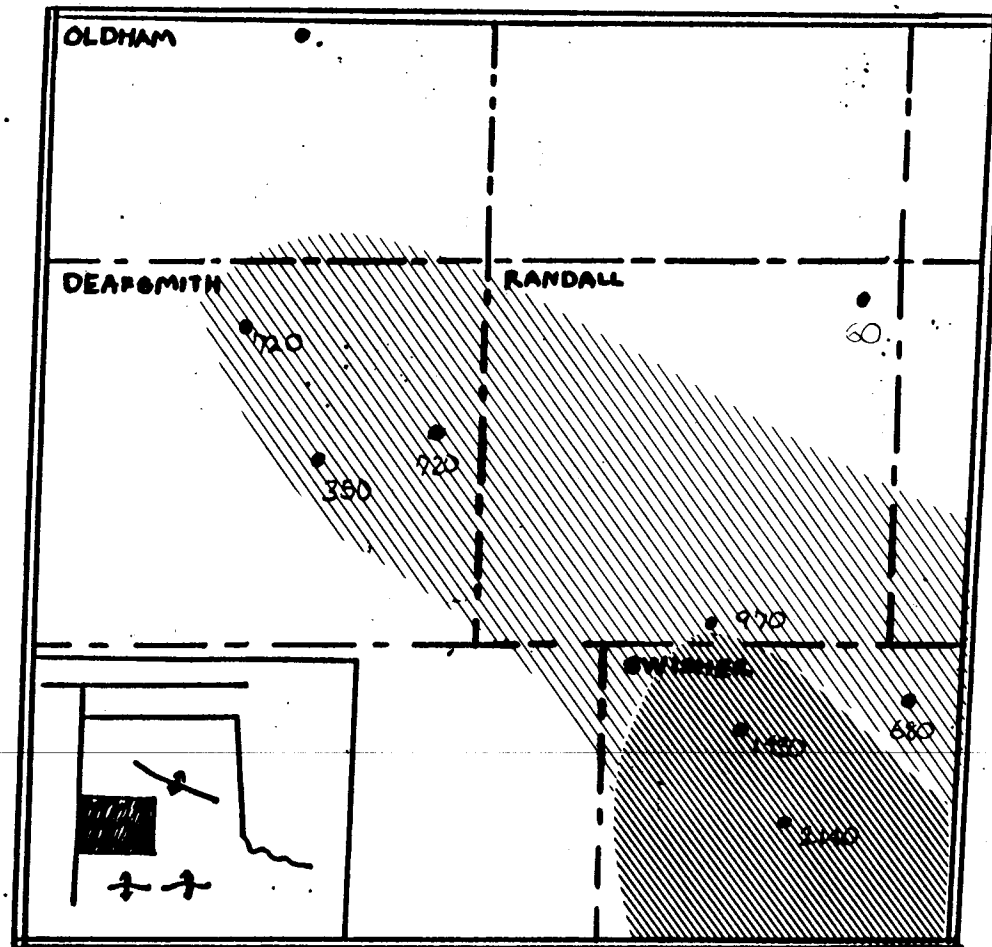


Thickness of zone 17 given in millimeters

Isopach of San Andres unit 5, zone 17

Figure 83. Isopach of unit 5, zone 17 showing increasing thickness of the anhydrite bed to the south in both Swisher and Deaf Smith counties.

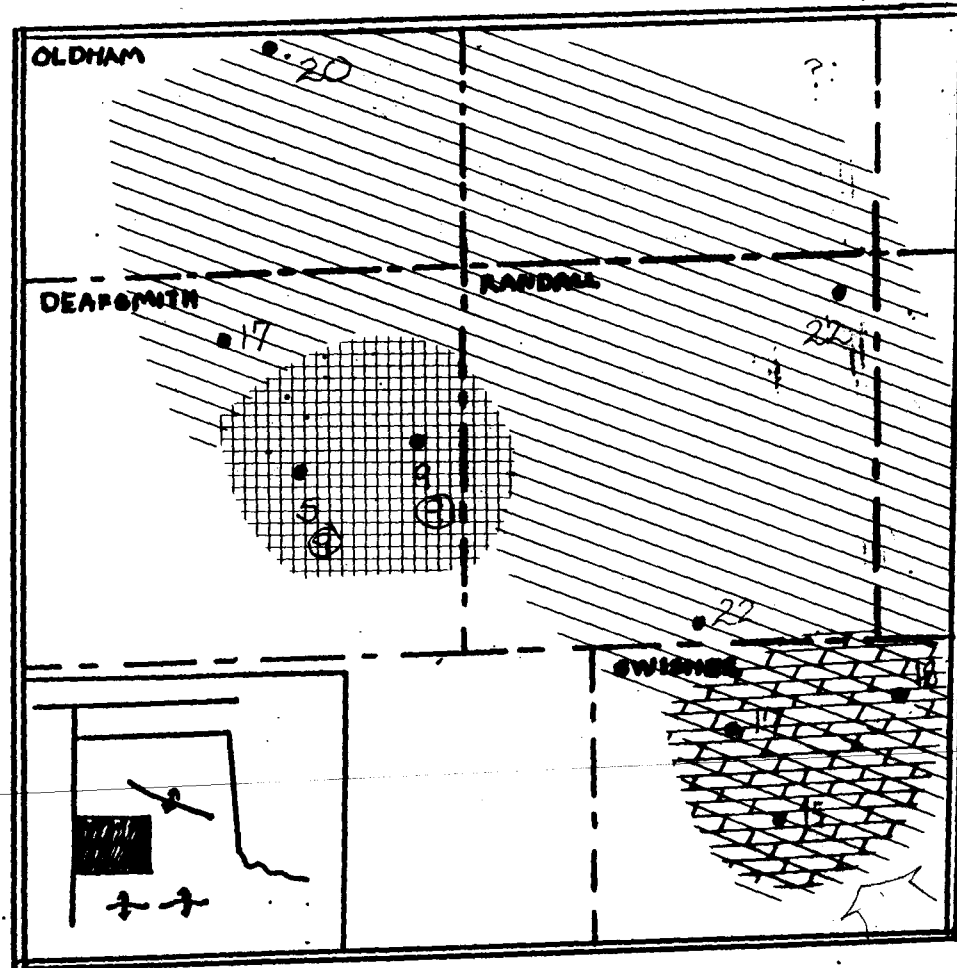
DRAFT


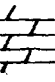



Isopach of San Andres units, zone 19

Figure 84. Isopach of unit 5, zone 19 showing increasing thickness of anhydrite bed to the south in Swisher County.

DRAFT



-  anhydrite in zone 23 and 25 thicker than 10 feet.
-  dolomite present in zone 23 or 25
-  Thickness of halite in zone 24 (circled)

Distribution of facies in San Andres unit 5, zone 23, 24 and 25

Figure 85. Distribution of facies in San Andres unit 5, zone 23, 24, and 25. The most marine facies are present in the south east with halite present within the interval in Deaf Smith County.

DRAFT